Characterization of Inherited Nephropathies in Pakistani Families Using Next Generation Sequencing

Naima Khan

Department of Biotechnology
Faculty of Biological Sciences
Quaid-i-Azam University
Islamabad, Pakistan
June 2021

Characterization of Inherited Nephropathies in Pakistani Families Using Next Generation Sequencing

Naima Khan

A thesis submitted in the partial fulfillment of the requirements of

Quaid-i-Azam University for the degree of Doctor of Philosophy in Biotechnology

Department of Biotechnology
Faculty of Biological Sciences
Quaid-i-Azam University
Islamabad, Pakistan

June 2021


بسم الله الرحمن الرحيم

Dedication

To my beautiful family for their endless love and support

ACKNOWLEDGEMENTS

In the name of **Allah**, *the Most Gracious and the Most Merciful Alhamdulillah, all praises to Allah for the strengths and His blessings in completing this thesis. Thanks to Allah Almighty for the wisdom that he has bestowed upon me during this research project, and indeed, throughout my life. Without the divine help of Allah, I would not have been able to achieve anything in life.*

I am immensely pleased to place on record my profound gratitude and heartfelt thanks to my supervisor **Prof. Dr. Muhammad Naeem** *for his interest, commitment to work, providing all facilities and inspiring guidance for successful completion of my research work. I deem it as my privilege to work under his able guidance. I ever remain grateful to him. I could not have imagined having a better advisor and mentor for my Ph.D study.*

Foremost, I would like to express my sincere gratitude to **Dr. Bilal Haider Abbassi**, *Chairman, Department of Biotechnology, Quaid-i-Azam University, Islamabad.*

I would also like to express my gratitude to all the **faculty members** *of the Biotechnology Department at Quaid-i-Azam University, Islamabad. To all of them, I appreciate what they have done to help me in my scholastic and professional growth.*

A very special gratitude goes out to all down at **Higher Education Commission Pakistan** *for helping and providing the funding for the work.*

I am grateful to my **sibling and parents** *who have provided me through moral and emotional support in my life.*

With a special mention to my dear friends and fellows **Fehmida Farid Khan, Dr. Sofia Hussain, Dr. Zain Aslam, Dr. Noreen Karim, Dr. Zubaida, Hajira Batool, Ghazala Zamani and Ribqa Akhter.** *It was fantastic to have the opportunity to work with all of them.*

I would like to acknowledge **Dr Naureen Akhter, The Children's Hospital and The Institute of Child Health Lahore** *for her help in this research work.*

And finally, last but by no means least, thanks to my caring **husband** *for his constant support who has been by my side throughout the last 3 years. living every single minute of it, and without whom, I would not have had the courage to embark on this journey in*

the first place. And to my dear daughter for being such a good little baby that past five months and making it possible for me to complete what I started.

Naima Khan

Author's Declaration

I, Ms. Naima Khan, hereby state that my Ph.D. thesis titled: **"Characterization of Inherited Nephropathies in Pakistani Families using Next Generation Sequencing"** is my own work and has not been submitted previously by me for taking any degree from Quaid-i-Azam University Islamabad or anywhere else in the country/world.

At any time if my statement is found to be incorrect even after I Graduate, the university has the right to withdraw my Ph.D. degree

Naima Khan

Plagiarism Undertaking

I solemnly declare that research work presented in the thesis titled: "**Characterization of Inherited Nephropathies in Pakistani Families using Next Generation Sequencing"** is solely my research work with no significant contribution from any other person. Small contribution/help wherever taken has been duly acknowledged and that complete thesis has been written by me.

I understand the zero-tolerance policy of the HEC and Quaid-i-Azam University Islamabad towards plagiarism. Therefore, I as an Author of the above titled thesis declare that no portion of my thesis has been plagiarized and any material used as reference is properly referred/cited.

I undertake that if I am found guilty of any formal plagiarism in the above titled thesis even after award of PhD degree, the University reserves the rights to withdraw/revoke my PhD degree and that HEC and the University has the right to publish my name on the HEC/University Website on which names of students are placed who submitted plagiarized thesis.

Student /Author Signature: _____

Ms. Naima Khan

PUBLICATIONS FROM THIS STUDY

Khan N, Khan FF, Akhtar N. Hussain S, Naeem M (2020). Molecular Diagnosis and Identification of Genetic Variants Underlying Distal Renal Tubular Acidosis (dRTA) in Pakistani Patients Using Whole Exome Sequencing. Genetic Testing and Molecular Biomarkers.24(2);85-91.

Khan N, Akhtar N. Hussain S, Naeem M. Digenic inheritance of novel heterozygous *NPHP4* and *ANKS6* missense variants identified by whole exome sequencing in a Pakistani patient affected with autosomal recessive nephronophthisis. (Manuscript prepared)

Khan N, Akhtar N. Hussain S, Naeem M. Whole exome sequencing as a diagnosis tool in hypokalemic Pakistani patients. (Manuscript prepared)

Khan N, Akhtar N. Hussain S, Naeem M. Molecular investigation of a Pakistani family affected with autosomal recessive nephronophthisis using whole exome sequencing. (In preparation)

SUMMARY

Inherited nephropathies represent the genetic diseases of kidney. A significant number of children and adults with ESRD have inherited kidney disease. Advanced genomic studies assisted by the next generation sequencing techniques have not only contributed to the identification of new genes and helped in the genetic diagnosis of highly heterogeneous inherited nephropathies but also broadened the phenotypic spectrum of known inherited nephropathies which might improve the diagnosis in puzzling cases, hence avoiding the invasive diagnostic procedures.

In the present study, six Pakistani families presenting two different inherited nephropathies (distal renal tubular acidosis and nephronophthisis) have been described at clinical and molecular level to identify the genetic causes of these inherited diseases. Families are labelled in sequel from Family A to Family F. Three families (A,B,C) demonstrated the clinical and diagnostic features of distal renal tubular acidosis while the other three families (D,E,F) were clinically diagnosed to have inherited nephronophthisis.

Family A with four affected individuals demonstrated the clinical and diagnostic features of inherited dRTA. Genetic diagnosis of the family using whole exome sequencing revealed a splice donor site variant c.2257+1G>A in *ATP6V0A4*. Sanger sequencing verified the identified variant and *in silico* prediction tools predicted the mutation to be damaging. The genetic variant c.2257+1G>A in *ATP6V0A4* identified in the family A was checked in the ten dRTA families whose gDNA was extracted previously. The variant was found in another family (designated as Family B in this dissertation) in heterozygous state in the patient II-1. Assuming compound heterozygous autosomal recessive inheritance, DNA sequencing of *ATP6V0A4* gene was carried out using Sanger sequencing method. A new heterozygous variant c.722+5G>A was identified in *ATP6V0A4* which was predicted to be disease causing by abolishing the canonical splice site. Both the splice site variants were co-segregated in the available members of family B through Sanger sequencing.

Family C comprised of two patients (II-1 and II-2). They were clinically diagnosed with dRTA based on polyuria and relatively high urine pH. Genetic investigation of these patients was carried out using whole exome sequencing and subsequent Sanger sequencing

to identify and verify the recurrent mutation [c.1049G>A; p.G350D] in *AGXT* gene. Parents were healthy and showed heterozygous variant c.1049G>A in *AGXT* gene. The mutations in *AGXT* gene is reported to cause PH1, an inherited kidney disorder and the mutation c.1049G>A was previously reported with PH1. The patients were later tested for their plasma oxalate levels which indicated higher serum oxalate levels (> 100µmol/L) compared to normal. Therefore, WES corrected the clinical diagnosis of dRTA to PH1 and the patients who reached CKD-IV were treated with high dose pyridoxine to maintain their GFR.

The three families D, E and F for whom NPH was diagnosed were ascertained at clinical and molecular levels. All the available members of these families were screened for recurrent homozygous *NPHP1* gene deletion and subjected to WES for identification of genetic cause upon negative *NPHP1* gene deletion. In family D, two novel variants (c.3145C>T; p.P1049S and c.1690C>G; p.P564A) were identified in *NPHP4* and *ANKS6* genes and a digenic mode of inheritance responsible for pathology was suggested. In family E, WES and Sanger sequencing identified a missense variant c.1424C>G; p.P475R in *NEK1* gene in three affected members of the family. Various bioinformatics-based tools predict this as a non-favored substitution and may disrupt the functional region of the protein thus disrupting its ciliary localization.

In family F, despite the complex filtration and careful analysis of the WES data no pathogenic mutation was identified in the genes linked to NPH, while the other potential shortlisted variants did not segregate with the disease phenotype within the family. Thus, whole genome sequencing is recommended to resolve the genetic cause of this family.

Thus, WES identifies the causative genetic variants in 5/6 of affected families, thereby presenting the correct diagnosis and allows identification of novel and recurrent variants in genes responsible for nephropathies.

CONTENTS

LIST OF FIGURES

LIST OF TABLES

LIST OF ABBREVIATIONS

%	Percentage
AD	Autosomal dominant
A-ICs	Alpha intercalated cells
AR	Autosomal recessive
BDS	Beckman dickinson syringes
B-ICs	Beta intercalated cells
CKD	Chronic kidney disease
CNVs	Copy number variations
DDR	DNA damage repair
DNA	Deoxyribonucleic acid
dRTA	Distal renal tubular acidosis
EDTA	Ethylene diamine tetraacetic acid
eGFR	Estimated glomerular filtration rate
ESRD	End stage renal disease
ExAC	Exome Aggregate Consortium
FSGS	Focal segmental glomerulosclerosis
GATK	Genome analysis tool kit
GWAS	Genome wide association studies
HCO_3	Bicarbonate
HDF	Hi-Di formamide
HGMD	Human genome database
KB	Kilobases
L	Liters
MAF	Minor allele frequency
MCKD	Medullary cystic kidney disease
mRNA	Messenger RNA
mTOR	mammalian target of rapamycin

NaOH	Sodium hydroxide
NC	Nephrocalcinosis
NGS	Next generation sequencing
NL	Nephrolithiasis
NPHP	Nephronophthisis
NPHP1	Nephrocystin 1
NPHP-RC	NPHP related ciliopathy
OMIM	Online Mendelian Inheritance inMan
PCR	Polymerase chain reaction
pH	Power of hydrogen
PH1	Primary hyperoxaluria type 1
Polyphen	Polymorphism phenotyping
POx	Plasma oxalate
pRTA	Proximal renal tubular acidosis
QC	Quality control
RNA	Ribonucleic acid
RPM	Rounds per minutes
RRT	Renal replacement therapy
RTA	Renal tubular acidosis
SAS	South Asians
SIFT	Sorting intolerant from tolerant
SNHL	Sensorineural hearing loss
SVD	Spontaneous vaginal delivery
TBE	Tris borate EDTA
UCSC	University of California, Santa Cruz
Ug	Microgram
Ul	Microliter
UTIs	Urinary tract infections

UTR	Untranslated regions
WES	Whole exome sequencing
WNT	Wingless-related integration site
XL	X-linked
XLD	X-linked dominant
XLR	X linked recessive

INTRODUCTION

1.1 Inherited nephropathies

Inherited nephropathies represent the hereditary diseases of kidney and are the fifth frequently occurring cause of end stage renal disease (ESRD), the first four are diabetes, high blood pressure, glomerulonephritis and pyelonephritis. Inherited kidney disease is the cause of leading ESRD in all children and approximately 10% of adults. No doubt, renal transplantation technique has substantially increased the lives of affected people, but they often have different health problems remain associated with them. Multiple organs are affected due to inherited renal diseases that offers challenges like phenotypic heterogeneity, scattered biochemical and clinical data, no standardization for diagnostics and limited insights into the mechanism of disease (Devuyst et al., 2009).

Kidney is an organ highly specialized for the regulated functions that are essential for acid-base and electrolyte homeostasis. Besides their homeostatic roles, kidneys are also involved in regulation of hormone and vitamin metabolism, oxygen supply to the tissues and immune functions. Secretion of drug metabolites and metabolic clearance is another essential role of kidneys. Therefore, kidney disfunctioning will have a direct effect on these cognitive functions. (Eckardt et al., 2013). Genetic studies were first used in nephropathies in 1985 with the mapping of autosomal polycystic kidney diseases and the identification of mutation responsible for Alport's syndrome (a monogenic kidney disorder)(Eckardt et al., 2013). These studies were followed by identification of genes for kidney disorders including nephrogenic diabetes insipidus, Liddle's syndrome, Dent's disease, Bartter's syndrome, nephronophthisis, Gitelman's syndrome, and nephropathic cystinosis (Boyer et al., 2011; Jouret et al., 2007; Lloyd et al., 1996; Rosenthal et al., 1992; Shimkets et al., 1994; Simon, Nelson-Williams, et al., 1996).

With the advent of techniques such as High-throughput and next generation sequencing, genetics of more than 160 rare nephropathies have been studied. Mutations in proteins encoding receptors, channels, enzymes, transporters, transcription factors and structural components result in these kidney disorders. (Figure 1.1, Table 1.1-1.5). In addition to the monogenic mutations, there are several kidney diseases which are caused by more than one

variant in the same gene or genes involved in related kidney pathways. This results in variable phenotypes that the conventional genotype-phenotype correlations are unable to explain.(Hildebrandt, 2010). The number of rare kidney disorders which were once considered as monogenic with tight genotype-phenotype correlations, is now increasing since previously and now they have been proven as heterogeneous (Devuyst, 2014). General classification of inherited nephropathies is shown:

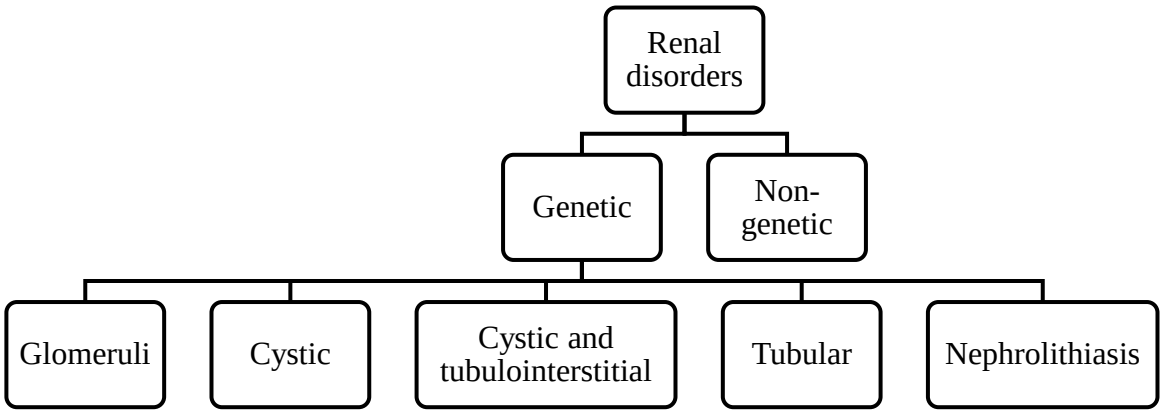

Figure 1.1: General classification of renal disorders.

Some of the inherited kidney diseases are presented below:

1.1.1 Glomerular diseases

Renal glomerular diseases are caused by structural defects in glomerular basement membrane, or the podocytes and endothelial cells that make the basement membrane. Glomerular diseases are diagnosed mainly on the basis of presence of urinary proteins or microhematuria. More than 50 genes have been described to cause several inherited glomerular diseases(Armstrong & Thomas, 2019). Alport syndrome caused by genetic mutations of *COL4A3, COL4A4* and *COL4A5* is the most frequent glomerular disease (Kruegel, Rubel, & Gross, 2013). Steroid resistant nephrotic syndrome (SRNS) is another commonly occurring primary glomerular disorder of the kidney. Many genes (>40) are known to cause the disease and except of few, all these single gene causatives of SRNS leads to CKD resistant to steroidal treatment(B. Hinkes et al., 2006; Machuca, Benoit, & Antignac, 2009). Age of onset of CKD is different with the different causative gene mutation for example *NPHS1, NPHS2, LAMB2* and *PLCE1* mutations lead to CKD at an

early age while *ACTN4* and *TRPC6* mutations result in adulthood CKD (B. G. Hinkes et al., 2007).An overview of glomerulopathies is shown in table 1.1 (Hildebrandt, 2010).

Table 1. 1: Renal glomerular diseases

Glomerular diseases	**Genes**	**Protein Product**	**Inheritance**	**Symptoms**
Steroid resistant nephrotic syndrome	*NPHS1*	Nephrin	AR	Congenital nephrotic syndrome, CKD
	NPHS2	Podocin	AR	CKD, FSGS
	PLCE1	Phospholipase C	AR	CKD, FSGS
	MYO1E	Non muscle class myosin 1E	AR	FSGS
	PTPRO	*Protein* tyrosine phosphatase, receptor type O.	AR	FSGS, tubulointerstitial fibrosis
	DGKE	Diacylglycerol kinase epsilon	AR	CKD
	ARHGDIA	Rho GDP dissociation inhibitor alpha	AR	CKD
	ACTN4	Alpha actinin 4	AD	FSGS, adult onset steroid resistant nephrotic syndrome

	TRPC6	Transient receptor potential cation channel C6	AD	FSGS, adult onset steroid resistant nephrotic syndrome
	WT1	WT1 transcription factor	AD	Wilms tumor, degenerative renal failure, hypertension
Denys-Drash syndrome,	*WT1*	WT1 transcription factor	AD	Wilms tumor, degenerative renal failure, hypertension
Pierson's syndrome	*LAMB2*	Laminin beta-2	AR	Congenital nephrotic syndrome, eye abnormalities, early onset ESRD
Fabry's disease	*GLA*	Galactosidase alpha	XL	Progressive renal disease, cardiac and cerebrovascular abnormalities
Nail-patella syndrome	*LMX1B*	LIM homeobox transcription factor 1 beta	AD	Congenital nephrosis, collagen fibrils at glomerular

				basement membrane
Alport's syndrome, ATS1	*COL4A5*	Collagen Type IV Alpha 5 Chain	XLD	Progressive ESRD, ocular disability, SNHL
Alport's syndrome, ATS2	*COL4A4*, *COL4A3*	Collagen Type IV Alpha 4 Chain Collagen Type IV Alpha 3 Chain	AR	Progressive renal failure, nephrotic syndrome, SNHL
Alport's syndrome, ATS3	*COL4A3*	Collagen Type IV Alpha 3 Chain	AD	Progressive renal function, microhematuria
Familial amyloidosis	*FGA* *APOA1* *LYZ* *B2M*	Fibrinogen alpha chain Apolipoprotein A1 Lysozyme Beta-2-microglobulin	AD	Chronic nephropathy, hematuria, edema

AD=autosomal dominant, AR=autosomal recessive, XLD=X-linked dominant, FSGS=focal segmental glomerulosclerosis, CKD=chronic kidney disease, ESRD=end stage renal disease, SNHL=sensorineural hearing loss

1.1.2 Renal cystic diseases

Cystic and glomerular diseases are amongst the most common inherited kidney diseases. Cystic diseases are characterized by the formation of renal cysts and disruption of nephrons (Alkanderi, Yates, Johnson, & Sayer, 2017;Vivante & Hildebrandt, 2016). Autosomal dominant polycystic kidney disease is the frequently occurring lethal disease that leads to CKD in late 60s. *PKD1* and *PKD2* are the culprit genes involved in ADPKD and their mutations segregate in autosomal dominant mode of inheritance. Renal cyst formation and growth of cysts in ADPKD shows somewhat recessive inheritance and depends upon second hit mutations. Diagnosis of more than 90% of ADPKD cases can now be done accurately using the molecular genetic techniques which helps in making the treatment decisions (Harris & Rossetti, 2008; Torres & Harris, 2009)**.**

Autosomal recessive polycystic kidney disease (ARPKD) is caused by *PKHD1* and characterized by the bilateral enlarged cysts that may arise before birth. Depending upon the severity of mutations in *PKHD1* gene, CKD may result directly after birth, in early or late childhood or at an adult age. Truncating mutations in *PKHD1* are correlated with perinatal onset of CKD (Hildebrandt, 2010).

1.1.3 Renal cystic and tubulointerstitial disease

Nephronophthisis (NPHP) is an autosomal recessive ciliary disease that progresses to cystic kidneys and eventually end stage renal failure (ESRD) before the age of 30 years (Hildebrandt & Zhou, 2007). On the basis of mean age at which ESRD develops in NPHP, three different forms have been described: infantile NPHP (<3 years), juvenile NPHP (13 years) and adolescent NPHP (19 years). Nephronophthisis is characterized by decreased ability to concentrate urine, polydipsia, enuresis, growth retardation, loss of corticomedullary differentiation, shrunken or normal sized cystic kidneys. The disease may be presented as isolated NPHP or there may be extrarenal manifestations i-e, retinal impairment, liver involvement, skeletal dysplasia or CNS abnormalities associated with renal disease. NPHP is caused by recessive mutations in 25 different genes (Salomon, Saunier, & Niaudet, 2009).

Medullary cystic kidney diseases now known as autosomal dominant tubulointerstitial kidney diseases (ADTKD) constitute a group of diseases that eventually results in decline in kidney function with a median age of 50s and onset at a variable age (Ayasreh et al., 2018; Eckardt et al., 2015). Interstitial fibroids and tubular atrophy upon renal imaging are usually seen in patients with ADTKD. Normal gap acidosis, increased creatinine and hyperkalemia are diagnostic but not the distinguishing clinical features in ADTKD. The renal images and histological features of NPHP and ADTKD are almost similar, therefore genetic testing is required to identify the disease pathogenesis. Age of onset and inheritance of both the diseases differ which can be helpful in differential diagnosis (Armstrong & Thomas, 2019).

An overview enlisting few cystic kidney diseases is given in table 1.2. (Hildebrandt, 2010)

Table 1. 2: Cystic and tubulointerstitial diseases.

Renal cystic and tubulointerstitial diseases	**Genes**	**Protein Product**	**Inheritance**	**Symptoms**
ADPKD Type 1	*PKD1*	Polycystin 1	AD	Polycystic kidneys and liver, intracranial aneurysm, ESRD
ADPKD Type 2	*PKD2*	Polycystin 2	AD	Polycystic kidneys, ESRD
ARPKD	*PKHD1*	Fibrocystin	AR	Polycystic kidneys, liver disease, ESRD
Medullary cystic kidney disease type 1	*MUC1*	Mucin 1	AD	Intramedullary and corticomedullary cysts, CKD

Medullary cystic kidney disease type 2	*UMOD*	Uromodulin	AD	Hyperuricemia, corticomedullary cysts, late onset CKD
Nephronophthisis types 1-9	*NPHP1-NPHP9*	Nephrocystins1-9	AR	Polyuria, polydipsia, anemia, ESRD
Meckel-Gruber syndrome (1-4)	*MKS1-MKS4* (Allelic with NPHP genes also)	Meckelin	AR	Polycystic kidneys, Organ dysplasia
Bardet-Biedl syndrome (1–12)	*BBS1-BBS12*	BBS protein	AR	Cystic kidney dysplasia, polydactyly, retinitis pigmentosa

ADPKD=autosomal dominant polycystic kidney disease, ARPKD=autosomal recessive polycystic kidney disease, AD=autosomal dominant, AR=autosomal recessive

1.1.4 Congenital abnormalities of the kidney and urinary tract (CAKUT)

Genetic CAKUT comprises a large group of diseases caused by developmental defects of kidney and urinary tract. CAKUTs show variable penetrance and are more common than recessive CAKUT cases. These defects are usually evident before birth, soon after birth or during early childhood but few cases may be identified at later ages. Patients may be diagnosed *in utero* during antenatal scan, childhood urinary problems, abnormal urinalysis or upon renal imaging in children with dysmorphic features (Capone, Morello, Taroni, & Montini, 2017; Pal & Reidy, 2017). Computed tomography scan or ultrasound can detect the phenotype including renal agenesis, horseshoe kidney, hypodysplasia (unilateral or

bilateral) and ectopic kidney. Single gene mutations in many genes result in different congenital anomalies of kidney (Table 1.3). Genetic investigation distinguish the genetic causes from environmental causes and helps in genetic counselling of the affected family (Armstrong & Thomas, 2019).

Overview of some congenital kidney abnormalities is given in table 1.3 (Hildebrandt, 2010).

Table 1. 3: Congenital abnormalities of the kidney and urinary tract (CAKUT)

CAKUT	**Genes**	**Protein product**	**Inheritance**	**Symptoms**
Renal agenesis	*RET*, *UPK3A*	Protooncogene ret, Uroplakin 3A	AD	VUR, renal agenesis, facial defects
Renal hypodysplasia (RHD)	*BMP4*, *SIX2*	Bone morphogenetic protein 4, Sine oculis 2	AD	RHD, cleft lip, microphthalmia
Multicystic renal dysplasia (MRD)	*CDC5L*, *USF2*	Cell division cycle, upstream stimulatory factor 2	AD	MRD
CAKUT	*FOXC1*	Forkhead transcription factor C 1	AD	CAKUT, eye abnormalities
Vesicoureteral reflux (VUR2)	*ROBO2*	Roundabout 2	AD	VUR, limbs and facial defects

Fraser syndrome	*FRAS1*, *FREM2*	ECM protein, Fras1-related ECM protein	AR	Renal agenesis, RHD, syndactyly

AD=autosomal dominant, AR=autosomal recessive, ECM=extracellular matrix protein

1.1.5 Renal tubulopathies

Renal tubulopathies are caused by defective renal tubular functions which comprise mainly reabsorption of water and solutes from filtrate produced by glomerular capillaries. The main clinical/diagnostic features of renal tubulopathies are electrolytes imbalance and polyuria. Most of the tubulopathies are being recognized as monogenic diseases caused by mutations in single gene. This forms the basis of unambiguous identification of tubulopathies by genetic diagnosis (Birkenhäger et al., 2001; Estévez et al., 2001; Simon et al., 1997; Simon, Karet, Hamdan, et al., 1996; Simon, Karet, Rodriguez-Soriano, et al., 1996; Simon & Lifton, 1996). All the genes involved mainly encode transport proteins or signaling proteins being expressed in certain specific tubular segments of the kidney, therefore mutations in these genes result in clinical and diagnostic signs of following diseases of renal tubules (Hildebrandt, 2010) (Table 1.4).

The term RTA includes many defects caused by metabolic acidosis due to defective bicarbonate reabsorption and hydrogen ions excretion in renal collecting tubules with the glomerular filtration unaffected or very little affected. Normal anion gap hyperchloremic metabolic acidosis are the clinical signs found in all forms of RTA and may lead to nephrolithiasis, growth retardation, bone diseases (osteoporosis and rickets) and eventually CKD if left untreated (Gregory & Schwartz, 1998; Ring, Frische, & Nielsen, 2005; Smulders, Frissen, Slaats, & Silberbusch, 1996; Soriano, 2002). At least seven different genes (*ATP6V0A4, ATP6V1B1, FOXI1*, *WDR72*, *SLC4A4*, *CA II* and *SLC4A1*) are involved in dominant and recessive forms of inherited renal tubular acidosis. Hearing impairment is associated with the first two genes with varying age of onset.

Proximal tubular defect results in renal Fanconi syndrome which manifests phosphaturia, glucosuria and acidosis in proximal tubules (RTA) whereas distal convoluted tubular

defects lead to Gitelman syndrome. Bartter syndrome is caused by mutations in different genes which are involved in sodium reabsorption in ascending loop of Henle. Nephrogenic diabetes insipidus (NDI) is caused by *AQP2* (aquaporin 2) mutations and X linked NDI is caused by gene encoding vasopressin-2-receptor (Deen et al., 1994; Glaudemans et al., 2009; Knoers, 2009; Konrad, Schlingmann, & Gudermann, 2004; Rosenthal et al., 1992; Simon, Nelson-Williams, et al., 1996). An overview of renal tubulopathies is described in Table 1.4. Secondary tubulopathies are not caused by genetic defect but are caused by nonspecific damage to renal tubular segments and cause their disfunctioning (Hildebrandt, 2010).

Table 1. 4: Renal tubulopathies

Renal tubular diseases	**Genes**	**Protein Product**	**Inheritance**	**Symptoms**
Renal glucosuria	*SLC5A2*	Sodium dependent glucose transporter	AR	Glycosuria, glucose/galactose malabsorption
Bartter syndrome (1-4)	*SLC12A1,*	sodium-potassium-chloride cotransporter-2	AR	Hypokalemia, alkalosis, growth failure, polyuria, Hypercalciuria
	KCNJ1,	Potassium channel ROMK		

	CLCNKB,	Kidney chloride channel B		
	BSND	Barttin		
Gitelman syndrome	*SLC12A3*	Sodium chloride cotransporter	AR	Hypotension, hypomagnesemia, hypocalciuria
Liddle syndrome (1-3)	*SCNN1B*	Renal epithelial sodium channel beta subunit	AD	Hypertension, Hypokalemia, Suppressed secretion of aldosterone
	SCCN1G	Renal epithelial sodium channel gamm a subunit		
	SCCN1A	Renal epithelial sodium channel alpha subunit		

Gordon syndrome	*WNK1*, *WNK4*, *KLHL3*, *CUL3*	Serine threonine protein kinases 1 and 4, Kelch-like protein *3*. component of ubiquitin E3 ligase complex	AD	Pseudohypoaldosteronism type 2, hyperkalemia, hyperchloremia, acidosis, hypertension
Distal renal tubular acidosis dRTA	*ATP6V1B1*, *ATP6V0A4*	Vacuolar ATPases	AR	Distal tubular acidosis, nephrocalcinosis, SNHL, osteomalacia, growth failure
dRTA type 1	*SLC4A1*	Anion exchanger 1	AD	
Proximal renal tubular acidosis	*CA2*, *SLC4A4*	Carbonic anhydrase 2, $NaHCO_3$ cotransporter	AR	Proximal tubular acidosis
Hypomagnesemia	*CLDN16*	Claudin 16	AR	Low magnesium levels in blood, nephrocalcinosis, CKD, hypotension

Hypomagnesemia	*ATP1G1*	FXYD2	AD	Low magnesium levels in blood, seizures
Nephrogenic diabetes insipidus	*AVPR2*	AVP receptor 2	XLR	Polyuria, polydipsia
	AQP2	Aquaporin 2	AD/AR	

AD=autosomal dominant, AR=autosomal recessive, XLR=X-linked recessive, CKD=chronic kidney disease, SNHL=sensorineural hearing loss

1.1.6 Nephrolithiasis

Nephrolithiasis (kidney stone formation) is a kidney disease caused by metabolic disorders including hypercalciuria, hyperoxaluria, hyperphosphaturia, hypocitraturia, cystinuria, defective urinary acidification and low urine volume. Their main clinical features are renal calculi. Genetic (Table 1.5), environmental (hypertension, obesity, high fructose diet, high animal protein diet etc.) and anatomical (medullary sponge kidney, horseshoe kidney, ADPKD, space travel) causes play role in nephrolithiasis (Sayer, 2008; West et al., 2008). There are many monogenic cases of nephrolithiasis which have been identified and the causative genes encode renal transport channels and transporters (Table 1.5) (Hildebrandt, 2010).

Table 1. 5: Nephrolithiasis.

Nephrolithiasis	**Genes**	**Protein Product**	**Inheritance**	**Symptoms**
Cystinuria type 1	*SLC3A1*	Amino acid transporter	AD, AR	Cystine stones
Cystinuria non-type	*SLC7A9*	Amino acid transporter	AD, AR	Cystine stones

Dent's disease type 1-2	*CLCN5* *ORCL*	Chloride-proton exchanger	XLR	Nephrocalcinosis; nephrolithiasis
Lowe's oculocerebroren al syndrome	*ORCL*	Enzyme inositol 5-phosphatase	XLR	Phosphaturia, cataracts, Fanconi syndrome
Primary hyperoxaluria type 1	*AGXT*	Alanine-glyoxylate aminotransferase	AR	Calculi, CKD
Primary hyperoxaluria type 2	*GRHPR*	Glyoxylate reductase/hydroxypyruvate reductase (peroxisomal enzyme)	AR	Nephrolithiasis
Primary hyperoxaluria type 3	*HOGA1*	4-Hydroxy-2-oxoglutarate aldolase (mitochondrial enzyme)	AR	Nephrolithiasis, hypercalciuria, hypocitraturia
Xanthinuria	*XHD*	Xanthine dehydrogenase	AR	Xanthine stones
Adenine-phosphoribosyl-transferase deficiency	*APR3*	adenine phosphoribosyl transferase	AR	Nephrolithiasis

AD=autosomal dominant, AR=autosomal recessive, XLR=X-linked recessive

1.2 Diagnosis, treatment and therapy through gene identification

Most of the inherited nephropathies are monogenic and identification of mutation itself present the disease etiology which offers a benefit of unequivocal diagnosis eliminating the need to perform invasive diagnostics in some disease e.g., nephronophthisis. In

addition, prenatal diagnosis is also possible. Prognosis of the disease can be made e.g., mutations in *PKD1* lead to ADPKD in early and *PKD2* mutations result in late onset ADPKD. Disease mechanism (using animal models) and assigning subtype to the disease (e.g., PH1 in case *AGXT* mutations and PH2 in *GRHPR*) after pathogenic mutation identification also becomes possible (Hildebrandt, 2010).

1.3 Nephropathies and modifier alleles

Monogenic diseases are caused by single gene mutations which exert strong causality on the phenotype and are rarely influenced by environmental effects. Linkage mapping usually easily detects the genetic cause of monogenic diseases. Polygenic diseases are more common than monogenic and exert weak causality on the disease phenotype. They are more influenced by environmental effects and require genome wide association studies i-e., GWAS, to be detected (Hildebrandt, 2010). Genetic variants that carries the risk of developing chronic kidney disease have been widely studied through GWAS. *UMOD* gene, which causes medullary cystic kidney disease type 2, carries a risk allele for chronic kidney disease e.g., a SNP located near the *UMOD* is strongly associated with CKD. Risk alleles have been associated and described hemolytic uremic syndrome, ureteropelvic obstruction and hypertension (Divers & Freedman, 2010).

Single-gene diseases (monogenic/Mendelian) are caused by mutations in one gene whereas polygenic kidney diseases are caused by multiple mutated alleles in many different genes. Until recently a strong relation between genotype and phenotype was thought to exist in monogenic diseases which is somewhat weak in polygenic diseases.(Hildebrandt, 2010). The scenario is now changed and the distinct margin between monogenic and polygenic diseases has become less distinct to some extent due to the interplay of modifier allelic effect. For example, in isolated nephronophthisis the genetic cause is *NPHP1* homozygous gene deletion, however a single allelic mutation of *NPHP6* along with *NPHP1* deletion result in retinal atrophy or ataxia (Hoefele et al., 2007). Here, single heterozygous mutation in *NPHP6* is a modifier allele which act in concert with the homozygous *NPHP1* to cause the additional phenotype in NPHP patient.(Tory et al., 2007).

1.4 Unknown genetics of nephropathies

Albeit the progress and advancement in genetic testing methods, genetic causes and pathways to understand the disease mechanism of most of the nephropathies are still unknown. The underlying genetics of only 30-40% of nephrotic syndrome, 40-50% of congenital tubulopathies and 50-60% of haemolytic uraemic syndrome are known. Genetic testing is considered rarely in clinical settings even for well explained genetic diseases Barter's, Gitelman's and Alport's syndrome because of the cost and time associated with them and also because of inadequate genetic literacy (Devuyst, Knoers, Remuzzi, & Schaefer, 2014).

1.5 Next generation sequencing in inherited nephropathies

There are five stages of chronic kidney diseases classified based on the estimated glomerular filtration rate (eGFR). The eGFR value of <60mL/min/1.73min^2 is known as first stage whereas eGFR value <15mL/min/1.73min^2 is known as fifth stage CKD or end stage renal disease (ESRD). (Hogg et al., 2003). Prevalence rates for chronic kidney diseases are 23.4% in general population (stage1-5) and 10.6% (stage 3-5) (Hill et al., 2016). In Pakistan the estimated prevalence of CKD is 21.2% (Hasan, Sutradhar, Gupta, & Sarker, 2018). The early stage of CKD is asymptomatic and cannot be distinguished merely by clinical data and this is why, in many individuals with a kidney failure, the exact cause remains unknown. About 10% to 25% of CKD cases represent a hereditary nephropathy (Lata et al., 2018; Shearer et al., 2010). Recently, microarray and next generation sequencing technologies has enabled the identification of molecular cause of many genetic kidney diseases in cost effective and timely manner (Lata et al., 2018).

Next generation sequencing technique has been successful in mutation screening of many renal diseases for example, Alport's syndrome, nephronophthisis and steroid resistant nephrotic syndrome by using the disease specific gene panels relevant to given phenotype at a low cost and turnaround times (Artuso et al., 2012; Koboldt, Steinberg, Larson, Wilson, & Mardis, 2013; McCarthy et al., 2013; Otto et al., 2011). The regions containing the exome of interest may only be captured to reduce the sequencing cost and data interpretation. In this method complementary baits are optimized to capture genes relevant

to renal diseases and are subjected to NGS and subsequent interpretation to identify variants, indels and CNVs (Shearer et al., 2010; Thomas et al., 2017). In addition, whole exome sequencing and the whole genome sequencing further improve the diagnostic efficiency of complex diseases. Massive molecular and genetic data provided by these technologies provide new challenges as the data analyses require bioinformatic methods which need development. The candidate genes and individual mutations need animal models for their characterization. Multilevel omics information created needs to be integrated, therefore, renal phenome database has been created to link the phenotypic features of rare nephropathies with genomic, transcriptomic and proteomics to reach the molecular insights of diseases (Devuyst et al., 2014).

Chapter **2**

MATERIALS AND METHODS

2.1 Recruitment of families and study approval

The current study comprises six Pakistani families with inherited nephropathies and the study protocol was approved from the institutional review board of Quaid-i-Azam University Islamabad, Pakistan. Written informed consent was provided by each family member for being participating in the study. It was impossible for young children being enrolled in the study to give their consent, so their consent was taken from their parents. Detailed family history, consanguinity kinship and renal disease history was obtained from the respective families to construct pedigree and assessing the inheritance pattern of disease. For the collection of blood samples, Becton Dickinson Syringes of 3ml, 5ml, and 10 ml were used. The blood was then transferred to ethylene-diamine-tetraacetic acid (EDTA) vacutainers and the tubes were kept at 4ºC in refrigerator.

2.2 Construction of family pedigrees

In view of the data provided by the family members, pedigrees were constructed manually for each family. Squares in the pedigree represented males and circles represented female members of the family. Filled squares and circles showed the affected status of the individual while normal or carrier individuals were represented by unfilled figures. Single horizontal line joining the two individuals was drawn to indicate the marriage between these individuals while a double line between two individuals was used to show consanguineous marriage. Descent line drawn from the marriage line showed the offspring and the sibs were connected through a horizontal line, joining each sib, drawn at the rear end of descent line. Roman numerals were used to show different generations of one family and Arabic numerals were used to show the members in each generation

2.3 Genomic DNA extraction and assessment of quality and quantity

2.3.1 Genomic DNA extraction

Genomic DNA was extracted using the standard protocol provided by Wizard genomic DNA purification kit (Promega, USA). 300 µl of the blood was taken from EDTA vacutainers and was transferred into 1.5 ml autoclaved Eppendorf. To this, 900 µl of Cell lysis solution was added and kept at incubation at room temperature. After 10

minutes, the tube was centrifuged for one minute at 13000rpm. Supernatant was discarded and 300 µl of nuclei lysis solution was added to the pellet. Pellet was resuspended and dissolved in nuclei lysis solution by vortexing. 100 µl of protein precipitation solution was added to this mixture and was again put on to vortexing for at least 20 seconds. After mixing, the tube was centrifuged at 13000rpm for three minutes and supernatant was carefully poured into a clean sterile Eppendorf. To this tube, add 300 µl chilled isopropanol to precipitate the DNA. The tube was centrifuged at 13000rpm for one minute and the DNA pellet obtained was washed with 70% ethanol twice. Washing was done carefully to preserve the DNA pellet which was then air dried for 15 minutes to aspirate the residual ethanol. The DNA pellet was then rehydrated by adding 100 µl of DNA rehydration solution and was kept at 65ºC for incubation. After one hour of this incubation, DNA was run on agarose gel and stored at 4ºC for further use.

2.3.2 Agarose gel electrophoresis

Extracted DNA was run on 1% agarose gel to see the quality of DNA. 1% agarose gel was made by using DNA grade agarose (cat. # No. 75000-500, Invitrogen) and TBE buffer TBE (0.89 mM Tris-Borate, 0.03 M EDTA; pH 8.3). Weighed amount of 0.5g of agarose was mixed to 50 ml of 1X TBE for preparing 50 ml agarose gel. The mixture was heated in microwave oven for 2 minutes and allowed to cool at room temperature. To the slightly warm mixture of molten agarose and 1X TBE, 5 µl ethidium bromide (10 mg/mL; cat. # No. 15585-001, Invitrogen) was added and mixed. It stains the DNA and DNA can then be visualized under UV. The mixture was poured in a casting tray which was set with combs and allowed to stand for 15-20 minutes at room temperature. After the solidification of agarose gel, extracted DNA mixed with loading dye (0.25% bromophenol blue and 40% sucrose) in equal proportions (1:1) was loaded in the wells on gel. Electrophoresis was done at 110 volts for 20 minutes and the gel was seen under ExtraGene UV transilluminator (UV3CL).

2.3.3 Quantification of genomic DNA

Quantity of DNA was checked through Promega Quantus fluorometer (cat # E6150) using QuantiFlour ONE dsDNA system (cat. # E4871). 199 µl of QuantiFlour ONE dsDNA system dye solution was taken in a tube and added to 1 µl of the DNA sample whose quantity was to be checked and was mixed thoroughly. The mixture was placed

at room temperature in darkness and incubated for 5 minutes. The tube was then placed on calibrated Quantus fluorometer and the concentration was recorded.

2.4 Candidate gene screening

2.4.1 Primer designing

Primers were designed for screening the candidate gene *ATP6V0A4,* deletion analysis of *NPHP1* gene and for segregation study of various shortlisted potential candidate variants obtained from WES data. Reference genomic sequence was downloaded from Ensembl genome browser (http://www.ensembl.org/index.html). Flanking regions (18-23 bp) of each exon and each variant was selected manually. GC content and melting temperatures were calculated by DNA/RNA GC content calculator (http://www.endmemo.com/bio/gc.php) and 4(G+C)+2(A+T) respectively. BLAT/BLAST tool (www.ensembl.org/Multi/Tools/Blast) of Ensembl and insilico PCR tool (genome.ucsc.edu/cgi-bin/hgPcr) of UCSC (University of California, Santa Cruz) were used to check out the rarity of sequence selected and the primers giving one hit were selected.

2.4.2 DNA amplification by PCR

DNA amplification was performed by polymerase chain reactions (PCR). The reaction was performed on thermocycler Multigene Optimax (Labnet International, Inc). A 50 µl reaction was prepared by adding 25 µl master mix (GoTaq 2X greebn mater mix, Promega Inc., USA) to the mixture containing 18 µl double distilled nuclease free water, 3 µl target DNA and 2 µl of forward and reverse primers each prepared in PCR tubes. Concentration of the primers used was 20pmol/ µl. The PCR tubes containing whole reaction mixture were placed in thermocycler set for 35 cycles at the conditions given below:

Initial denaturation temperature= 95ºC for 5 minutes

Final denaturation temperature= 95ºC for 1 minute

Annealing temperature= optimized temperature for each primer for 1 minute

Initial extension temperature= 72ºC for a time depending upon the fragment length (1kb= 1min)

Final extension temperature= 72ºC for 10 minutes.

After amplification, the amplified DNA fragments were checked by running on 2% agarose gel with the concentration of agarose being used was twice as compared to the 1% gel. Amplification of DNA was performed to obtain the enough DNA required for sequencing.

2.4.3 Purification of PCR products

Amplified products were purified before sequencing reaction. Thermo Scientific GeneJET PCR purification kit (cat. # K0702) was used for this purpose. Protocol provided with the kit was followed and binding buffer (available with the kit) was added to PCR product in 1:1 volume and mixed thoroughly. This mixture was poured in to the GeneJET purification columns and placed in a centrifuge at 13000 rpm for 1 minute. Amplified product bound to the membrane of column and the eluent which flowed through it was discarded. Column was placed in a clean collection tube and 700 µl of wash buffer was poured carefully in the column without disturbing its membrane. Centrifugation was done again at 13000 rpm for 1 minute to wash the amplified DNA retained in the column membrane and flow through was discarded again. The empty column was recentrifuged at 13000 rpm for 2-3 minutes to completely wash out the wash buffer. Column was placed on to 1.5 ml eppendorf and allowed to stand for 15 minutes to aspirate wash buffer. After this, 20 µl of DNA elution buffer was poured in to the GeneJET column and centrifuge step was performed at 13000 rpm for 1 minute. Amplified DNA was eluted from the column membrane and collected in the 1.5 ml eppendorf below it. To confirm the purified DNA, 2% agarose gel was made, and electrophoresis was performed. Quantity of the DNA was checked using QuantiFlour ONE dsDNA system discussed in the section 2.3.3.

2.4.4 DNA sequencing

DNA sequencing was performed following the purification step. Big Dye terminator cycle sequencing kit V3.1 (PE Applied Biosystems, Foster City, CA, USA) was used to prepare sequencing reactions. 10 µl reaction mixture was prepared using 1.5 µl reaction mix, 1.5 µl of 5X sequencing buffer (PE Applied Biosystems, Foster City, CA, USA), 1 µl DNA, 1 µl of each of forward and reverse primers and 5.5 µl PCR water for

sequencing. Reaction mixture was placed in the thermocycler set for 30 cycles at following conditions:

Initial denaturation temperature= 95ºC for 5 minutes

Final denaturation temperature= 95 ºC for 30 seconds

Annealing temperature= 50-55 ºC for 10 seconds } 30 cycles

Initial extension temperature= 60ºC for 4 minutes

Final extension temperature= 60ºC for 10 minutes.

After the completion of sequencing reaction, 100% chilled ethanol was added, and the reaction was placed at incubation for 15 minutes at room temperature. This step precipitates the extension products. Sequencing reaction was then subjected to centrifugation at 13000 rpm for 22 minutes. Precipitated extension products were separated out in the form of pellets at the bottom of the tube and supernatant was discarded. 250 µl of 70% ethanol was used for washing purpose and added to the pellets. Centrifugation followed this step and supernatant containing ethanol was discarded. Pellets were dried in incubator at 37 ºC. 20 µl of HDF (Hi-Di formamide) (PE Applied Biosystems, Foster City, CA, USA) was added to the dried pellets and pellets were re-suspended. The samples were injected into Applied Biosystems 3730XL Automated DNA analyzer (Applied Biosystems, Foster City, CA, USA) and the sequencing data was obtained in the form of chromatograms.

2.4.5 Mutations analysis

BioEdit sequence alignment tool (Version 7.0.5.3) was used to align the sequencing data obtained above with the reference genome. Reference sequence was downloaded from two Ensembl and NCBI (National Centre for Bioinformatics) genome browser (https://www.ncbi.nlm.nih.gov/). This alignment allowed to check any variation in the DNA sequence by comparing it with reference sequence. Potential variations whenever found were checked in Ensembl, HGMD (Human Genome Mutation Database) (http://www.hgmd.cf.ac.uk/ac/index.php) and ExAC Exome Aggregation Consortium (http://exac.broadinstitute.org/) databases. Minor allele frequencies (MAF) of the variations were found out through ExAC and 1000 GP data provided in Ensembl. Mutations reported earlier with disease phenotype and new mutations found were

subjected to *in silico* analysis by MutationTaster, SIFT, PolyPhen or PredictSNP2 to predict their effect on protein structure. Effect of splice site mutations were predicted by HSF, CRYP-SKIP and NNSplice and the scores were calculated.

2.5 Whole exome sequencing and Quality control

Whole Exome Sequencing (WES) was performed in the probands of family A, C, D, E and F. Prior to DNA library preparation for WES, this DNA was analyzed for quality and quantity. Quantification of DNA (discussed in section 2.3.3) was done again to ensure the high quantity of DNA in proband samples. Gel electrophoresis was used to assess the quality of DNA. The sharp intact DNA bands without smear were considered to pass the QC. Extracted DNA passed the Quality Control and was employed in construction of DNA libraries. Libraries were enriched and sequenced using Illumina platform (Illumina HiSeq4000). Sequencing procedure used is as follows:

2.5.1 Library preparation

SureSelect V4 kit (Agilent Technologies, Santa Clara, CA, USA) was used to prepare DNA library for WES. Steps involved during library preparation were as follows:

2.5.2 DNA shearing

DNA shearing was performed using Covaris E-220 sonicator (Adaptive Focused Acoustics™) which produced 150-200bp DNA fragments. The optimized procedure used was as follows: 3 µg of purified DNA was taken in 1.5 ml Eppendorf tube and filled with 1X Low TE Buffer to dilute the DNA upto the 120 µl volume. Covaris E-220 sonicator was adjusted and set at 200 cycles/burst for 430 seconds. The DNA diluted with the buffer was transferred to microtube strip and placed in the sonicator and run with pre-set conditions mentioned above. Ultrasonication sheared the DNA. 2% agarose gel was made, and the sheared DNA was run to verify DNA fragmentation.

2.5.3 Amplicons purification

The 120 µl sheared DNA was mixed with homogenized Agencourt AMPure XP reagent (Beckman Coulter Life Sciences Brea, California, United States). Mixture was vortexed and placed in incubator at 25˚C for 5 minutes. Afterwards, the mixture was transferred on magnetic stand and allowed to stand 1-2 minutes. DNA bounded to magnetic beads

were separated from clear supernatant which was discarded. Magnetic beads bounded DNA was washed with 200 µl of 70% ethanol twice followed by air drying. After being dried up, beads were mixed with 50 µl of nuclease free water to extract the DNA from magnetic beads. One minute later, this solution containing tubes were placed on magnetic stand again to allow the separation of beads and rehydrated DNA. Supernatant containing DNA was pipetted out in clean Eppendorf.

2.5.4 Ends repair

PCR amplification of the DNA purified with Agencourt AMPure XP reagent (as discussed in section 2.4.3) was performed using the protocol and reagents provided with the SureSelect V4 kit. A reaction mixture containing 50 µl of the purified DNA fragments, 10X end-repair buffer (10 µl), mixture of dNTPs (1.6 µl), enzyme mix (5.2 µl) and nuclease-free PCR water (94.8 µl) was prepared and run in a thermal cycler at 20˚C for half hour. This procedure repaired the DNA ends and was subjected to purification through the protocol discussed in section 2.4.3.

2.5.5 Adaptor ligation

Adaptor (universal primers) ligation requires the end-repaired DNA to be adenylated at its 3'end. For this purpose, the end-repaired purified DNA was mixed with 3 µl of 10X Klenow polymerase buffer [Exo (-) Klenow] and 46 µl of nuclease-free PCR water. The mixture was incubated for half hour at 37 ˚C. The adenylated DNA thus formed was purified again using Agencourt AMPure XP reagent as mentioned in section 2.4.3. For adaptor ligation, 10 µl of SureSelect adaptor oligo mix provided with SureSelect V4 kit was added to this adenylated DNA (28.5 µl) along with 10 µl of 5X T4 DNA ligase buffer and 38.5 µl of PCR water and the whole solution was kept at 20˚C for 15 minutes. This resulted in an adaptor-ligated DNA library which was purified again as mentioned above (section 2.4.3).

2.5.6 PCR amplification of adaptor-ligated DNA library

Adaptor-ligated DNA library was subjected to PCR amplification. 15 µl of library solution was mixed with following reagents along with the quantities mentioned according to the manufacture's guidelines:

SureSelect primers = 1.25 µl

SureSelect ILM indexing pre-capture PCR reverse primer = 1.25 µl

5X Herculase-II reaction buffer = 10 µl

Herculase-II fusion DNA polymerase =1 µl

100mM dNTPs mix = 0.5 µl

Nuclease-free PCR water = 21 µl

DNA library was amplified in a thermal cycler pre-set at the given conditions:

Initial denaturation temperature= 98ºC for 2 minutes

Final denaturation temperature= 98ºC for 30 seconds

Annealing temperature= 65ºC for 30 seconds } 6 cycles

Initial extension temperature= 72ºC for 1 minute

Final extension temperature= 72ºC for 10 minutes.

Quality of amplified DNA was checked by using DNA 1000 kit (5067-1504) and analyzing it on 2100 Bioanalyzer (Agilent) according to manufacturer's protocol.

2.5.7 Hybridization

The samples containing amplified DNA were now converted into lyophilized form and were rehydrated afterwards by suspending them in 3.4 µl of nuclease-free PCR water. Rows of thermal cycler were marked with numbers 1,2 and 3 and three mixtures (block mix, hybridization buffer and capture library mix) were prepared according to the guidelines provided by manufacturer. To the second row (#2), DNA samples mixed with 5.6 µl of block mix were placed and set at incubation for 5 minutes at denaturation temperature (95˚C). The temperature was reduced to 65˚C after 5 minutes. 40 µl of hybridization buffer was loaded in the first row (#1) and incubated at 65˚C for 5 minutes. 7 µl of Capture library mix was loaded in the third row (#3) and incubated at 65 ˚C for 2 minutes. Afterwards, when incubation times were completed, the mixtures in row 1 and 2 were transferred in row 3.

2.5.8 Hybridized DNA capture

Hybridized DNA library was then captured on magnetic beads (Dynabeads MyOne streptavidin T1, Life Technologies 65602). Before use, beads were washed thrice with wash buffer and binding buffer. These beads were mixed with the hybridization buffer in first row of the thermal cycler mentioned in previous section. Thorough mixing was done by pipetting and the mixture was incubated at 65˚C for half hour. Magnetic beads were separated on magnetic stand and supernatant was discarded. Resuspended with 500 µl of wash-1 buffer, the beads were placed at incubation for 15 minutes. Washing was done with wash-1 buffer twice. After this, tubes were vortexed for 5 seconds and placed at 65 ˚C for 10 minutes. Samples were then washed with 500 µl of wash-2 buffer thrice and placed on magnetic stand to separate magnetic beads from wash-2 buffer. 50 µl of elution buffer was added to these beads and kept at room temperature for 10 minutes after vortexing for 5 seconds. Centrifugation of the beads followed by separation on magnetic stand produced supernatant containing DNA which was transferred to 1.5 ml Eppendorf. The Eppendorf was supplemented with 50 µl of neutralization buffer and both solutions were thoroughly mixed through pipetting. The samples were again subjected to purification using the protocol discussed in section 2.4.3 and eluted finally with 30 µl of nuclease free PCR water.

2.5.9 Final amplification

Each hybridized DNA library prepared in the previous step was supplemented with indexes through PCR amplification. The protocol required the addition of following reagents to 14 µlof captured DNA library:

5X Herculase II reaction buffer = 10 µl

Herculase II fusion DNA polymerase = 1 µl

PCR primer (Index 1 to index 16) = 1 µl

SureSelect ILM indexing forward PCR primer = 1 µl

100 mM dNTPs mix = 0.5 µl

PCR water = 22.5 µl

Each captured library was amplified in a thermal cycler pre-set at the given conditions:

Initial denaturation temperature= 98ºC for 2 minutes

Final denaturation temperature= 98ºC for 30 seconds
Annealing temperature= 65ºC for 30 seconds
Initial extension temperature= 72ºC for 1 minute
} 6 cycles

Final extension temperature= 72ºC for 10 minutes.

Amplicons were subjected to purification using AMPure XP reagent (90 µl) and eluted with 30 µl of elution buffer.

2.5.10 Pooling of libraries and multiplex sequencing

1 µl of amplified DNA was analyzed through 2100 Bioanalyzer. Libraries were pooled based on the molar concentrations provided by Bioanalyzer. Pooled libraries were sequenced through Illumina HiSeq4000 (Illumina, San Diego, California, USA). For multiplex sequencing, cluster generation was performed as a first step. Single clusters on the flow cell were generated using the guidelines provided by the manufacturers of HiSeq cluster kit V4 (cat. # PE-401-4001). Hybridization buffer (HT1) was added to DNA fragments and kept at 96 ˚C for denaturation. Washing buffer (HT2) was added following denaturation. Both the buffers were provided with the kit. To this mixture, Amp premix (AMP1) was added for template extension. Mixture was kept at 20 ˚C and was supplemented with HT2 after 90 seconds. Bridge amplification of the hybridized DNA was performed as follows:

Denaturation by adding formamide (AT1)
Annealing by adding AMP1
Extension by adding AMX1
} 35 cycles

Finally, after the completion of 35th cycle, HT2 and HT1 were added for washing and hybridization respectively.

Next step was to amplify, linearized and block the clusters generated with the help of guidelines provided by manufacturer of HiSeq SBS kit V4 (cat. # FC-401-4002). Amplification was done using AMP Manifold and HT1 buffer, whereas LMX1 mix was used to linearize the amplicons. Incubation was done afterwards at 38 ˚C for half hour. HT2 buffer was added again at this stage. Blocking reagent BMX1 was added and

placed for incubation followed by washing with HT1 and HT2. DNA strands were denatured by 0.1 N NaOH and sequencing primers were hybridized. Washing with HT1 and HT2 buffers was performed. Thereafter, sequencing of first read was obtained. Blocked sites were deprotected after sequencing and second strand was synthesized for sequencing using linearization, blocking and hybridization. Repeated many times, this process created approximately 25 Gb reads with an average size of 101 bp.

2.5.11 Bioinformatics analysis of the sequencing reads

Bioinformatic analysis was used to convert the enormous number of raw sequencing reads into readable form. FastQC was used to filter the raw sequencing reads which were then mapped to reference genome (UCSC assemble hg19/Grch38) using BWA tool (version: bwa-0.7.10). The properly paired reads that were uniquely mapped were filtered out using Picard tools (version: picard-tools-1.118) (http://broadinstitute.github.io/picard/). Variant calling (SNPs and INDELS) was performed by GATK (GATK 3.v4). Variants that passed the quality filters were processed and annotated with snpEff (snpEff_v4.1)

2.5.12 Variant filtering

Filtering criteria mentioned above produced an average of eighty thousand variants in probands of the families A, C, D, E and F respectively. At first, Intronic (except splice site) and synonymous variants which do not affect the protein structure were excluded. In the next step, the variants were screened for recurrent and new mutations in the previously reported genes with the phenotype. If no such mutation was found, variants were filtered to select only those with unknown minor allele frequency (MAF) or MAF< 0.01 from Ensembl genome browser, ExAC database, and 1000Genomes (http://www.internationalgenome.org/). Afterwards, input file was filtered to include the variants found to follow the autosomal recessive mode of inheritance. Next criteria used were to annotate the selected variants for predicted effect of mutation on protein structure. Effects were predicted using PolyPhen (genetics.bwh.harvard.edu/pph2), SIFT (sift.jcvi.org/), PredictSNP2 (https://loschmidt.chemi.muni.cz/predictsnp2/) and MutationTaster (www.mutationtaster.org/). Expression in relevant tissue was also an additional step used at this stage for variants filtering. Variants predicted to have low confidence score were excluded for further analysis. Rare variants predicted to be damaging with higher expression in relevant tissue were proceeded further for

segregation study. Segregation study of selected list of variants for each proband was performed.

2.6 Segregation Analysis

Variants identified in *ATP6V0A4, ATP6V1B1, C2CD3, AGXT, AQP12B, FOXD1, CANT1, NPHP4, ANKS6, TUB, FOXQ1, PCNT, NEK1, ZNF154, NAF1, ABCG5, MYOM3, HLA-DQB1, RAET1L* and *KCTD19* were checked using Sanger sequencing in all the available family members of respective family. Primers were designed manually using the approach discussed in section 2.4.1.

2.7 *In Silico* analysis

Variants identified from WES analysis were subjected to web-based bioinformatics analyses to predict their pathogenicity. To predict the splice site variants, Mutation Taster (http://www.mutationtaster.org/cgibin/MutationTaster/MutationTaster69.cgi), Human Splicing Finder (http://www.umd.be/HSF3/HSF.shtml), NNSplice (http://www.fruitfly.org/seq_tools/splice.html),NetGene2 (http://www.cbs.dtu.dk/services/NetGene2/) and CRYP-SKIP (http://cryp-skip.img.cas.cz/) were used. Missense variants were evaluated for their pathogenicity using Mutation Taster, Polyphen (http://genetics.bwh.harvard.edu/pph/), SIFT (https://sift.bii.a-star.edu.sg/) and PredictSNP2 (https://loschmidt.chemi.muni.cz/predictsnp2/). STRING (https://string-db.org/) was used to see the interaction between different proteins.

Chapter **3**

DISTAL RENAL TUBULAR ACIDOSIS

3.1 Introduction

Kidneys play an important role in regulation of acid-base homeostasis. This acid-base balance is basically performed in the kidney tubules mainly the proximal tubules and collecting duct system (Enerbäck et al., 2018).Three major ways are employed by these tubules to maintain and regulate the acid-base balance:1. Bicarbonate reabsorption and filtration by proximal tubule, loop of Henle and distal tubule 2. Proton secretion by intercalated cells of collecting duct system, 3. Bicarbonate synthesis to compensate the dissipated bicarbonate in metabolic reactions (Mohebbi et al.,2018). The reabsorption of bicarbonate in kidney is coupled with another biochemical reaction of acid synthesis and secretion mainly in the form of ammonium Sulphate and dihydrogen phosphate. Multiple specific transporter systems present in the collecting tubules of nephrons are involved in this coupling biochemical process (Escobar, Mejía, Gil, & Santos, 2013). The transporters present on alpha intercalated cells (AICs) perform proton secretion while type B intercalated cells are involved in exudation of bicarbonate (Enerbäck et al., 2018). Impaired proteins of transporter systems, defective enzymes located in the acid intercalated cells or malformed kidneys lead to the disturbances in normal renal acidification process results in a group of disorders called renal tubular acidosis. The term RTA was first formulated by Mudge and Pines in 1951 and then endorsed by Elikinton in 1960 (Batlle & Haque, 2012). When excretion of acid charge (Protons and Ammonium) is defected in the intercalated cells of collecting tubule, acid load is accumulated in the distal convoluted tubules which results in the bicarbonate consumption leading to decreased HCO_3 buffer in blood. This condition results in the symptoms of disease known as Distal renal tubular acidosis. Distal RTA is also termed as Classic RTA or Type 1 RTA based on order of discovery The characteristic feature of classic dRTA is the diminished ability of tubules to acidify urine despite the metabolic acidosis and reduced bicarbonate excretion (Roy, Al-bataineh, & Pastor-Soler, 2015).

3.2 Molecular pathophysiology of distal renal tubular acidosis

Humans generate 1 to 1.5 mmol of hydrogen /kg of their body weight daily which may result in urinary acidification resulting in urine pH as low as 4. This Acid secretion is

vital to the acid-base homeostasis, one of the key role played by kidneys. Collecting duct system in the nephron are designated to perform acid secretion coupled with the reabsorption of filtered bicarbonate (app. 10%) (Gong et al., 2010). Epithelial cells of collecting duct system are the principle and intercalated cells that forms a 'salt and pepper' epithelium. Intercalated cells have been classified into three categories A-type (alpha intercalated cells), B-type (beta intercalated cells) and non-A, non-B intercalated cells based on their morphology. Additionally, intercalated cells classification has also been modified based on the presence or absence of chloride-bicarbonate anion exchanger (AE1), pendrin protein and localization of H+-ATPase on the apical cell membrane. A-ICs are defined as having lack of pendrin expression, localization of H+-ATPase at apical membrane and AE1 expression at basolateral membrane. On the other hand, B-ICs express pendrin and AE1 exchanger at their apical membrane and H+-ATPase at their basolateral membrane. Non-A, non-B intercalated cells have expression of H+-ATPase and pendrin at their apical membranes while AE1 at their basolateral membrane. Carbonic anhydrase is expressed by all the three categories of intercalated cells in their cytoplasm(Xu et al., 2011).

3.2.1 Major transport proteins of type A intercalated cells and their function

Urinary acidification is performed by entire collecting duct but the type A intercalated cells (A-ICs) in its outer medullary part are most important for this function. These A-ICs express H^+-ATPase and SLC4A1 at their apical and basolateral membranes respectively. H^+-ATPase pump secretes H^+ into the lumen of tubules resulting in the formation of bicarbonate within the cells by the action of carbonic anhydrase II. The bicarbonate is then reabsorbed in the tubulointerstitial regions and in exchange chlorides are absorbed in the cells via anion exchanger AE1. Metabolic acidosis results in the upregulation of H^+-ATPase and AE1 in the kidney. In addition, H^+/K^+-ATPase, at apical membrane of A-ICs, can secrete H^+ into the urine in exchange for each potassium ion (Roy et al., 2015).

Transport proteins of the A-ICs are activated via changes in pH or bicarbonate levels. pH sensing pathways have been studied in A-ICs which regulate the activities of these transport proteins. For example, protein kinase A (PKA) activates the H^+-ATPase while AMP activated kinase (AMPK) inhibits it. Soluble adenylyl cyclase is a bicarbonate sensor and it is involved in regulation of proton secretion in A-ICs of collecting

duct.9Another important regulator, electrogenic Cl^- transporter, SLC26A11, colocalized with H^+-ATPase, has recently been identified as stimulant to the function of H^+-ATPase in type A intercalated (Xu et al., 2011).

3.2.2 Major transport proteins of type B intercalated cells and their function

SLC26A4 PDS encodes pendrin which is expressed on apical membrane of B type intercalated cells (B-ICs). It is an important chloride-bicarbonate exchanger. On the basolateral membrane, B-ICs express H^+-ATPase and anion exchanger 4 (SLC4A9). Na^+ driven chloride/bicarbonate exchanger colocalizes with the pendrin in B-ICs and bring about the NaCl reabsorption in the collecting ducts. Metabolic acidosis results in many changes in B-ICs transport proteins (Roy et al., 2015). For example, diminished expression of pendrin at apical and AE4 at basolateral membranes of B-ICs (Wagner et al., 2004).Transport proteins or associated enzymes of the intercalated cells are encoded by respective genes and the changes at DNA level of these transport proteins may lead to disfunctioning of their normal regulated activities. This may result into distal renal tubular acidosis, a disease in which the ability to acidify urine to a normal pH is reduced along with other conditions i-e, hypokalemia, hyperchloremia and metabolic acidosis. The patient fails to excrete his/her daily proton load, consequently accumulate this proton load resulting in metabolic acidosis with normal anion gap and bicarbonatemia (Escobar et al., 2013).

3.2.3 Mechanism of urinary acidification

The filtered bicarbonate HCO_3^- from glomerulus is reabsorbed in the lumen of proximal tubules of nephron. Protons present in the tubular lumen combine with HCO_3^- to form H_2CO_3. Carbonic anhydrase IV catalyzed reaction then takes place in the luminal membrane of the proximal tubules which converts H_2CO_3 into CO_2 and H_2O, both molecules quickly diffused into the tubular cells and combine again resulting into the intracellular production of H^+ and HCO_3^- by another enzyme called carbonic anhydrase II. Na+/H+ exchanger (NHE3) secretes these H^+ into the tubule lumen and Na^+/HCO_3^- cotransporter (NBC1) located on the basolateral membrane of cell, transport HCO_3^- with Na^+ ions into the blood (Laing, Toye, Capasso, & Unwin, 2005). The net acid secretion in proximal tubules is less because most of the H^+ is utilized in reclamation of HCO_3^- and the remaining will be buffered by phosphate as titratable acid. Glutamine taken up from blood in the proximal tubules undergoes deamination and

gluconeogenesis results in the production of NH_4^+ and HCO_3^-. Ammonium generated is then excreted into the tubular lumen and bicarbonate is reclaimed via basolateral membrane (Laing et al., 2005; Pereira, Miranda, Oliveira, & Simões e Silva, 2009). Proton secretion into the urine is mainly performed by the H^+-ATPases in the luminal membrane of A-ICs. These hydrogen pumps and H+/K+-ATPase secrete protons into the lumen of distal tubule and collecting ducts. Function of H^+-ATPases is coupled with bicarbonate exit into interstitial fluid and hence into the blood by AE1 exchanger located on basolateral surface. Disfunctioning of any of the transporters involved in overall process of urinary acidification can be attributed to the cause of dRTA (Batlle & Haque, 2012).

3.3 Classification of distal renal tubular acidosis

Distal renal tubular acidosis can be studied by classifying it into following four types based on the defective genes associated with the disease (Table 3.1).

(1) *ATP6V0A4* associated dRTA
(2) *ATP6V1B1* associated dRTA
(3) *SLC4A1* associated dRTA
(4) *FOXI1* associated dRTA

3.3.1 *ATP6V0A4* associated dRTA

ATP6V0A4 gene is located on chromosome 7 and encodes 840 amino acids containing a4 subunit belonging to V0 domain of large complex V-ATPase. V-ATPases are the proton pumps having a cytoplasmic V1 domain and a transmembrane V0 domain. The V0 domain is composed of six different subunits (a, c, c", d, e, Ac45) among which subunit a is reported to be involved in pathogenesis of various human diseases. The subunit a has four isoforms (a1-a4) among which a4 subunit is expressed in all types of kidney intercalated cells, proximal tubules, thick ascending loop of Henle and in some parts of inner ear (Stehberger et al., 2003; Wagner et al., 2004). The a4 isoform of subunit a is involved in the assembly and functioning of V-ATPase pump (Borthwick & Karet, 2002). Mutations in a4 encoded by *ATP6V0A4* gene results in autosomal recessive dRTA with or without sensorineural hearing loss (Pereira et al., 2009).

3.3.2 *ATP6V1B1* associated dRTA

ATP6V1B1 gene is located on q arm of chromosome 2 and encodes the 513 amino acids containing B1 subunit of membrane bound V1 domain of vacuolar ATPase. The V1 domain is composed of eight (A-H) subunits which are involved in proton translocation across the membrane and hydrolysis of ATP. Subunit B has two isoforms; B1 and B2, isoform B1 is expressed in apical membranes of kidney A-ICs, male genital tract, ciliary segment of the eye, endolymphatic sac and cochlea in the inner ear (Karet, 2002). Screening of this gene for mutations revealed recessive and compound heterozygous mutations which disrupt the structure or abolish the production of B1 isoform leading to dRTA and sensorineural hearing loss(Pereira et al., 2009; Yenchitsomanus, Kittanakom, Rungroj, Cordat, & Reithmeier, 2005) .

3.3.3 *SLC4A1* associated dRTA

SLC4A1 gene is located on chromosome 17q and encodes an 846-amino acid protein called kidney Anion exchanger 1 (kAE1) which is expressed on basolateral surface of A-ICs in distal parts of nephron. An isoform of this protein named as erythrocyte Anion exchanger 1 (eAE1) is expressed in red blood cells which is also encoded by *SLC4A1* gene using a separate promoter. Unlike kAE1, eAE1 is involved in interacting with cytoskeletal proteins such as stomatin and ankyrin (Enerbäck et al., 2018; Karet, 2002; Mohebbi & Wagner, 2018). kAE1 is a chloride-bicarbonate exchanger and is involved in the exchange of intracellular bicarbonate ions generated during urinary acidification for the extracellular chloride ions. The bicarbonate ions are then reabsorbed into the kidney interstitium (Batlle & Haque, 2012). This is the key step in maintenance of acid-base balance and reflects how its disfunctioning may lead to impaired urinary acidification. Mutations in *SLC4A1* gene results in inherited forms of dRTA or red blood cells abnormalities or rarely both (Yenchitsomanus et al., 2005). Most common recessive mutation G170D is mostly associated with both dRTA and hemolytic anemia. *SLC4A1* associated dRTA is inherited either in autosomal dominant or autosomal recessive manner (Mohebbi & Wagner, 2018).

3.3.4 *FOXI1* associated dRTA

The genetic causes of about one third of known cases of dRTA have been unknown suggesting that some other genes encoding membrane transport proteins or the genes

encoding their regulatory DNA binding proteins might be involved in the pathogenesis of the disease. Recently, Enerback et al described *FOXI1* gene as a cause of autosomal recessive dRTA and deafness in two unrelated consanguineous UAE families. *FOXI1* is located on chromosome 5 and encodes a transcription factor named forkhead box I 1 which binds with the cis elements of genes (AE1, AE4, V-ATPase subunits B1, a4, E2, A) associated with dRTA thus involved in regulating these genes. Mutations in *FOXI1* gene results in loss of functional FOXI1 protein which fails to bind the target genes leading to impaired functioning in the respective tissues with altered pH of the endolymphatic fluid in the inner ear and inability of kidney tubules to produce the required acid in urine. Therefore, distal renal tubular acidosis with sensorineural hearing loss results due to the inactive membrane transport proteins because of recessive mutations in *FOXI1* (Enerbäck et al., 2018).

Table 3. 1: Classification of inherited dRTA (Fry & Karet, 2007):

Type of dRTA	**Genes associated**	**Inheritance pattern**	**Protein affected**	**Clinical features**
Type 1 dRTA (classic dRTA)	*SLC4A1* associated dRTA (1a)	Dominant	AE1 exchanger	Mild/compensated metabolic acidosis Hypokalemia (variable) Hypercalciuria Hypocitraturia Nephrolithiasis Nephrocalcinosis Metabolic bone disease, Secondary erythrocytosis
	SLC4A1 associated dRTA	Recessive	AE1 exchanger	Metabolic acidosis Hemolytic anemia
	ATP6V1B1 associated dRTA (Type 1b)	Recessive	B1 subunit of V-ATPase	High urinary pH, Metabolic acidosis, nephrocalcinosis Vomiting, FTT, Delayed growth,

				hypokalemia, hyperchloremia, hypercalciuria, Rickets, Early onset of Bilateral sensorineural hearing loss
	ATP6V0A4 associated dRTA (Type 1c)	Recessive	V-ATPase subunit a4	Same symptoms as above except that the onset of Bilateral SNHL is usually delayed.
	FOXI1 associated dRTA	Recessive	Forkhead box I 1	Hypokalemia, Hyperchloremic metabolic acidosis, FTT, high urine pH bilateral nephrocalcinosis, rickets, early onset SNHL.

FTT=failure to thrive, SNHL=sensorineural hearing loss

3.4 Diagnosis of distal renal tubular acidosis

Diagnosis of primary distal renal tubular acidosis is based on family history, clinical symptoms including failure to thrive, polyuria, diarrhea or dehydration and laboratory findings which shows inappropriately high pH of urine despite metabolic acidosis with normal anion gap and normal glomerular filtration rate, hyperchloremia, hypokalemia or normokalemia and bicarbonatemia. Presentation of dRTA Type 1b and Type 1c usually occurs during the first year of life while dRTA Type 1a presents milder symptoms at adolescence (Mohebbi & Wagner, 2018). Specialized basal and functional tests are used to approach the correct and timely diagnosis of dRTA. These include serum anion gap ((Na) - [(HCO3 + Cl)]) and urinary anion gap ((Urine Na^+ + Urine K^+) – Urine Cl^-) for evaluation of hyperchloremic metabolic acidosis, ammonium chloride loading test or furosemide with fludrocortisone test for defects in urinary acidification (Santos, Ordóñez, Claramunt-Taberner, & Gil-Peña, 2015). Further ultrasonography examinations revealing nephrocalcinosis and or nephrolithiasis prove helpful in correct

diagnosis. Genetic testing can be used to confirm the diagnosis. Extrarenal manifestations may include SNHL, bone diseases and hemolytic anemia depending upon the underlying genetic changes (Santos, Gil-Peña, & Alvarez-Alvarez, 2017; Zhang et al., 2015).

3.5 Management of distal renal tubular acidosis

Fortunately, clinical outcome of the dRTA is excellent if correct diagnosis is made early. Alkali therapy remains the mainstay of managing the disease symptoms including vomiting, metabolic acidosis, failure to thrive and growth retardation. Potassium citrate and sodium citrate are administered orally as alkali formulations. Potassium supplements are preferred in cases where patients present with hypokalemic metabolic acidosis. Dosage requirements vary in adults who require low doses of alkali in contrast to higher doses which may be required for growing children and infants (Mohebbi & Wagner, 2018). In classic dRTA patients and children also have calcium oxalate and calcium phosphate which may get saturated in the urinary tract causing the chances of nephrolithiasis to be high. Therefore, citrate salts help to treat hypocitraturia and prevent the likelihood of nephrolithiasis in these patients. Patients with inherited dRTA requires this alkali therapy throughout their life and the prognosis remains good if correct administration of alkali is continued. Unfortunately, hearing impairments associated with this disease cannot be corrected by alkali treatment and hence the patients having severe unilateral or bilateral sensorineural hearing loss or conductive deafness needs hearing devices and language teachings to ensure their social and intellectual development (Batlle & Haque, 2012).

3.6 Objectives of the study of dRTA families

The study of dRTA was conducted to fulfill the following objectives:

(1) To find out the genetic basis of inherited distal renal tubular acidosis in families presented with the disorder recruited from Pakistani population.

(2) To determine the potential pathogenicity of the identified mutation on the corresponding protein products.

RESULTS AND DISCUSSION

3.7 dRTA families enrolled in the study

Protocol to conduct the current study was approved from the Institutional Review Board of Quaid-i-Azam University Islamabad, Pakistan. Four affected children belonging to three unrelated families were enrolled in this study. Affected families were referred to Department of Nephrology, The children's Hospital and Institute of Child Health Lahore for the evaluation of vomiting, polyuria and dehydration. Clinical and Biochemical investigations suspected the diagnosis of distal renal tubular acidosis. BD syringes were used for blood sample collection and immediately transferred to ethylene-diamine-tetraacetic acid (EDTA) vacutainers. EDTA tubes containing blood were later stored at 4^{o}C until further processing for DNA extraction. Peripheral blood samples were collected from the patients and family members after written informed consent. The patients belonged to Southern Punjab and were born to the consanguineous parents with significant family history of renal disease.

3.7.1 Construction of family pedigrees

Pedigrees were drawn immediately during blood sample collection provided by the information provided by the family members.

3.8 Family A (Lab ID: dRTA 17)

Family A was recruited from Lahore, Pakistan. Diagnosis of dRTA was confirmed based on the initial presenting symptoms and laboratory tests in the local Government hospital, Lahore and family history established the autosomal recessive dRTA. Pedigree construction (Figure 3.1) was done based on the information provided by the parents of proband (III-4). One of his brothers (III-2) and two paternal cousins (III-6 and III-7) were affected with similar symptoms as the proband and were died at the ages of 12, 11 and 16 months respectively.

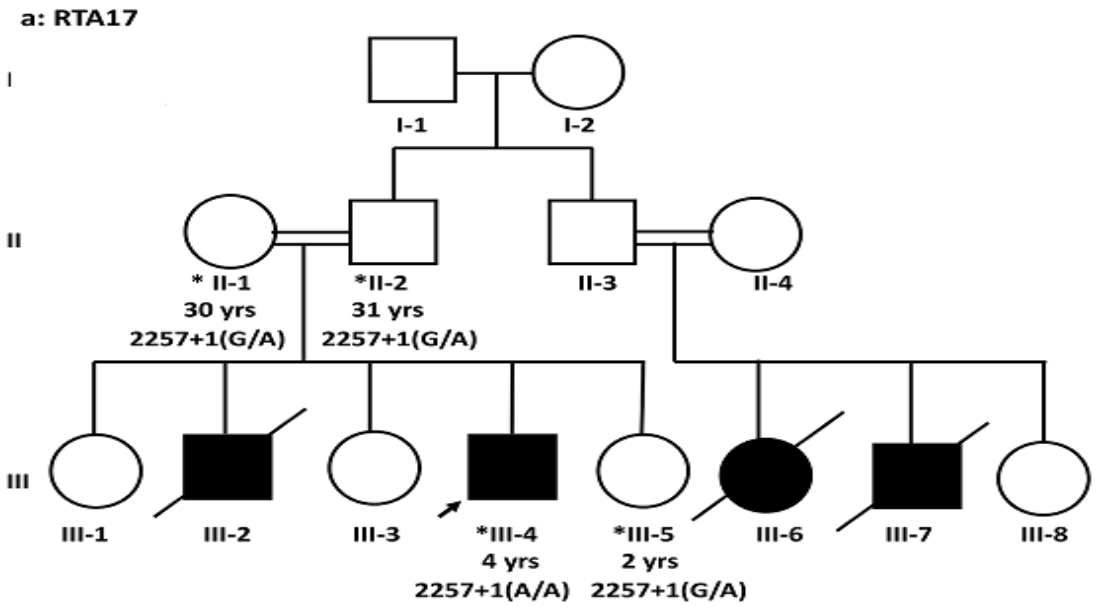

Figure 3.1 Pedigree of family A. Male and female members of the family are represented by squares and circles respectively.

3.8.1 Clinical and biochemical features

Laboratory findings of the proband are listed in Table 3.2. The proband III-4 showed hypokalemia (Normal range=3.7-5.0mmol/l) hyperchloremia, (Normal range =99-107 mmol/l). The patient had severe metabolic acidosis and a normal anion gap with bicarbonatemia mmol/l. Disease management was being done by alkali therapy and potassium citrate for acidosis and hypokalemia and the follow up of family showed improved electrolyte balance.

Table 3.2: Laboratory findings of family A; patient III-4

Sr.No.	Serum Biochemistry (Normal values)	Results
1	Sodium (135-145mmol/l)	131
2	Potassium (3.4-4.7mmol/l)	2.4
3	Phosphate (2.7-5.4mg/dL)	3.5
4	Chloride (98-106mmol/l)	111
5	Bicarbonate (22-28mmol/l)	12
6	Alkaline phosphatase (50-100U/L)	300
7	Urea (7-20mg/dL)	31
8	Urine pH	6.5
9	Creatinine (0.7-1.3mg/dL)	0.7
10	Nephrocalcinosis	Present bilaterally

3.9 Molecular genetic analysis

Molecular study of the patient III-4 was performed using whole exome sequencing.

3.9.1 Whole exome sequencing data analysis

WES of the patient III-4 presented total of 64,531,56 reads with an average length of 102bp. These reads were mapped to the reference human genomic sequence (UCSC hg 19) employing Burrows-Wheeler algorithm. Subsequent variant identification then left us with 83,914 variants in a single patient.

Following step-wise criteria was set to reduce the large number of variants and to reach the pathogenic variant: Analysis of the whole exome sequencing data of the patient III-4 (family A) revealed 83,914 variants. These included 10,430 missense, nonsense, splice donor/splice acceptor site, indels and frameshift variants. These variants were further sorted based on autosomal recessive inheritance pattern within the families (homozygous or compound heterozygous), MAF<0.01 in 1000 Genomes Project and ExAC databases (106 variants) and in silico prediction of the effect on protein function

(22 variants). Finally, these remaining variants were checked in in-house exome data to exclude the common variants in local population. Eight of these 22 variants were ruled out and remaining 14 variants were prioritized according to their biological functions and associated phenotypes with reference to OMIM, HGMD and NCBI databases. Three variants were identified as principal candidates: a homozygous splice donor site variant c.2257+1G>A in *ATP6V0A4;* a homozygous missense variant c.6236C>T in *C2CD3*; and a heterozygous missense variant c.1394G>A in *ATP6V1B1* (Table 3.3). Owing to the recessive mode of inheritance of dRTA being observed in the family, we stick to the homozygous mutation and performed the segregation study for the mutation in all the available members of family.

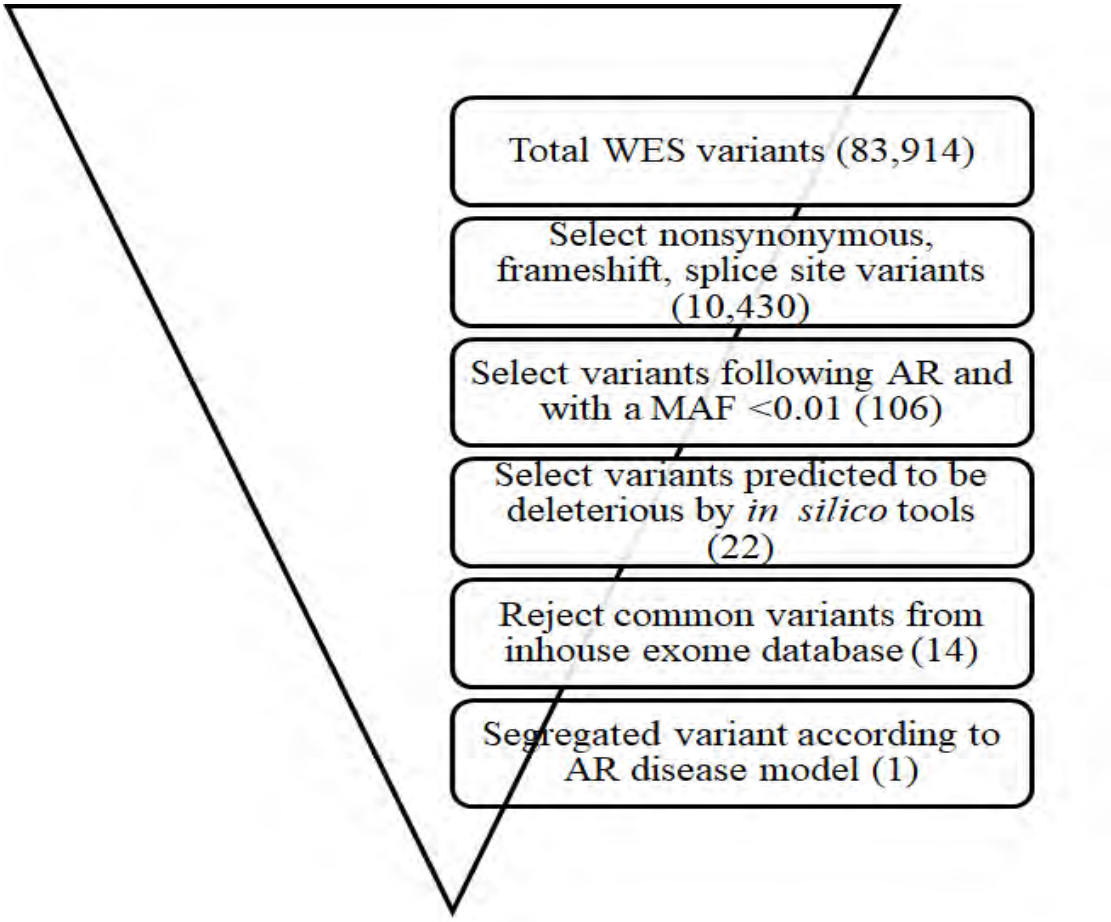

Figure 3. 2: Step-wise approach used to identify pathogenic variants

Table 3.3: Short listed variants from the WES analysis

Chrom	Position	Gene Name	HGVS.c	Zyg-osity	Effect	AF	ExAC
7	138,400,508	*ATP6V0A4*	c.2257+1G>A	Hom	Splice_donor site variant	NA	8.2e-06
2	71,192,103	*ATP6V1B1*	c.1394G>A	Het	Missense variant	0	0.003
11	73,744,969	*C2CD3*	c.6236C>T	Hom	Missense variant	0.004	3.13e-3

Chrom = chromosome. HGVS.c = Human Genome Variation Society. cDNA position, AF = allele frequency from 1000 genome project3, Hom = homozygous, NA = not available, ExAC=Exome Aggregation Consortium.

3.9.2 Segregation analysis

The variant c.2257+1G>A was verified by Sanger sequencing in the patient and the whole family was screened for this variant. All the available members co-segregated the mutation showing mendelian recessive inheritance. The three healthy members (II-1, II-2and III-5) were found to be heterozygous for the mutant allele and the patient (III-4) was homozygous for the mutant allele (Figure 3.3).

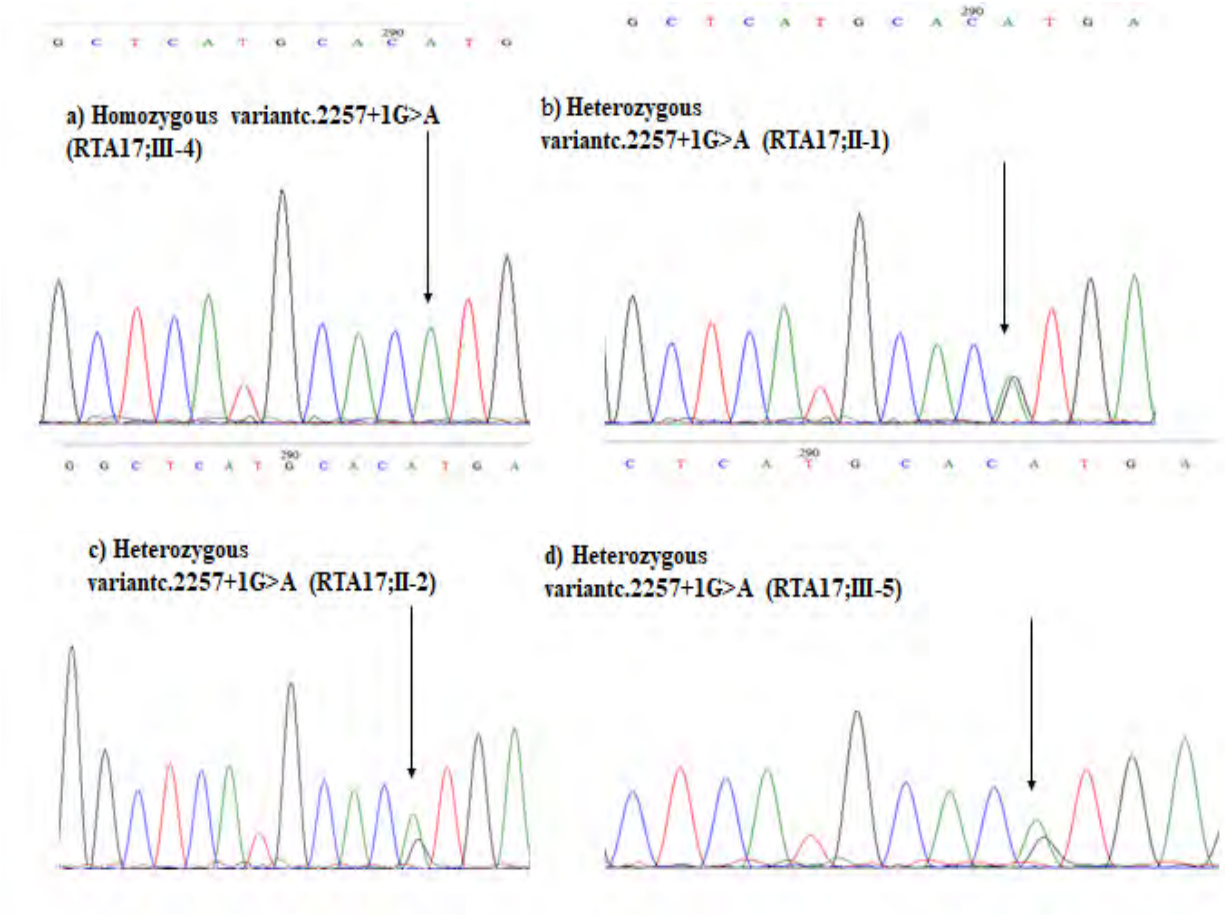

Figure 3.3: Electropherograms showing c.2257+1G>A variant in family A

(a) III-4 (b) II-1 (c) II-2 (d) III-5.

3.9.3 *In silico* analysis

Insilico analysis was performed using the computational programs including MutationTaster, Human Splicing Finder, NNSplice, NetGene2 and CRYP-SKIP to predict the pathogenic effect of mutation which changes the first base G of consensus splice donor site at c.2257+1 position into A. MutationTaster predicted c.2257+1G>A to be disease causing and CRYP-SKIP indicated exon skipping due to the invariant nucleotide change immediately after the last nucleotide of exon 20. The last nucleotide of exon 20 and first two nucleotides of exon 21 in a normal mRNA make up codon 753, therefore skipping of exon 20 leads to frameshift and a premature termination at position 723 in aberrantly spliced transcript. The most frequent outcome of consensus 5' splice site variants in humans and mammals is exon skipping against inclusion of intron which happens as infrequent pattern of aberrant splicing (Nakai & Sakamoto, 1994). Loss of the remaining codons due to exon skipping and stop-gained event might result in the truncated protein and loss of function of the C-terminus. *ATP6V0A4*

encodes 840 amino acids long protein having its large intracellular N-terminal region, six transmembrane domains and a very short C- terminus present intracellularly. The nucleotide variant c.2257+1G>A predicts the loss of last transmembrane domain and the intracellular C terminus of protein which might be playing role in normal acidification of urine through proton secretion. The results show that this invariant nucleotide change has a remarkable effect on the normal splicing of mRNA which subsequently alter the protein structure and function (Table 3.4).

3.10 Discussion

A definitive molecular diagnosis of genetic diseases can aid in the assessment and prognosis of the disease thus helping in the early management in addition to improved genetic counselling of the affected families. Such diagnosis using the first-generation sequencing is often costly and time consuming where large number of variations in more than one gene are rule. Performing whole exome sequencing is therefore a matter of choice in such clinical and research settings. Variants in *ATP6V0A4*, *ATP6V1B1* and *SLC4A1* underlying dRTA phenotype have been reported previously. To reduce the time and cost in sequencing the amplicons of 58 coding exons and adjacent splice sites of these genes by Sanger sequencing, we took advantage of whole exome sequencing. Genetic and clinical heterogeneity make dRTA a good candidate for whole exome sequencing (Gómez et al., 2016). Moreover, it allows identification of any comorbid variants like deleterious alleles in related genes.

In this family, we started with index case of an eight years old male patient III-4 whose clinical and laboratory findings (failure to thrive, polyuria, alkaline urine due to metabolic acidosis) suspected distal renal tubular acidosis. Whole exome sequencing in this patient revealed a homozygous *ATP6V0A4* variant c.2257+1G>A in the splice donor site of intron 20. This variant was reported earlier in heterozygous condition in a Chinese patient affected with dRTA and progressive sensorineural hearing loss (Li et al., 2012).

A heterozygous missense variant c.1394G>A (p.R465H) in *ATP6V1B1* was also found in patient III-4 (family A) in addition to homozygous *ATP6V0A4* variant c.2257+1G>A. This *ATP6V1B1* variant was reported earlier in a dRTA patient in heterozygous state in the absence of another *ATP6V1B1* variant (Ruf et al, 2003). Since the patient III-4 (family A) exhibits autosomal recessive dRTA without SNHL,

therefore the likely cause of the phenotype in this patient is homozygous splice donor site variant c.2257+1G>A in *ATP6V0A4*. The dominant negative effect of *ATP6V1B1* p.R465H allele is ruled out as the parents of the patient were not affected. Moreover, *ATP6V1B1* variants are classically associated with early SNHL while *ATP6V0A4* variants result in dRTA with intact hearing or loss of hearing after the first decade of life, although there are few reports of dRTA with SNHL within the first decade of life (Vargas-Poussou et al, 2006; Kose et al., 2014). The patient in family A carrying *ATP6V0A4* variant has completed first decade of life and his hearing status is normal. Follow up will be necessary to elucidate whether this variant results in later onset of hearing problems.

We reported a splice donor site variant c.2257+1G>A in *ATP6V0A4* as the likely cause of disease in patient belonging to family A. Molecular diagnosis of dRTA for the early and exact diagnosis of the recessive disease in the affected family will be helpful in prenatal diagnosis and genetic counselling among the family members.

3.11 Family B (Lab ID; dRTA 15)

Family B was sampled from Hafizabad, Pakistan. Proband II-1 was evaluated in general OPD (The Children Hospital Lahore) for his initial presenting symptoms which includes vomiting, polyuria and dehydration. Further biochemical tests (Table 3.3) and family history revealed diagnosis of inherited distal renal tubular acidosis. Pedigree was drawn according to the information obtained from father (I-1) of the proband. Family history showed renal disease in paternal side. Parents of the proband II-1 were first cousins and gave rise to three children (II-1, II-2 and II-3) of which II-2 and II-3 showed no signs of the disease (Figure 3.4).

3.11.1 Clinical and biochemical features

Clinical and biochemical investigations of the patients II-1 (family B) explained dRTA (Table 3.4). He had normal anion gap with hyperchloremic metabolic acidosis and high urine pH (≥6), hypokalemia and hypercalcemia. The phosphates, urea and creatinine levels were normal. Ultrasound examination revealed bilateral nephrocalcinosis. He was treated with regular doses of potassium and sodium citrate. Patient's sensorineural hearing capability was intact.

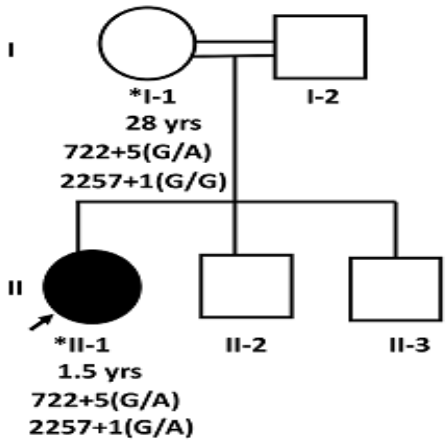

Figure 3.4: Pedigree of family B Squares and circles represent male and female members respectively. Healthy members are represented by unfilled shapes while filled shapes represent affected members; double lines show the cousin marriage. Arrow head points towards proband.

3.12 Molecular genetic analysis

The homozygous *ATP6V0A4* variant c.2257+1G>A identified in family A was screened through Sanger sequencing in ten other dRTA patients whose gDNA was previously available in our laboratory. It was not identified in these patients except in one patient II-1 of the family B in heterozygous state

3.12.1 Sanger sequencing

Assuming compound heterozygous segregation of the causative variants in this family, we screened all coding regions and splice sites of *ATP6V0A4* **(**NC_000007.14**)** in the patient II-1. Primers were made manually using the flanking regions the coding exons of *ATP6V0A4* gene. Two heterozygous splice region variants c.722+5G>A and c.2257+1G>A in *ATP6V0A4* were identified in the patient II-1.

3.12.2 Segregation analysis

Segregation study was performed, and the two variants were screened in available healthy sample (mother, I-1) of the family. Mother I-1 was heterozygous for one splice site variant (c.722+5G>A) and wild type homozygous for second splice site variant c.2257+1G>A(Figure 3.5). The biological samples for the rest of family members of this patient were not available for analysis.

Table 3.4: Laboratory findings of family B; patient II-1

Sr.No.	Serum Biochemistry (Normal values)	Results
1	Sodium (135-145mmol/l)	131
2	Potassium (3.4-4.7mmol/l)	2.5
3	Phosphate (2.7-5.4mg/dL)	3.5
4	Chloride (98-106mmol/l)	110
5	Bicarbonate (22-28mmol/l)	11.1
6	Alkaline phosphatase (50-100U/L)	380
7	Urea (7-20mg/dL)	31
8	Urine pH	6.0
9	Creatinine (0.7-1.3mg/dL)	0.7
10	Nephrocalcinosis	Present bilaterally

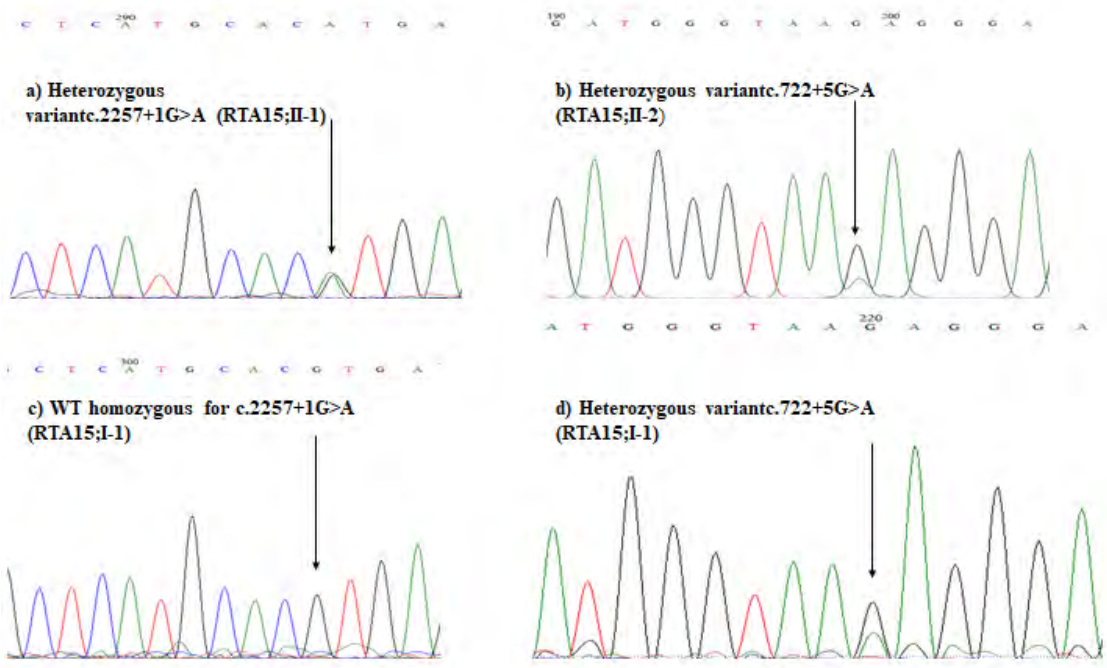

Figure 3.5: Electropherograms showing *ATP6V0A4* variants c.2257+1G>A and c.722+5G>A in family B

(a) III-4 (b) II-1 (c) II-2 (d) III-5.

3.12.3 *In silico* analysis

Two heterozygous *ATP6V0A4* variants were identified in the patient II-1 (family B). In silico analysis of the two *ATP6V0A4* variants (c.2257+1G>A and c.722+5G>A) predicted their deleterious effects on the protein function (Table 3.5). The variant c.722+5G>A was inherited from mother and the second variant c.2257+1G>A might come from father whose sample was not available for analysis. c.722+5G>A is not reported in HGMD (http://www.hgmd.org/) and ExAC (http://exac.broadinstitute.org/) databases. This splice region variant is predicted to abolish the canonical splice donor site in intron 9 (Table 3.5). The +5 position may be decisive during the splicing process of premature transcript as it plays a crucial role in the spliceosome formation and in determining the cleavage site for introns to be spliced out.

3.13 Discussion

The proband II-1 of family B was diagnosed with dRTA based on her initial presenting symptoms. She was investigated at molecular level to find out the genetic cause of disease. Results of this investigation revealed two splice site variants in *ATP6V0A4*

(c.2257+1G>A and c.722+5G>A).The variant c.2257+1G>A was reported earlier in heterozygous condition in a Chinese patient affected with dRTA and progressive sensorineural hearing loss (Li et al., 2012). The presence of identical variant in two unrelated families in Pakistan (A and B) may suggest the idea of founder variant that has evolved with population movements. Otherwise, it might be a mutational hotspot in *ATP6V0A4* gene, and our data can be considered as an evidence to confirm the functional importance of truncated region of *ATP6V0A4.*

The proband (II-1) from family B was compound heterozygote for the variant c.2257+1G>A with another splice region variant c.722+5G>A. A recent study described the pathogenic effect of +5 position in intron 11 *of ATP6V0A4* gene (Yamamura et al., 2017; Park et al., 2018). The exon 9/intron 9 splice junction variant in patient II-1 of family B might interfere with the normal mRNA splicing leading to aberrant splicing, mRNA instability and exon skipping (as identified by the results of HSF and CRYP-SKIP). However, the possibility of non-sense mediated mRNA decay cannot be ruled out (in both variant alleles, c.2257+1G>A and c.722+5G>A) (Lesser et al.,1993; Hwang et al, 1996; Zhuang et al, 1986). Consequently, the functional evaluation of such variants lying outside the consensus splice sites is important and should offer new insights into the molecular causes of disease pathogenesis. The patient in family B carrying *ATP6V0A4* variants has completed first decade of life and her hearing status is normal. Follow up will be necessary to elucidate whether this variant results in later onset of hearing problems.

We reported two splice site variants in *ATP6V0A4* in the patient belonging to family B affected with dRTA without sensorineural hearing loss . Molecular diagnosis of dRTA and other inherited kidney diseases through whole exome sequencing needs to be promoted in Pakistan and other developing regions where consanguinity is prevalent for the early and exact diagnosis of the recessive diseases in the families and to propose antenatal diagnosis.

Table 3.5: Functional predictions of splice site variants by in silico tools

Variant → / *Program ↓	c.2257+1G>A (WT*[1]) scores	c.2257+1G>A (M*[2]) scores	c.722+5G>A (WT) scores	c.722+5G>A (M) scores	Interpretation
Maxent	9.3	1.1	8.91	3.2	Abolition of splice site
NNSplice	0.94	Below threshold	0.96	Below threshold	Abolition of splice site
HSF	87.83	60.99	90.83	78.66	Altered WT splice site
FATHMM	NA	0.99521	NA	0.98896	Deleterious effect (P value > 0.5)
CRYP-SKIP	NA	0.29	NA	0.30	Lower value speaks in favor of exon skipping
Mutation Taster	NA	NA	NA	NA	Disease causing

*Default settings were used in all in silico tools; *[1]WT: Wild type; *[2]M: mutant

3.14 Family C (Lab ID: dRTA3)

Family C was recruited from Lahore, Pakistan. The family comprised of two affected sibs and healthy parents. dRTA was suspected by the clinicians based on the initial presenting symptoms and results laboratory tests performed in The Children Hospital and The Institute of Child Health Lahore. The exact molecular diagnosis required the genetic testing, so the family was referred to Medical Genetics Research Laboratory,

Quaid-I-Azam University Islamabad. We drew the family pedigree along with the ages as told by the father. II-1 and II-2 were the only children of healthy parents born as a result of cousin marriage with unknown family history of any genetic disease (Figure 3.6).

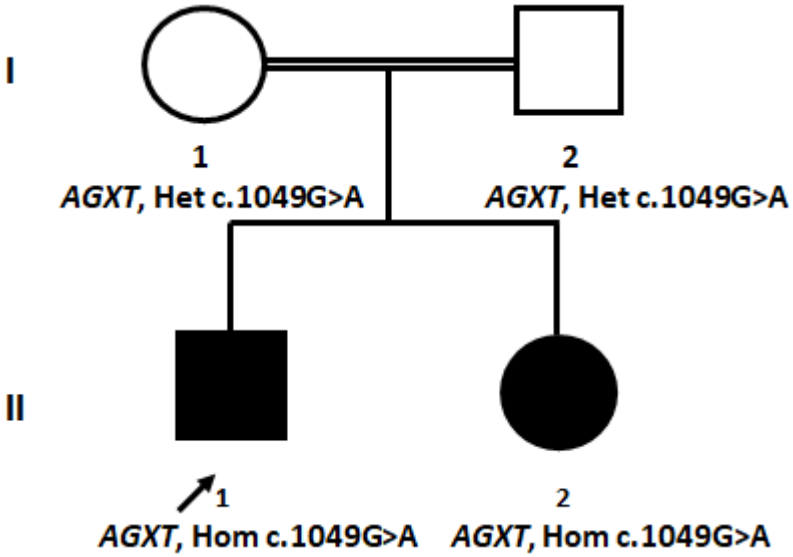

Figure 3.6: Pedigree of family C Male and female members of the family are represented by squares and circles respectively. Healthy members are represented by unfilled shapes while filled shapes represent affected members; lines across the shapes represent the deceased members in the family; double lines show the consanguinity. Arrow head points towards proband.

3.14.1 Clinical and biochemical features

3.14.1.1 Patient II-1

The proband (II-1) was the first male child of consanguineous parentage born after smooth gestation period. The patient had hyponatremia and metabolic acidosis with an alkaline urine of pH 7.0. Renal ultrasound revealed bilateral nephrolithiasis and a right kidney smaller in size (5.0X1.5cm) with increased parenchymal echogenicity and loss of corticomedullary differentiation. Left kidney is 8.8X3.7cm in size and shows multiple calculi of 1.5 to 2.0cm at upper, middle and lower pole. Clinical diagnosis of distal renal tubular acidosis was suspected based on alkaline urine and metabolic acidosis. Various biochemical parameters of the patient are shown in Table 3.6. Acidosis and electrolytes were managed by giving usual treatments of oral alkaline supplements to correct fluids. He developed CKD stage IV at the age of 16 years.

3.14.1.2 Patient II -2

Patient II-2 was a female child and presented with similar symptoms as of her brother. Distal renal tubular acidosis was suspected because of metabolic acidosis and relatively high urine pH. KUB scan was performed which showed smaller kidneys (right kidney=5.5X2.5cm and left kidney=7.5X3.5cm) with increased echogenicity. Her ABG results and electrolytes are shown in Table 3.6. She also developed CKD stage IV at the age of 15 years.

3.15 Molecular genetic study

Genetic investigations of the family C were undertaken to find out the exact molecular cause underlying their pathology. For this, power of whole exome sequencing was employed.

3.15.1 Whole exome sequencing analysis

Proband's DNA (II-1) underwent WES and gave a total of 63,763,000 reads. The average size of read length was 101bp and average depth of target regions was 125.8. Reads were mapped to reference human genome and subsequent filtering steps provided 79,871 variants. Initially we searched the WES data for dRTA associated genetic variants to relate the clinical and genetic diagnosis. The variants were checked for previously associated genes with dRTA (*ATP6V0A4,ATP6V1B1,SLC4A1* and *FOXI1*). No potential variants were identified in the genes previously identified for dRTA. Afterwards we used the following strategy to identify the pathogenic variant responsible for the disease:

Firstly, the synonymous and intronic variants were filtered out to reduce the large number of variants and only those variants were considered which could either alter the protein function or truncate the protein product, i-e, missense, splice acceptor site and splice donor site, frameshifts, nonsense, stop gained and stop-lost. The number of such variants was 10,851. From these variants, we further reduced the number to 539 by selecting variants that had minor allele frequency MAF <1% in Ensembl, ExAC or 1000 Genome Project. keeping in mind the pedigree inheritance mode, we looked for the variants that followed autosomal recessive inheritance i-e, homozygous or compound heterozygous. This step reduced the number to 30 which were further sorted out based on their *in-silico* prediction and inhouse Exome of 100 individuals. Finally, four

variants were identified as potential candidates which were not present in inhouse exome data of 100 individuals (Table 3.7, Figure 3.8).

3.15.2 Segregation analysis

The other family members were screened for these variants for segregation analysis. Variant in *AGXT* gene was found to be segregating with the affected and unaffected status of family members (Figure 3.7). None of the other variants co-segregated with the phenotype (Table 3.7).

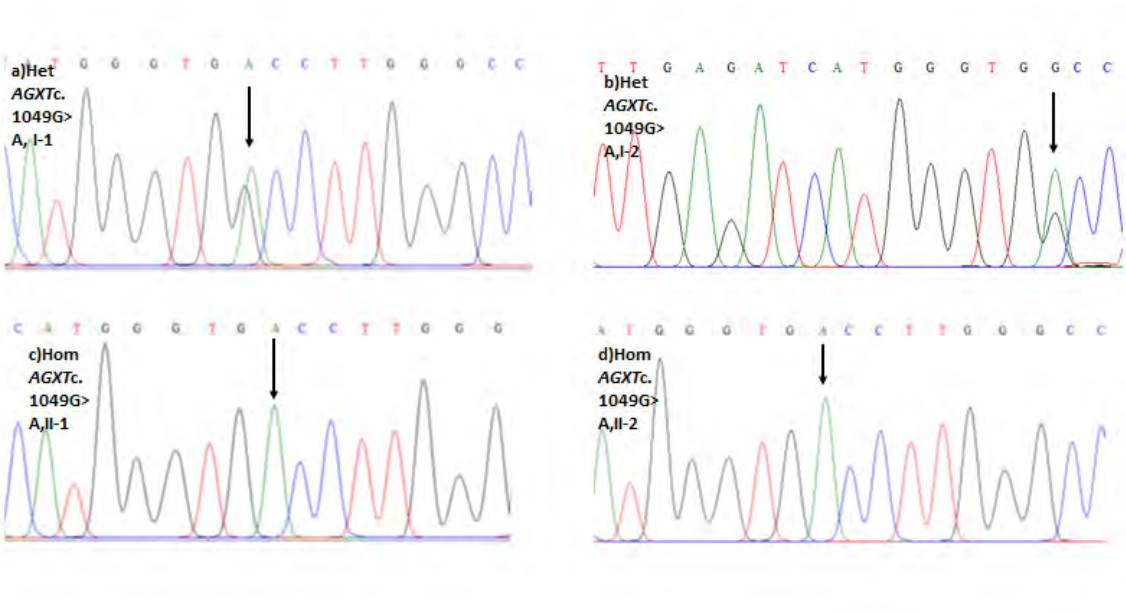

Figure 3.7: Electropherograms showing c.1049 G>A variant in AGXT in family C (a) I-1 (b) I-2 (c) II-1 (d) II-2.

3.15.3 *In silico* analysis

In silico analysis of *AGXT* gene variant c.1049 G>A was performed using SIFT, Polyphen and Predict SNP2 predicting the nucleotide change as damaging.

Table 3.6: Laboratory findings affected members of family C.

Sr.No.	**Serum Biochemistry**	**Results**			**Arterial Blood Gas**	**Results**		
		Patient II-1	**Patient II-2**	**Reference values**		**Patient II-1**	**Patient II-2**	**Reference values**
1	Sodium (mmol/l)	131	130.3	135-145	Temp. (℃)	37.0	37.0	37.0
2	Potassium (mmol/l)	2.4	2.36	3.5-5.5	pH	7.440	7.34	7.35-7.45
3	Phosphorous (mmol/l)	2.0	2.4	1.45-2.1	pCO_2 (mmHg)	22.3	23.1	35-45
4	Chloride (mmol/l)	104	101	96-108	pO_2 (mmHg)	122.2	121.8	80-100
5	Alkaline phosphatase (IU/L)	125	200	50-100	BEecf (mmol/L)	-9.4	-9.1	-3-3
6	Urea (mg/dL)	40	35	12-45	sO_2(%)	98.8%	95.5%	>95
7	Urine pH	6.5	6.2	Morning urine (5.5-6.0)	Baro (mmHg)	744.5	744.5	
8	Creatinine (mg/dL)	2.8	2.6	0.3-0.7	cHCO3 (mmol/L)	14.8	15.0	22-28
9	Calcium (mmol/l)	2.5	2.0	2.1-2.7	Hct	29.0	29.2	>30%
10	POx (μmol/l)	120	140	25-30	----------			

BEecf= base excess in the extracellular fluid compartment, Hct= hematocrit, pCO_2= partial pressure of carbon dioxide, pO_2= partial pressure of oxygen, sO_2= oxygen saturation in blood, POx=plasma oxalate

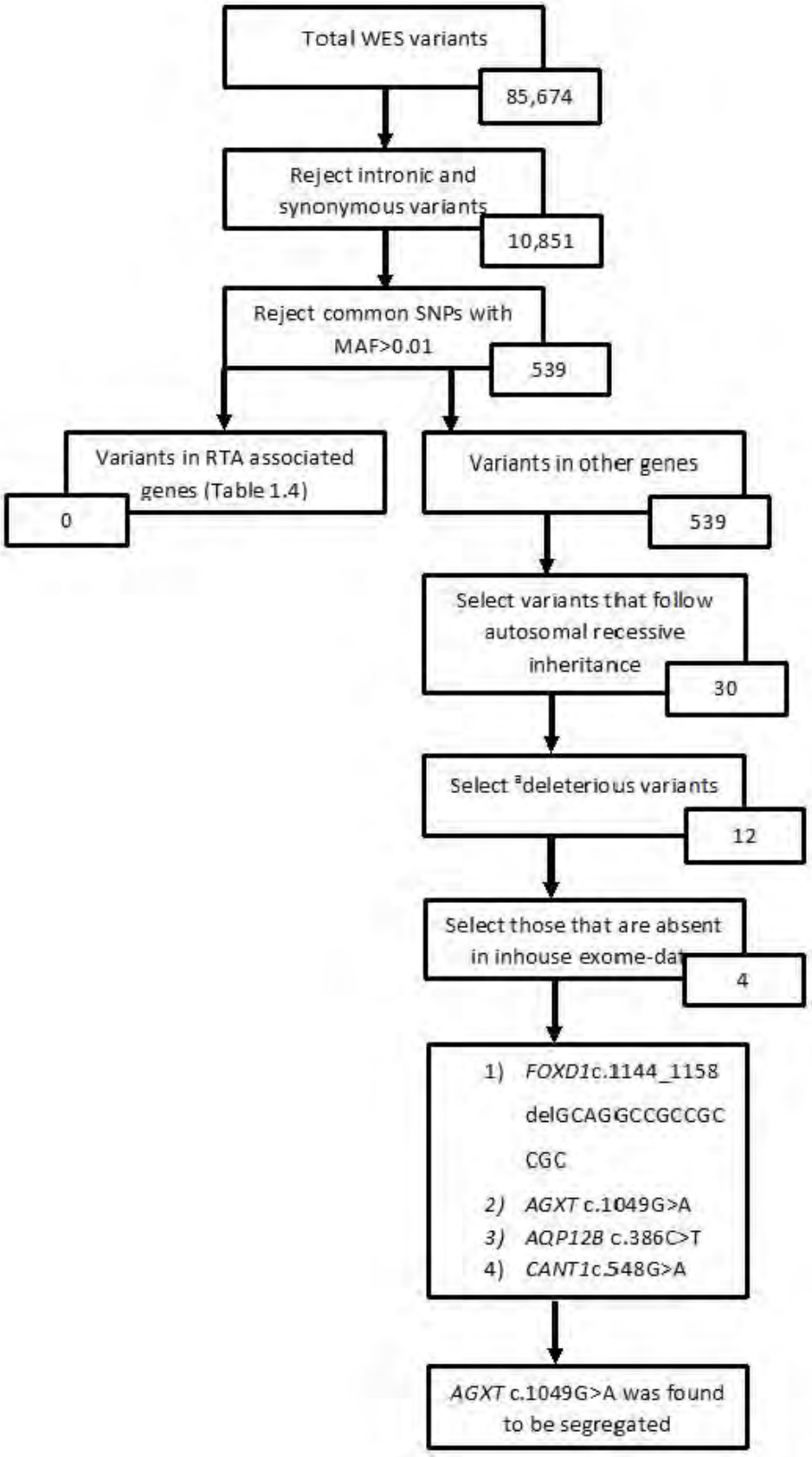

Figure 3.8: Flow sheet to understand the variant filtering process

a=Damaging according to PredictSNP2, Polyphen and SIFT.

Table 3.7: Short listed variants from the WES analysis

Chrom	**Position**	**Gene Name**	**HGVS.c**	**Zyg-osity**	**Effect**	**AF**	**ExAC**	**PolyPhen2 scores**	**SIFT Scores**
5	72,743,029	*FOXD1*	c.1144_1158delGCAGGCCGCCGCCGC	Hom	Inframe deletion	--	--	--	--
2	*241,817,545*	*AGXT*	c.1049G>A	Hom	missense	--	0.000003994	1.0	0
16	*2,284,330*	*E4F1*	c.1534G>T	Hom	missense	--	--	1.0	0.005
17	*76,993,157*	*CANT1*	c.548G>A	Hom	missense	--	9.94e-5	1.0	0.003

Chrom = chromosome. HGVS.c = Human Genome Variation Society. cDNA position, AF = allele frequency from 1000 genome project3, Hom = homozygous, NA = not available, ExAC=Exome Aggregation Consortium.

3.16 Discussion

We report the genetic and clinical investigations of two sibs who presented with polyuria, failure to thrive, hypokalemia, alkaline urine and incorrect acid-base balance. Inability to acidify urine made clinicians to suspect dRTA and they were kept on polycitra to correct the electrolytes. However, their urinary or plasma oxalate levels were not checked at that time. As of this writing, follow up of both patients (II-1 and II-2) revealed that they had developed chronic kidney disease stage IV at the ages of 15 and 16 years. Patients underwent genetic study using whole exome sequencing in combination with Sanger sequencing and a recurrent mutation in c.1049G>A;[p.Gly350Asp] in *AGXT* gene was identified. This gene is responsible for Primary hyperoxaluria type 1 (PH1) and the mutation c.1049G>A was reported earlier in a Pakistani boy with PH1 and had blocked urethra due to calcium oxalate stones (Rumsby, 1998). Therefore, WES corrected the clinical dRTA diagnosis to (PH1).

PH1 is a rare autosomal recessive disease characterized by deficiency of alanine-glyoxylate aminotransferase also abbreviated as AGT enzyme encoded by *AGXT* gene (Picca, Colombini, & Cochat, 2017). This enzyme is required to convert glyoxylate to

glycine. In the absence of functional AGT enzyme, glyoxylate is converted into oxalate which is responsible for oxalate stones in kidney or other organs (Williams et al., 2009). Diagnosis of PH1 is often done based on elevated urinary oxalate levels in the absence of CKD or ESRD. These levels may appear normal due to reduced eGFR (<15mL/min/173m^2) once disease progresses to ESRD. Measuring plasma oxalate levels (POx) when eGFR is <60mL/min/173m^2 are recommended (Perinpam et al., 2017). Although POx generally increases when GFR falls and there is no clear cut-off to categorize patients with PH from those with any other cause of kidney failure, values >100ɥmol/L are considered to be the more likely cause of PH (Cochat et al., 2012). A noninvasive approach to diagnose PH1 is *AGXT* gene screening which is considered as an accurate diagnosis eliminating the need to perform enzyme assays (Milliner, 2005).

Reviewing the previous literature, we came across with few reports of dRTA associated with PH1. In one study, the patient showed hypokalemia and hyperchloremic metabolic acidosis and increased oxalate levels in his 24h urine analysis. However, the genetic study to determine the cause underlying clinical diagnosis of dRTA and PH1 in the same patient was not performed (Cheng et al., 1987). In another study reported in 2010, the patient was diagnosed to have had PH1 based on her urinary oxalate levels and nephrocalcinosis. She also showed hyperchloremic metabolic acidosis and alkaline urine which were consistent with dRTA. Later, molecular analysis was done which confirmed dRTA (Pela, Provenzano, & Giglio, 2011). Atypical presentation of dRTA in a 7-month old patient reported by Copelovitch and Kaplan along with the diagnosis of PH1 and Dents disease led authors to perform molecular study of *ATP6V1B1* gene to identify *ATP6V1B1*mutations and confirm the dRTA diagnosis (Copelovitch & Kaplan, 2010).

Primary hyperoxaluria shows heterogeneous clinical signs including recurrent nephrolithiasis, nephrocalcinosis, UTIs, and oxalosis in tissues and organs. Several atypical features in PH1 are also reported which includes failure to thrive and metabolic acidosis (Yang et al., 2019). Our patients might escaped correct diagnosis due to presence of metabolic acidosis which is considered as hallmark of dRTA, therefore, we here want to suggest while evaluating clinically, the dRTA signs and symptoms and performing ammonium chloride test to detect acid load, 24h urinary oxalate test or plasma oxalate test must also be performed in routine to exclude PH1 diagnosis.

Metabolic acidosis though not very rare in PH1 disease, it might be explained on the basis of low potassium levels and GI loss due to diarrhea in our patients.

Our study highlights the fact that molecular investigations become necessary in such settings where confused findings hinders the correct diagnosis. In addition, this study is an excellent example of utility of whole exome sequencing as a diagnostic tool for the identification of correct cause of CKD in children which are often difficult to diagnose even on renal ultrasound and clinical evaluation (Daga et al., 2018). WES reached the noninvasive and unbiased diagnosis in family C, where identification of *AGXT* mutation established the correct diagnosis of PH1 which was misdiagnosed as dRTA. This could be helpful in delaying ESRD by using high dose pyridoxine therapy for the patients and maintaining stable eGFR.

NEPHRONOPHTHISIS

4.1 Introduction

Nephronophthisis (NPHP), an autosomal recessive inherited cystic kidney disease, is the most frequent cause of end stage renal disease (ESRD) before 30 years of age (Delous et al., 2007). The literal meaning of the word nephronophthisis is "disappearance of nephrons" (Simms, Eley, & Sayer, 2009). Previously, the worldwide incidence of NPHP was estimated to fall between the ranges of 1: 50,000 to 1: 900,000 with the prevalence of 5-6.5% among pediatrics (Ala-Mello, Koskimies, Rapola, & Kääriäinen, 1999; Waldherr et al., 1982); however recent advancements in molecular and genetic diagnostics have identified many chronic kidney disease in young adults as NPHP which might cause an increase in the estimated frequency of disease (Bollée et al., 2006; Hoefele et al., 2011). Early clinical features associated with the disease are polyuria due to inability of an individual to concentrate urine (<400mosm/kg), polydipsia, enuresis, regular intake of fluids at night, anemia, lethargy and growth retardation. Malfunctioning of cortical collecting part of nephron results in salt wasting and production of dilute urine through the kidneys (Krishnan, Eley, & Sayer, 2008; Luo & Tao, 2018). Renal ultrasound may reveal normal or reduced size kidneys, one or few cysts along the corticomedullary junction and increased parenchymal echogenicity (Hildebrandt, Attanasio, & Otto, 2009). Histological examinations show disrupted and thickened tubular basement membrane and tubulointerstitial fibrosis (Luo & Tao, 2018). Based on the age of onset of ESRD, NPHP can be classified into four distinct forms; infantile NPHP presents ESRD at median age of 1 year, juvenile NPHP manifests symptoms of ESRD at 13 years on an average, adolescent NPHP progresses to ESRD at median age of 19 years and late onset NPHP is cited in number of reports which progress to ESRD between the ages of 42 and 56 years (Georges et al., 2000; Hildebrandt, Strahm, et al., 1997; Hoefele et al., 2011). Clinical features associated with each of the NPHP subtypes are summarized in Table 4.1. Another classification of NPHP can be made based on the presence or absence of extrarenal manifestations in addition to NPHP. Most of the NPHP cases have no extrarenal symptoms i-e they have isolated NPHP while others have extrarenal manifestations that create a class of NPHP called syndromic NPHP (Halbritter, Porath, et al., 2013). Syndromic NPHP

comprises a number of syndromes having NPHP as a renal defect with other clinical findings including Senior-Løken syndrome, Joubert syndrome, Sensenbrenner syndrome, Jeune syndrome, COACH syndrome and Meckel-Gruber syndrome (Srivastava, Molinari, Raman, & Sayer, 2018). Nephronophthisis-Related Ciliopathies (NPHP-RC) is a term coined for isolated NPHP, NPHP with extrarenal findings but with no recognizable syndrome and syndromic NPHP (Halbritter, Porath, et al., 2013). The number of identified genes in NPHP has reached to almost 25 till date, however it is anticipated that more genes will be identified underlying this genetic defect since 70-75% NPHP cases have an unidentified molecular cause (Simms, Hynes, Eley, & Sayer, 2011).

Table 4.1: Clinical subtypes of Nephronophthisis (Georges et al., 2000).

Subtype	Median age at ESRD	Clinical features	Other findings
Infantile NPHP	Before 3 years	Polyuria, anemia, growth retardation, ultrasound image reveals enlarged hyperechogenic cystic kidneys.	Hypertension secondary to renal failure, limb contractures, pulmonary hypoplasia, facial dysmorphism
Juvenile NPHP (most prevalent subtype)	13 years	Polyuria, polydipsia, anemia, growth retardation, reduced echogenicity and corticomedullary differentiation upon renal imaging, renal cysts in 50% of affected individuals, normal or reduced kidney size.	Findings related to CKD are metabolic bone disease, metabolic acidosis, uremia and proteinuria (late finding).
Adolescent NPHP	19 years	As above	As above

Late onset NPHP	After 30 years	Polyuria, polydipsia, nocturia, enuresis, multiple renal cysts	Mild proteinuria and unremarkable sediment upon urinalysis

4.2 Nephronophthisis as a ciliopathy

The unifying theory of kidney disease as a renal cystic disease is based on very first findings that nephrocystins (NPHP1 and Inversin/NPHP2) are localized on primary cilia of cells present in kidney tubules (Otto et al., 2003). The theory states that mutations in the genes encoding cystoproteins which are expressed on primary cilia, basal bodies or centrosomes cause renal cystic diseases in humans, mice or zebrafish (Watnick & Germino, 2003). Primary cilia are extremely conserved structures, they are assembled from the basal bodies and anchored to them by microtubule-based structure called axoneme (Hildebrandt et al., 2009). Transition zone lies between cilia and axoneme and act as a gateway for the selective molecules to enter or exit from the cilium (Shi et al., 2017). Several genes encoding nephrocystins *NPHP1, NPHP2, NPHP3, NPHP4, NPHP5, CEP290, NPHP7, RPGRIP1L, NPHP9* have been identified by positional cloning that encode the components localized to primary cilia, basal body and transition zone. These are monogenic recessive genes and their normal protein product is necessary for normal kidney function and mutations in any of these genes can produce NPHP phenotype (Hildebrandt et al., 2009). Several other nephrocystins are found to be present in inversin compartment and intraflagellar transport complexes (Srivastava & Sayer, 2014). However, some of the identified nephrocystins NPHP1L and NPHP2L are localized to mitochondria (Simms et al., 2009).

4.3 Nephrocystins modules

Nephrocystins interact with each other at ciliary compartments to modulate the cilia functioning. At present, there are four recognizable nephrocystins modules, each of these four modules comprise two or more interacting nephrocystins and function in different signaling pathways for example Wnt signaling pathway, Sonic Hedgehog pathway, DNA damage response pathways and mTOR pathway. The four modules are represented as;

NPHP1-4-8 module, NPHP5-6 module, NPHP2-3-9-16 module and MKS module (MKS1-CC2D2A-TCTN2) (Luo & Tao, 2018).

The first two modules (NPHP1-4-8 and NPHP5-6) are specifically localized to transition zone and constitute Group I nephrocystins. In renal epithelial cells, NPHP4 binds directly to NPHP1 and NPHP8 and regulate the trafficking of ciliary components at transition zone. The exact function of the complex is not known, however it is not required for ciliogenesis (Sang et al., 2011). NPHP5 binds to NPHP6 and controls the ciliary assembly and trafficking. Depletion of any one of these two result in ciliogenesis defect in renal epithelial cells (Shiba & Yokoyama, 2012). Group II nephrocystin (NPHP2-3-9) are involved in functioning of renal epithelial cells cilia and nodal cilia. Nodal primary cilia are important in determining left right asymmetry during early embryogenesis (Bergmann et al., 2008).

4.4 Molecular and genetic analysis

There are almost 25 known genes, which, if mutated lead to NPHP pathogenesis. These are identified by positional cloning, homozygosity mapping and exome capture techniques. Next generation sequencing techniques allowed the identification of NPHP genes at a faster rate (M. T. Wolf & Hildebrandt, 2011).

4.4.1 *NPHP1*

NPHP1 is the first identified gene responsible for 25% cases of isolated nephronophthisis (Hildebrandt, Otto, et al., 1997). It encodes nephrocystin 1 which interacts with tensin, filamin A and B, Protein tyrosine kinase 2B (PTK2B), ack, jouberin and is shown to involve in all cell-cell adhesion and cell signaling events (M. T. Wolf & Hildebrandt, 2011). In the primary cilium of renal epithelia, nephrocystin 1 interacts with nephrocystin 4 and RPGRIP1L and form a link with inversin (Sang et al., 2011). *NPHP1* also expresses its protein product in retinal epithelial cells which support the fact that *NPHP* mutations can also cause SLS and JS. *NPHP1* is reported in cases where oligogenic inheritance has been identified; mutations in both *NPHP1* and *NPHP3* genes, *NPHP1* and *NPHP4*, and *NPHP1* and *AHI1* have been detected (Hoefele et al., 2007; Utsch et al., 2006). Homozygous *NPHP1* full gene deletions are most prominent cause of NPHP cases reported (Halbritter, Porath, et al., 2013).

4.4.2 *NPHP2/INVS*

NPHP2/INVS encodes 1062 amino acid inversin protein, bipartite nuclear localization signal, an IQ domain and 16 ankyrin repeats. Calmodulin directly binds to inversin through its IQ domain (Morgan et al 2002a). Inversin localizes to primary cilium and centrosome where it not only acts as a molecular switch between non-canonical (planar cell polarity) and non-canonical Wnt signaling but also regulate the tubular architecture. Depletion of the *NPHP2* gene product may result in sustained Wnt signaling pathway which has been shown to cause abnormal cell division and proliferation leading to cystogenesis (Simons et al., 2005). *NPHP2* mutations cause distinct form of NPHP called infantile NPHP which presents ESRD before the age of 2 years and enlarged cystic kidneys resembling the polycystic kidneys as compared to other forms of NPHP where kidneys are normal sized or reduced. Extrarenal findings observed in patients with *NPHP2* mutations are heart anomalies, situs inversus and rarely SLS (Gagnadoux, Bacri, Broyer, & Habib, 1989; Phillips et al., 2004).

4.4.3 *NPHP3*

NPHP3 was mapped on chromosome 3q21-q22 by whole genome search for linkage in large kindred by applying the strategy of homozygosity mapping. It encodes a 1330 amino acid nephrocystin 3 that links directly to nephrocystin 1. It also interacts with inversin in primary cilia (Olbrich et al., 2003). Mutations in NPHP3 have been reported in isolated NPHP patients and with variety of extrarenal organs involvement including SLS, MKS, liver fibrosis, situs inversus. The pleiotropy observed in *NPHP3* cases reflects its expression in primary cilia (Bergmann et al., 2008).

4.4.4 *NPHP4*

Nephrocystin 4/nephroretinin is encoded by *NPHP4* located on chromosome 1p36 (Schuermann et al., 2002). Nephrocystin is highly conserved protein and expressed and colocalized with primary cilia, centrosomes, alpha tubulin, PTK2B and actin cytoskeleton (Mollet et al., 2005; M. T. Wolf & Hildebrandt, 2011). Mutations in *NPHP4* gene result in nephronophthisis and retinitis pigmentosa. Retinal ciliopathy is the most common extrarenal manifestation associated with mutation in this gene that's why the name

nephroretinin is used. NPHP4 interacts with nephrocystin 1, inversin, nephrocystin 3 and retinitis pigmentosa GTPase regulator interacting protein 1(RPGRIP1L) (Raj, Gordillo, Warnecke, & Chand, 2016). NPHP4 is a negative regulator of Wnt signaling pathway suppressing its overactivation which may lead to abnormal cell proliferation (Habbig et al., 2011).

4.4.5 *NPHP5/IQCB1*

NPHP5/IQCB1, located on chromosome 3q21.1, encodes nephrocystin 5 which consists of two calmodulin binding sites (Otto et al., 2005). Individuals presenting mutations in *NPHP5* have characteristic features of NPHP with early onset retinitis pigmentosa (Simms et al., 2011). An investigation to find the link between NPHP and retinal degeneration leads to the novel findings that *IQCB1* binds to RPGP and calmodulin in retinal cilia (Otto et al., 2005). Nephrocystin 5 interacts with NPHP6 (nephrocystin 6) and colocalizes with nephrocystins (1 and 4) in primary cilia (Sayer et al., 2006; Schäfer et al., 2008).

4.4.6 *NPHP6/CEP290*

CEP290 is located on chromosome 12q21.32 and encodes centrosomal protein of 290 kDa (CEP290) also known as nephrocystin 6 (Sayer et al., 2006). NPHP6 interacts with NPHP5 at primary cilia in renal epithelium (Shiba & Yokoyama, 2012). CEP290 mediates cyst formation by interacting with transcription factors such as ATF4 which is involved in cAMP dependent renal cyst formation and coiled coil and c2 domain (CC2D2A) protein (Sayer et al., 2006). Zebrafish models containing mutant *CC2D2A* combined with mutant *NPHP6* has been shown to cause renal cysts (Gorden et al., 2008). Patients with mutations in *NPHP6* gene present a variety of extrarenal symptoms with no clear genotype phenotype correlation. These include isolated NPHP, JS, MKS, SLS and BBS. (Coppieters, Lefever, Leroy, & De Baere, 2010). *NPHP6* mutations are most frequently reported in patients with Leber's Congenital Amaurosis (LCA) (den Hollander et al., 2006).

4.4.7 *NPHP7/GLIS2*

GLIS2 is located on chromosome 16p13.3 and encodes GLI similar 2 protein (Attanasio et al., 2007). GLIS2 localizes to nucleus and primary cilia (Raj et al., 2016). *GLIS2* mutations

were first identified in 2007 as a novel cause of NPHP providing further insights into NPHP pathogenesis. GLIS2 is a zinc finger transcription factor and its depletion results in enhanced tissue fibrosis and cell death. (Attanasio et al., 2007). The involvement of GLI transcription factors provides a link of NPHP pathogenesis with Hedgehog signaling pathway since this pathway has a major role in tissue maintenance (Huangfu et al., 2003).

4.4.8 *NPHP8/RPGRIP1L*

Retinitis pigmentosa GTPase regulator interacting protein 1-like (RPGRIP1L) is encoded by *NPHP8* which is located on chromosome 16q12.2 (M. Wolf et al., 2007). RPGRIP1L interacts with nephrocystin 1 and 4 at centrosomes and basal bodies (Delous et al., 2007). RPGRIP1L defects due to mutations in NPHP8 are the frequent cause of cerebello-oculo-renal syndrome (M. Wolf et al., 2007). A study published in 2007 revealed patients who harbored mutations in *NPHP8* with JS features from three unrelated families (Arts et al., 2007).

4.4.9 *NPHP9/NEK8*

NPHP9 is located on chromosome 17q11.1 encodes NIMA Kinase 8 (NEK8) protein (Otto et al., 2008). The protein product of *NPHP9* colocalizes with many nephrocystins at primary cilia and centrosomes and involved in regulating cell cycle (M. T. Wolf & Hildebrandt, 2011). Recent evidences support its role in DNA damage response (DDR) since mutated *NPHP9* results in increased DNA damage leading to NPHP phenotype (Choi et al., 2013). Defects in NEK8 are also associated with deregulated hippo pathway and severe renal cystic disease (Grampa et al., 2016).

4.4.10 *NPHP10/SDCCAG8*

The first NPHP gene to be identified using next generation sequencing was *NPHP10* encoding SDCCAG8 (Serologically Defined Colon Cancer Antigen 8). The gene is located on chromosome 1q44 (Otto et al., 2010). The protein is located at centrioles and interacts directly with OFD1, a ciliopathy associated protein. SDCCAG8 cause kidney disease by increased DDR signaling (Airik et al., 2014). Moreover, SDCCAG8 also interacts with

retinal ciliopathy protein, RPGRIP1L, and has been implicated as a rare cause of BBS and SLS (Raj et al., 2016).

4.4.11 *NPHP11/TMEM67*

NPHP11 is present on chromosome 8q22.1 and encodes transmembrane protein 67 (Otto et al., 2009). The protein is localized to primary ciliary membrane and help in maintaining the cellular structures (Raj et al., 2016). Mutations in *NPHP11* have been found in NPHP patients with liver involvement as extrarenal clinical feature. TMEM67 should be screened in NPHP patients with liver involvement, JS or MKS (Vilboux et al., 2017).

4.4.12 *NPHP12/TTC21B*

NPHP12/TTC21B encodes intraflagellar transport protein 139 (IFT139). IFT139 is a retrograde transport protein and is involved in NPHP pathogenesis through Hedgehog signaling pathway. It may cause isolated NPHP or NPHP with JS manifestations (McMahon, Ingham, & Tabin, 2003).

4.4.13 *NPHP13/WDR19*

WDR19 encodes a retrograde protein called IFT144. IFT144 is a part of IFT A complex that functions in ciliogenesis and ciliary transport (Bredrup et al., 2011). The mutations in *WDR19* have been implicated in patients with isolated NPHP, Sensenbrenner syndrome, JS and SLS (Coussa et al., 2013).

4.4.14 *NPHP14/ZNF423*

NPHP14/ZNF423 encodes a DNA binding zinc finger transcription factor which binds to poly ADP-ribose polymerase 1 (PARP1). ZNF423 protein is connected to DDR pathway and links the pathogenesis of NPHP with mechanism of DDR. The protein is also shown to interact with CEP290 protein encoded by *NPHP6*. Mutations in *ZNF423* are a rare cause of JS with NPHP (Chaki et al., 2012).

4.4.15 *NPHP15/CEP164*

CEP164 is located on chromosome 11q23.3. Centrosomal protein CEP164 encoded by this gene colocalize specifically to distal appendages of mature centriole (DAP) and might be involved in the transport between primary cilium and interior of the cell (Graser et al., 2007). Impaired and depleted CEP164 might result in ciliopathy diseases in humans such as NPHP and SLS (Chaki et al., 2012).

4.4.16 *NPHP16/ANKS6*

ANKS6/NPHP6 encodes a protein , Ankyrin repeats Sterile Alpha Motif (SAM) domain containing 6 (ANKS6), which was identified as a member of NPHP family in 2013 (Hoff et al., 2013). ANKS6, localized to at proximal part of primary cilium of medullary collecting duct, makes a direct connection with NEK8/NPHP9 and connects it to INVS and NPHP3 with the whole complex of four proteins forming an NPH module (INVS-NPHP3-NPHP9-ANKS6) (Hoff et al., 2013; Shiba, Manning, Koga, Beier, & Yokoyama, 2010). In a study comprising six NPHP patients, *NPHP16* truncating mutations are reported in patients with heart anomalies, hepatic fibrosis or situs inversus while missense mutations presented isolated NPHP (Hoff et al., 2013).

4.4.17 *NPHP17/IFT172*

IFT172 encodes a member of IFT-B subcomplex, IFT172 protein. IFT-B subcomplex, a part of IFT (intraflagellar transport) complex, comprises 14 proteins subunits all of which are involved in human ciliopathies except the subunit IFT80. IFT172 is one of these subunit and has been demonstrated to cause renal, retinal, hepatic and thorax abnormalities in a cohort of patients belonging to 12 families, some of which also presented with NPHP-RC (Halbritter, Bizet, et al., 2013). Loss of functional IFT172 is also implicated in JS (Schaefer et al., 2016).

4.4.18 *NPHP18/CEP83*

CEP83 is one of the DAP-encoding gene which encodes centrosomal protein 83. It is localized to distal appendages of centriole which are involved in docking centriole to the cell membrane during assembly and disassembly of primary cilia (Failler et al., 2014).

Biallelic mutations were found in *CEP83* gene in a cohort of eight patients with early onset of nephronophthisis (Failler et al., 2014).

4.4.19 *NPHP19/DCDC2*

The product of NPHP19/*DCDC2* is located on ciliary axoneme of renal tubular cells and liver cholangiocytes. It interacts with disheveled 3 (DVL3) and inhibits the Wnt signaling pathway along with the Wnt inhibitors. Absence of DCDC2 results in overactivation of Wnt pathway and contributes to NPHP-RC with liver fibrosis (Schueler et al., 2015).

4.4.20 *NPHP20/MAPKBP1*

MAPKBP1 is a newly identified gene, the product (MAP-kinase binding protein 1) of which is located at mitotic spindles. Knockdown of *MAPKBP1* in murine cells produces elevated DDR signaling. Mutations in this gene may result in juvenile or late onset non syndromic NPHP (Macia et al., 2017).

4.4.21 *AHI1*

AHI1 is located on chromosome 6q23.3 and encodes an AHI1 protein also called jouberin. AHI1 is localized to cell-cell junctions and basal bodies. AHI1 mutations are frequently involved in Joubert syndrome without renal disease (Dixon-Salazar et al., 2004). However, few cases have been described which individuals with NPHP associated JS had mutations in *AHI1* gene (Utsch et al., 2006).

4.4.22 *CC2D2A*

CC2D2A encodes a CC2D2A protein having three coiled coil domains and one C2 domain. The gene resides on 4p15 locus and its product localizes to primary cilium and interacts with CEP290/NPHP6 protein. Mutations in this gene cause cystic kidney diseases and JS (Gorden et al., 2008).

4.4.23 *XPNPEP3/NPHP1L*

Unlike most other NPH family members, *XPNPEP3* encodes a mitochondrial protein which localize to mitochondria present in kidney cells. The gene is located on 22q13.2

locus. *XPNPEP3* mutations have been implicated in patients manifesting NPHP like nephropathy and heart and mental abnormalities as extrarenal manifestations (O'toole et al., 2010).

4.4.24 *SLC41A1*

SLC41A1 encodes a Mg^{+2} transporter SLC41A1. The first transporter to be included as a member of NPH family is SLC41A1. The protein localizes to corticomedullary junction of renal tubular cells, a cystogenic region observed in NPHP and related ciliopathies (Hurd et al., 2013).

4.4.25 *ATXN10*

ATXN10 gene residing on chromosome 22 encodes Ataxin 10 protein. Ataxin 10 interacts with ciliary nephrocystin NPHP5/IQCB1. Depletion of ATXN10 resulted in ciliation defects when mutated protein was induced in IMCD3 cells. *ATXN10* mutations resulted in infantile NPHP in a study reported in 2011 (Sang et al., 2011).

4.5 Diagnosis

Clinical diagnosis of NPHP relies on early presenting symptoms of the disease which include polyuria, polydipsia, nocturia, and enuresis. Protein/creatinine ratio and early morning urine osmolality are investigated early in the disease course to evaluate NPHP. Low osmolality indicates the reduced ability of patients to concentrate their urines. Urinalysis is often bland and absent or low proteinuria is observed (Raj et al., 2016). Anemia, lethargy and growth retardation are also observed as initial presentation of the disease (Krishnan et al., 2008). Renal function tests, complete blood picture, liver function tests and parathyroid hormone examination help in establishing the chronic kidney disease diagnosis (Raj et al., 2016). Abdominal ultrasound is performed to see the normal or shrunken kidneys, except in infantile NPHP in which the imaging studies show enlarged kidneys resembling the polycystic kidneys (Oud et al., 2014). Increased cortical echogenicity and diminished corticomedullary differentiation with cysts along the corticomedullary junction indicate nephronophthisis (Soliman et al., 2012). These diagnostic features help in establishing the diagnosis, while confirmation can be done by

molecular genetic testing which is the only method currently available and reliable for NPHP exact diagnosis (Luo & Tao, 2018). *NPHP1* gene screening accounting for almost 25% NPHP cases, should be done first using standard PCR assays and whole exome sequencing or targeted exome capture should be performed for a definite diagnosis in case of absence of *NPHP1* gene deletion or mutation (Gee et al., 2014; Hussain, Akhtar, Qamar, Khan, & Naeem, 2018; Luo & Tao, 2018). Histologic findings may reveal characteristic tissue fibrosis on renal parenchyma and tubular membrane disruption, small number of inflammatory cells, normal glomeruli which may show sclerosis upon disease progression, but these are not required for establishing the NPHP diagnosis (Hurd & Hildebrandt, 2011; Soliman et al., 2012; Zollinger et al., 1980). Renal biopsy should be performed in cases where the differential diagnosis is required to distinguish NPHP from other chronic kidney diseases or when no genetic mutation is identified in known NPHP genes (Luo & Tao, 2018; Raj et al., 2016). Ophthalmological and neurological examinations are recommended if retinal changes or CNS abnormalities are observed in association with NPHP in case of NPHP-RC (Raj et al., 2016).

4.6 Treatment

Currently, there is no treatment for NPHP or related ciliopathies. NPHP is managed by delaying the progression from chronic kidney disease to ESRD. The focus of clinicians is to transplant kidneys where possible. (Simms et al., 2011). Large number of genes identified in NPHP has provided a wider insight into the disease pathophysiology and zebrafish models of NPHP have been proven useful in determining the effect of drugs on kidney function and development. There is a hope that personalized medicines will be provided to affected individuals in future (Molinari, Srivastava, Sayer, & Ramsbottom, 2017). Vasopressin is a major adenyl cyclase agonist and binds to V2 receptors present in collecting duct. Its elevated levels are correlated with cystic phenotype of NPHP. V2 receptor antagonists, OPC31260 and tolvaptan, have been recently shown to inhibit renal cyst formation when used in murine model of human NPHP3 (Gattone II, Wang, Harris, & Torres, 2003). Tolvaptan has moved into the clinical practice through successful preclinical and clinical trials (Müller, Haas, & Sayer, 2018).

At present. the treatment is only symptomatic to lessen the symptoms and prevent complications. Corrections of electrolyte and acid-base imbalance and hypertension, if present, is treated. Potassium supplements are provided to the affected individuals to alleviate polyuria which is caused by hypokalemia. Vitamin D therapy and calcium supplements help in management of osteodystrophy in individuals with such abnormalities. Anemia and growth retardation can be treated by administering erythropoietin and growth hormones (Hildebrandt, 2009). Chronic dialysis and renal transplantation as the two modes of renal replacement therapy (RRT) are the only available treatment options left, once the disease has developed to ESRD. Ideal mode of RRT is renal transplantation as the disease does not reappear in this case (Srivastava et al., 2018).

4.7 Objectives of the study of NPH families

The study of NPH families was conducted to fulfill the following objectives:

(1) To find out the genetic basis of nephronophthisis and/ or NPHP-RC in families recruited from Pakistani population.

(2) To determine the potential pathogenicity of the identified mutation on the corresponding protein products.

RESULTS AND DISCUSSION

4.8 NPH families enrolled in the study

The current study protocol was approved from the Institutional Review Board of Quaid-i-Azam University Islamabad, Pakistan. A sum of 5 probands from 3 unrelated families were enrolled in this study. Affected families were referred to Department of Nephrology, The children's Hospital and Institute of Child Health Lahore for the evaluation of polyuria, treatment resistant anemia, polydipsia and secondary enuresis. Investigations carried thereafter lead to the diagnosis of nephronophthisis. Becton Dickinson syringes were used for blood drawing from all the available members of each family. The blood was transferred to ethylene-diamine-tetraacetic acid (EDTA) vacutainers and stored at 4^{o}C until

further processing for DNA extraction. All the families provided written informed consent for participating in the study.

4.9 Family D (Lab ID: NPH11)

Family D was recruited from Hafizabad, Pakistan. Diagnosis of NPHP was confirmed based on the initial presenting symptoms and laboratory tests in the local Government hospital, Lahore and family history established the autosomal recessive NPHP associated with severe developmental delay and eye abnormalities. Pedigree construction (Fig.4.1) was done based on the information provided by the parents of proband (II-2).

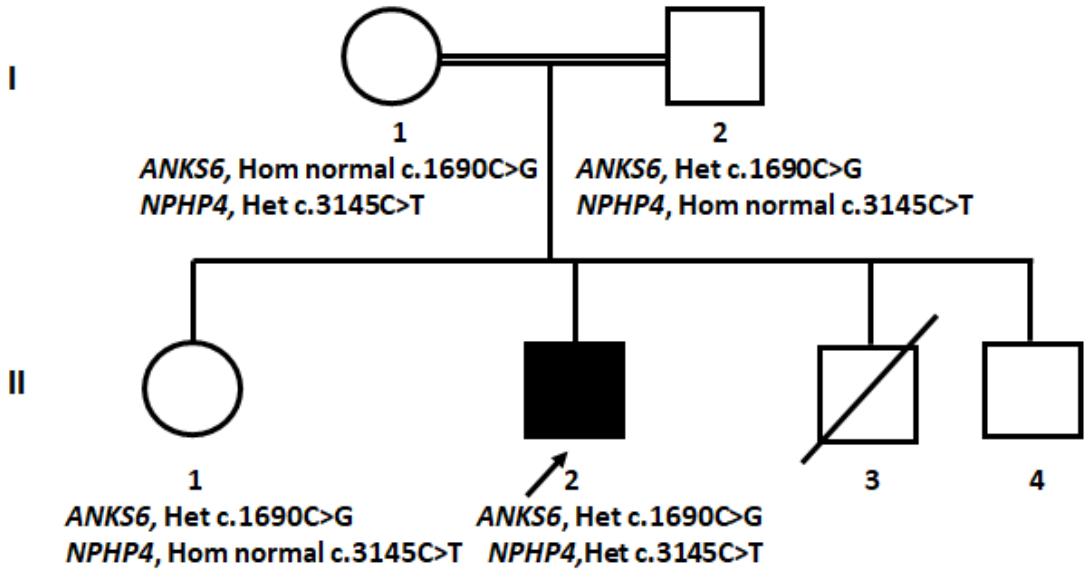

Figure 4. 1: Pedigree of family D. Male and female members of the family are represented by squares and circles respectively. Healthy members are represented by unfilled shapes while filled shapes represent affected members; lines across the shapes represent the deceased members in the family; double lines show the consanguinity.

4.9.1 Clinical features of the patient (Family D; II-2)

We investigated an NPH patient (II-2) born to first cousins in a Pakistani family. The patient's history stated his birth via SVD after an uneventful gestation. The patient presented with severe vomiting at an age of 4 months which remained persistent for two years. Nystagmus and developmental delay were noted within the first year of life. He was

unable to walk till the age of 3 years and slowly lost the control to move his right arm. At the age of four years, he was diagnosed with lower limb immobility and renal disease, which progressed slowly. He was diagnosed with NPH at eight years of age when he presented with polyuria, polydipsia, growth retardation and severe anemia. Renal ultrasound revealed parenchymal hyperechogenic kidneys and cysts at corticomedullary junction which was poorly differentiated. The laboratory findings are listed in Table 4.2. Family history showed his younger brother (II-3) died at the age of six months without a clinical diagnosis, appropriate follow-up and treatment. The parents lacked a detailed history of the patient except severe vomiting. Biological samples were collected from the family members (I-1, I-2, II-1 and II-2) after informed written consent for participating in the study and to publish clinical history of the patient.

Table 4.2: Clinical findings of the patient.

Sr. No.	**Serum biochemistry**	**Results**	**Reference range**
1	Sodium	140 mmol/L	136-145 mmol/L
2	Potassium	5.3 mmol/L	3.5-5.3 mmol/L
3	**Phosphorous**	***12.6 mg/dL**	**2.7-5.4 mg/dL**
4	Chloride	100 mmol/L	90-110 mmol/L
5	Calcium	9.8 mg/Dl	8.5-10.2 mg/dL
6	Urea	35 mg/Dl	10-50 mg/dL
7	Creatinine	1.2 mg/Dl	0.6-1.3 mg/dL

*indicates higher than normal levels.

4.10 Molecular genetic study

Homozygous *NPHP1* gene deletion was screened and excluded in all the three NPHP families (D,E and F) before they underwent whole exome sequencing. This was necessary

because *NPHP1* deletion is the frequent genetic cause of 25% nephronophthisis cases and cannot be identified by whole exome sequencing (Braun et al., 2016).

4.10.1 *NPHP1* deletion screening

Genomic DNA extraction from whole peripheral blood of the study participants was performed following phenol-chloroform method. *NPHP1* deletion was tested in the patient (II-2) and his parents by PCR amplification of gDNA for the coding exons of the gene located on chromosome 2q13 as homozygous *NPHP1* deletions are reported in almost 25% cases of NPH. This is an established noninvasive diagnostic approach for NPH that allows diagnosis of the disease without renal biopsy (Konrad et al., 1996). Negative amplification indicated homozygous gene deletion while positive amplification indicated intact *NPHP1* on one or both alleles.

4.10.2 Whole exome sequencing data analysis

We shortlisted non-sense, missense, frameshift and splice site variants (10,450) as these are more likely to affect the protein structure and function (Figure 4.2). From these variants we selected variants with unknown allele frequency or MAF<0.01 in public databases: 1000Genomes (http://www.1000genomes.org/data) and ExAC (http://exac.broadinstitute.org/). We divided these rare homozygous and heterozygous variants (1002) in two groups: 1) variants in genes previously linked to NPHPand NPHP-RC) and 2) variants in other genes. Group 1 variants (3) were subjected to Sanger sequencing and in silico analysis. Group 2 variants (999) were prioritized according to the autosomal recessive mode of inheritance, the biological function of the respective gene with reference to OMIM and published literature and in-silico prediction. Variant effect on protein structure and function was tested through following bioinformatics tools: PredictSNP2 (combining the DANN, CADD and FATHMM), SIFT, Polyphen-2 and MutationTaster. These analyses provided us with three variants, which were absent from our in-house exome database of 100 healthy samples. Sanger sequencing was performed for validation and segregation analysis.

4.10.3 Segregation analysis

Segregation analysis was performed in all the family members using Sanger sequencing. Primers were designed manually for both the variants identified. The healthy members were all wild type homozygous or heterozygous for either of the variants found to be pathogenic in patient II-5 (Figure 4.3).

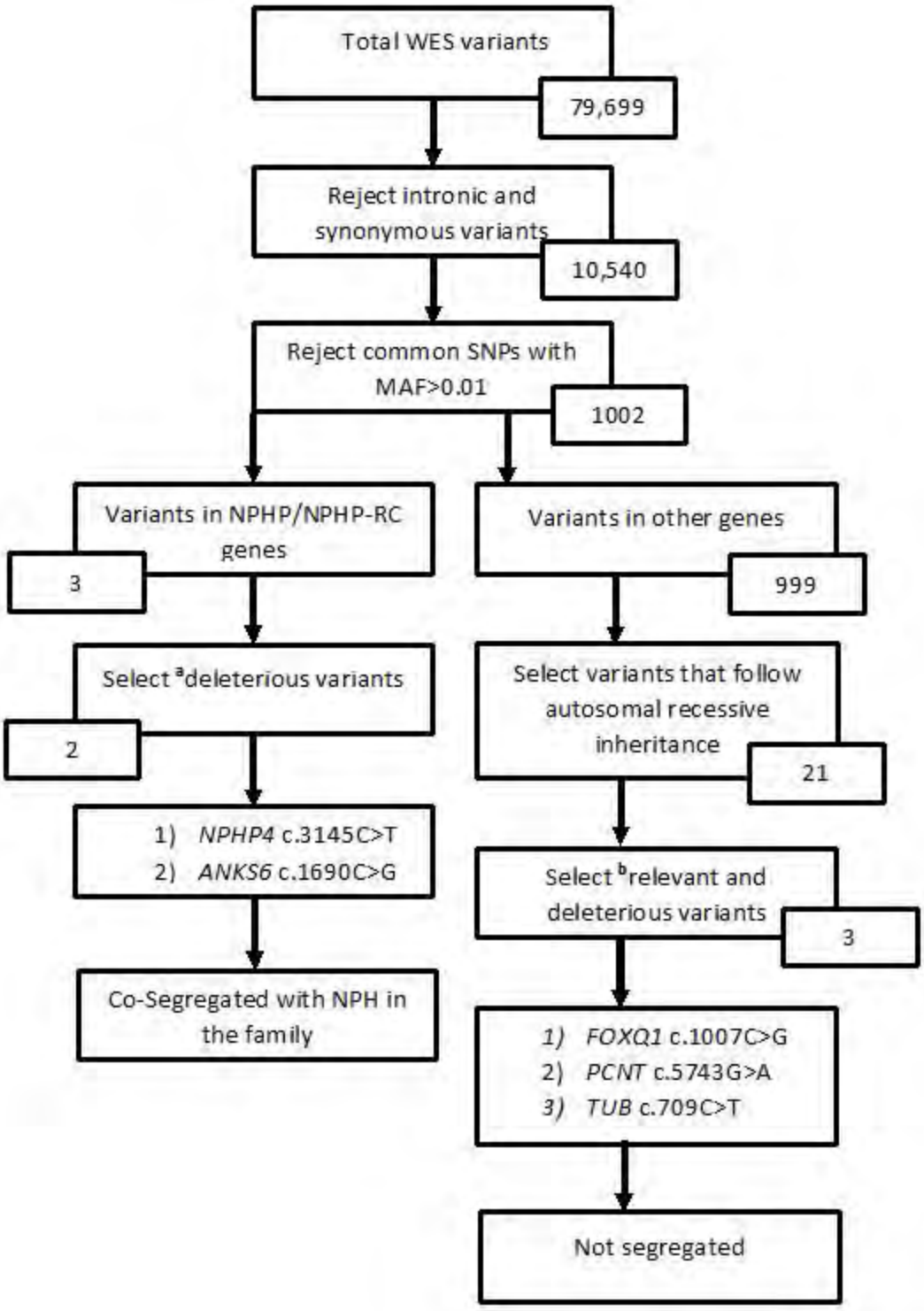

Figure 4.2: Flow sheet to understand the filtering process to identify a genetic cause underlying phenotype in II-2. a = variants are considered deleterious by in silico tools, b =

variants are said to be relevant according to biological functioning of respective genes by literature review and OMIM.

4.10.4 *In silico* prediction

Different bioinformatics tools i-e, PredictSNP2 (combining the DANN, CADD and FATHMM), SIFT and MutationTaster were used to predict the effect of nucleotide change on structure and function of protein. Furthermore, STRING pathway (https://string-db.org/) was used to see the possible interactions NPHP4 and ANKS6 proteins (Figure 4.4). Results of this analysis showed some common pathways being shared by these two proteins (Table 4.3).

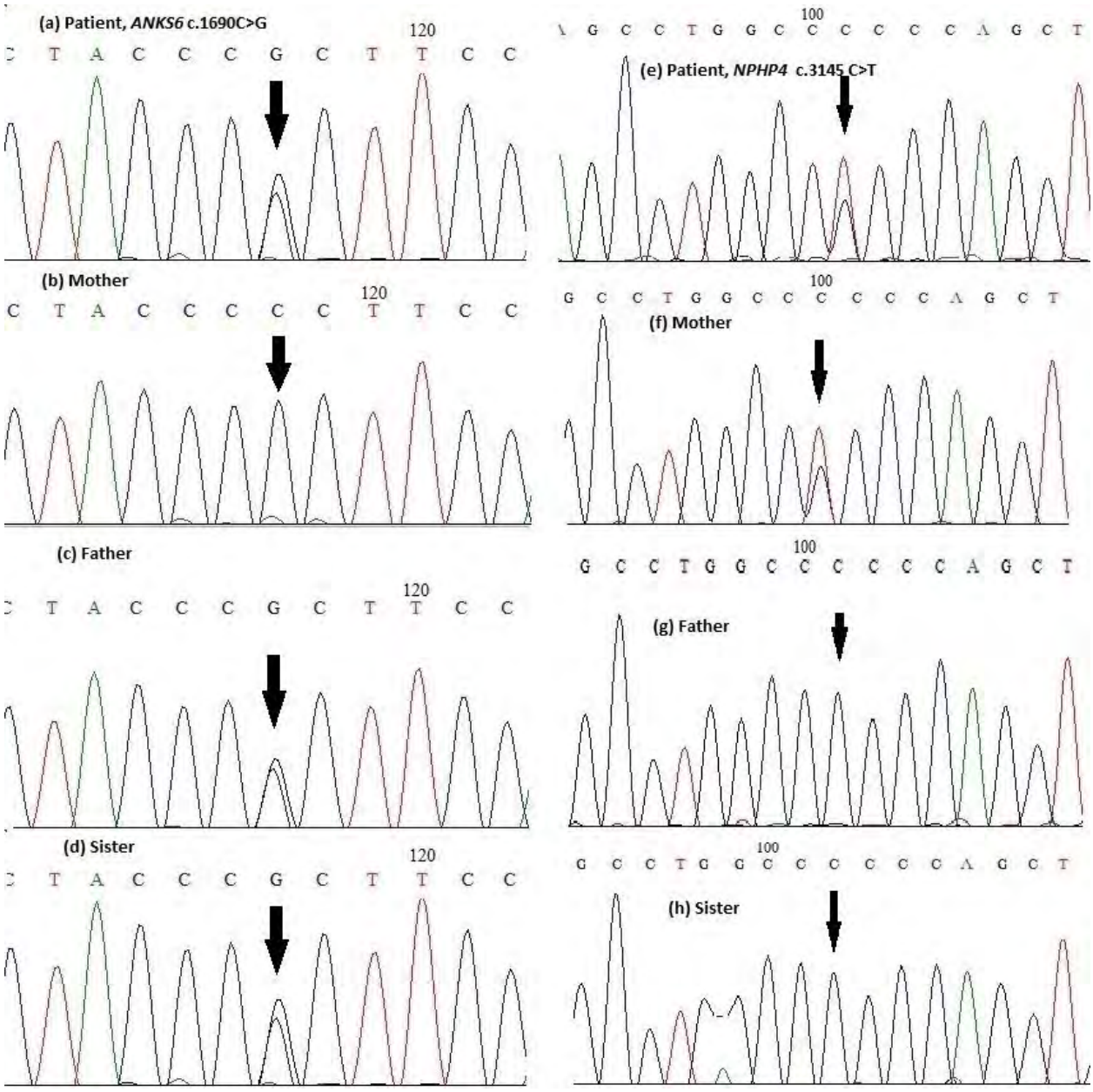

Figure 4.3: Sequencing chromatograms obtained using Sanger sequencing of family D. Sequencing results from (a) to (d) are showing *ANKS6* c.1690C>G in Patient and his unaffected family members. Sequencing results from (e) to (h) are showing *NPHP4* c.3145C>T in Patient and his unaffected family members.

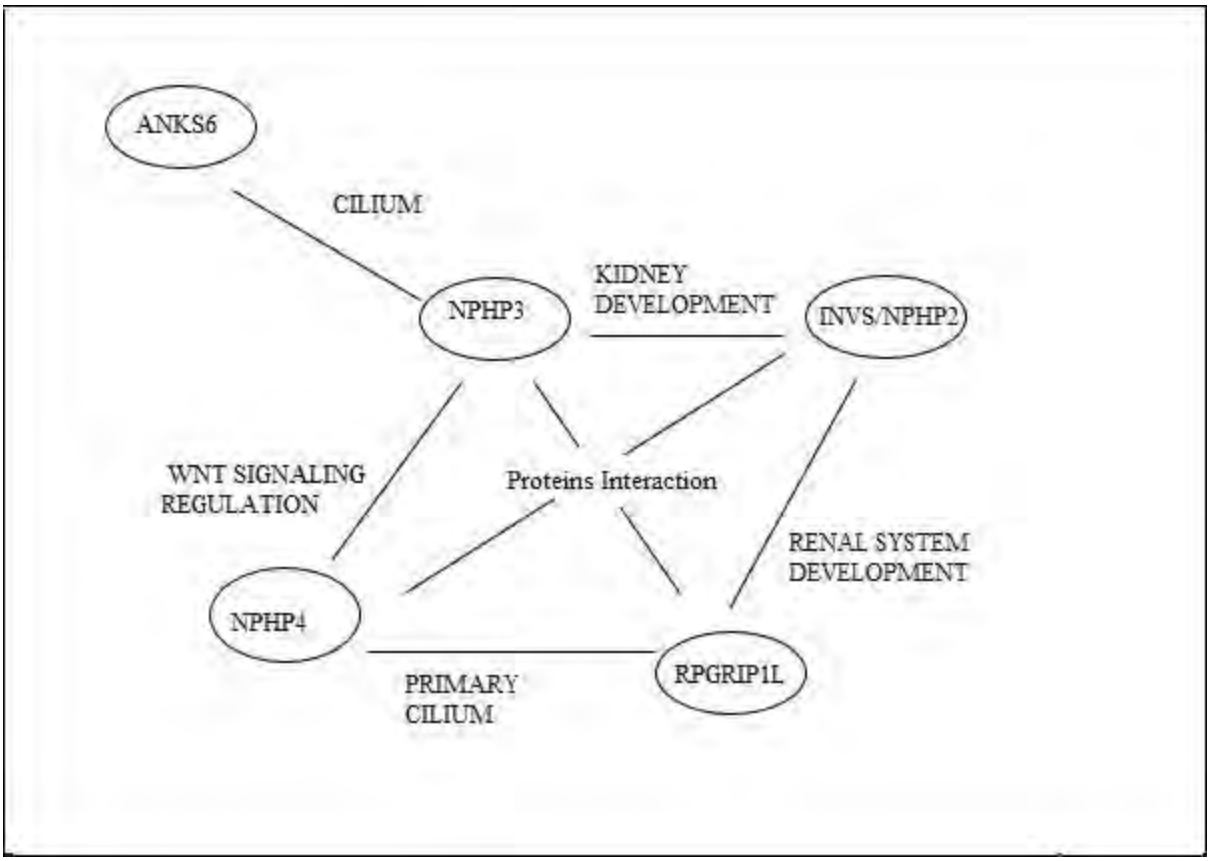

Figure 4.4: Predicted common interactions of protein products of *NPHP4* and *ANKS6* genes.

4.11 Results

The proband (II-2) was first tested for *NPHP1* deletion using PCR amplification. The gDNA of all family member was successfully amplified through PCR for coding exons of *NPHP1* indicating an intact gene. Whole exome sequencing of the proband revealed three missense variants in NPH linked genes; two heterozygous variants in *NPHP4*: [GRCh37/hg19; chr1: 6,046,228G > A; NM_015102.4: c.122C> T; p.(Pro41Leu)] and [GRCh37/hg19; chr1: 5,934,617 G > A; NM_015102.4: c.3145C> T; p.(Pro1049Ser)], and one variant in *ANKS6* (*NPHP16*): [GRCh37/hg19; chr9: 101,536,290 G > C; NM_173551.3: c.1690 C> G; p.(Pro564Ala)]. Sanger sequencing in all family members showed that both *NPHP4* variants were present on paternal allele. Moreover, c.122C>T variant was predicted as benign by SIFT and PolyPhen-2. The variants c.3145C> T (*NPHP4*) and c.1690 C> G (*ANKS6*) were found to be co-segregating in the family in accordance with digenic (oligogenic) inheritance.

Table 4.3: Common pathways predicted by STRING analysis of *NPHP4* and *ANKS6*

Pathway ID	Pathway description
Biological Process (GO)	
GO:0090090	Negative regulation of Wnt signaling pathway
GO:0001822	Kidney development
GO:0009968	Negative regulation of signal transduction
GO:0072001	Renal system development
GO:0001655	Urogenital system
Cellular Component (GO)	
GO:0005929	Cilium
GO:0072372	Primary cilium
GO:0035869	Ciliary transition zone
GO:0097546	Ciliary base

Three more variants were found in genes *PCNT*, *TUB* and *FOXQ1* after applying the various filtering steps. These genes have role in kidney function or damaging effects on protein function according to various prediction tools but none of these segregated with disease in the family. The NPHP4 variant: [c.3145C> T; p. (Pro1049Ser)] has a CADD score of 23.7 and it is predicted to be deleterious according to PredictSNP2, Mutation Taster, and SIFT. It has a minor allele frequency of less than 0.01 in 1000 Genome Project, 0.0001 in ExAC database and no homozygotes reported. The ANKS6 variant [c.1690 C> G; p. (Pro564Ala)] has a CADD score of 22.1 and it is damaging according to PredictSNP2, SIFT and Mutation Taster. The variant has a minor allele frequency <0.01 in 1000 Genome Project and 0.00009 in ExAC database with no homozygote reported. Additionally, we found a heterozygous missense variant [c.1501G> A; p.(Ala501Thr)] in ANKS3 gene with less than 0.01 MAF in public databases and no homozygotes found in these databases. In silico predicting tools mentioned above showed deleterious effect of this mutation on protein function.

4.12 Discussion

Next generation sequencing particularly the whole exome sequencing has enabled not only to uncover new genes associated with diseases but also to resolve the genetic heterogeneous diseases with unknown genetic etiology (Bamshad et al., 2011). Molecular study of nephronophthisis and nephronophthisis related ciliopathies sometimes present complicated approach to identify the causative genetic mutations (Srivastava et al., 2018). Here in this patient we were able to find out the genetic variants at two different loci using WES and gave a digenic model as a most parsimonious analysis to describe the genetic defect underlying NPHP related ciliopathy.

There are few patterns of digenic inheritance including mutations in directly or indirectly interacting genes, genes in common pathway, similar functions of the two different genes mutated or the genes not linked to each other i-e, belonging to different pathways (Gazzo et al., 2015). Digenic inheritance is more likely when the two different genes encoding different proteins have a function in a singular pathway. There have been several publications reporting digenic inheritance in inherited diseases. Examples include retinitis pigmentosa, Bardet Biedel syndrome, Joubert syndrome, nephronophthisis, hypercholesteremia (Beales, Elcioglu, Woolf, Parker, & Flinter, 1999; Schäffer, 2013).

In the current study, we reported two novel heterozygous variats in *NPHP4* and *ANKS6* genes encoding the ciliary protein and cilia interacting protein respectively. Nephrocystin 4 encoded by *NPHP4* is a ciliary protein component of transition zone gate and act to regulate the movement of other dissolved and membrane bound proteins across the flagellar and cytoplasmic compartments. (Awata et al., 2014). NPHP4, at the primary cilium, also negatively regulates the Wnt signaling to prevent the cysts formation in kidneys during tubular and glomerular development of kidney, a process which requires balanced Wnt signaling. Variant in *NPHP4* might result in overactivation of Wnt pathway which lead to cystic kidneys in NPHP phenotype (Borgal et al., 2012)[*]). *ANKS6* also known as *NPHP16* encodes ankyrin repeat and SAM domain-containing protein 6 with nine N terminal ankyrin repeats and sterile alpha motif at its C terminal. ANKS6 interacts with many primary cilia proteins i-e, /INVSNPHP2, NPHP3 and NEK8/NPHP9 through its ankyrin repeat domain to inhibit the canonical Wnt signaling pathway. Mutations in *ANKS6*

have been shown to cause the NPHP and extrarenal manifestations cardiac defects, situs inversus and laterality defects.(Hoff et al., 2013) Digenic inheritance (heterozygous variants in *ANKS6* and *NPHP2)* has been reported previously in an NPHP patient who also had cardiac defect and mental and motor retardation as extrarenal manifestations (Taskiran et al., 2014). Digenic inheritance in NPH with different combinations of NPH genes (heterozygous mutations in *ANKS6* and *NPHP2/INVS, NPHP2/INVS* and *NPHP4* and *NPHP2/INVS* and *NPHP3*) have been reported previously which might suggest the close interaction of proteins encoded by these genes. (Hoefele et al., 2007; Taskiran et al., 2014). We used STRING pathway (https://string-db.org/) to see the possible interactions of products encoded by *NPHP4* and *ANKS6.* Analysis showed some common pathways which are shared by NPHP4 and ANKS6 proteins (Fig.4). This supports our results that how the proteins encoded by these variations could interact to produce the NPH phenotype in II-2.

To our knowledge, the current study is the first report of oligogenic inheritance in Pakistani patient affected with NPHP. Pro1049Ser in *NPHP4* and Pro564Ala in *ANKS6* might also act in concert with each other since both the genes encode proteins which act to inhibit Wnt signaling pathway and therefore might be responsible to develop the disease phenotype in our patient. Both the genes have been previously reported in NPHP cases and pathogenic mutations in these genes prospect the likelihood of digenic inheritance. A study on phenotypic spectrum of NPHP-RC showed that subjects with mutations in *NPHP4* develop ESRD at relatively older age and extrarenal manifestations in these subjects are rare except for one subject who presented severe developmental delay. (König et al., 2017) These phenotypes are also observed in our patient. Interestingly, the mutation in *ANKS3* found in this patient may also act as a modifier allele in our proposed digenic model. This is in line with the recent findings that ANKS3 protein interact with a complex containing *NPHP1, NPHP4* and *NPHP8* formed at transition zone of primary cilium and contribute to mediate their function. ANKS3 is also an interacting partner of ANKS6 (Yakulov et al., 2015). Although the possibility of mutant allele in non-coding regions in *ANKS6* or *NPHP4* genes cannot be excluded and expression studies with double mutants will confirm and validate our results, the most obvious interpretation of our WES data and deleterious effects of the subsequently identified mutations reported in this study suggest the digenic inheritance as a disease mechanism in this patient.

In summary we report two novel variants in *NPHP4* and *ANKS6* genes in a Pakistani NPHP patient. We devised a digenic model responsible for pathology in this patient, these findings are based on WES data analysis, Sanger validation and subsequent *in silico* prediction. The two genetic variants presented in this study may expand the mutation spectrum of NPHP-RC. In addition, our data may provide further evidence to support oligogenicity in NPHP and related ciliopathies. Being aware of limited evidence we provided for the digenic inheritance in the observed pathology in a single patient, we suggest functional investigations to prove the findings presented in the current study.

4.13 Family E (Lab ID: NPH6)

Family E was recruited from Lahore, Pakistan. Diagnosis of NPHP was confirmed based on the initial presenting symptoms and laboratory tests in the local Government hospital, Lahore and family history established the autosomal recessive NPHP. The consanguineous family had five children three of which were affected with NPHP. Pedigree construction (Figure 4.5) was done based on the information provided by the parents of proband (II-4).

4.13.1 Clinical features of family E

Different biochemical parameters of the patients (II-1, II-2 and II-4) belonging to family E were tested which are shown in Table 4.4 and their brief history is described below

4.13.1.1 Patient 1 (II-1)

The patient II-1 was the first-born male child of the family. He was born after an uneventful pregnancy and remain healthy. He was suffered with mild disease symptoms polyuria, polydipsia and secondary enuresis at 14 years of age. Anemia and growth retardation were also observed. The exact NPHP diagnosis was made at 16 years of age by ultrasound imaging which revealed bilaterally cystic kidneys along the diminished differentiation of corticomedullary junction. Kidney size was normal. Various biochemical values are given in Table 4.4. He died with ESRD at 22 years of age during this study.

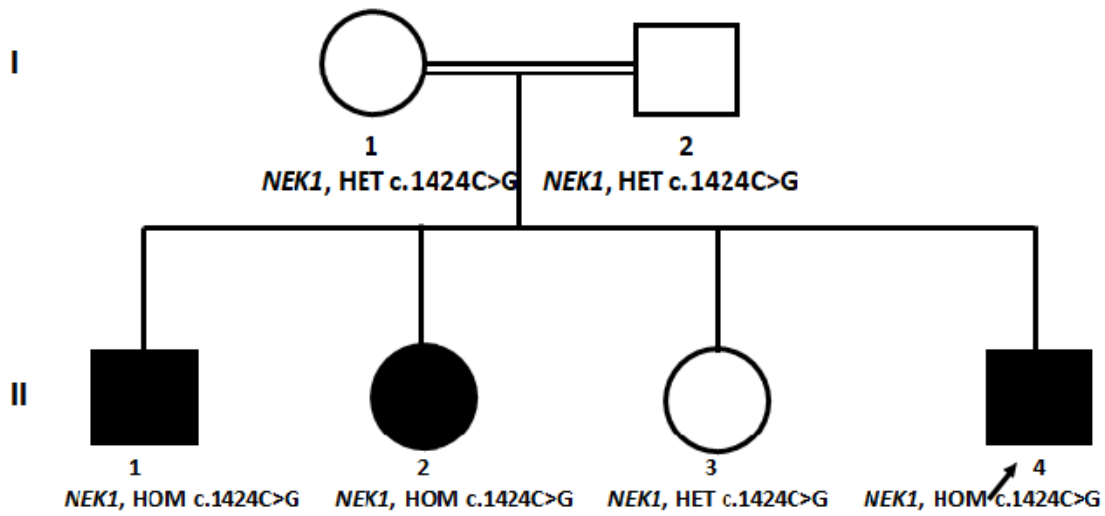

Figure 4.5: Pedigree of family E. Male and female members of the family are represented by squares and circles respectively. Healthy members are represented by unfilled shapes while filled shapes represent affected members; lines across the shapes represent the deceased members in the family; double lines show the consanguinity. Arrow head points towards proband.

4.13.1.2 Patient 2 (II-2)

The second patient was a young female, died with ESRD at 15 years of age. She was alive at the time of sample collection. The clinical symptoms polyuria, polydipsia, anemia and secondary enuresis appeared at 9-10 years of age and ultrasound examination revealed cysts along the poorly differentiated corticomedullary border. Kidney size was shrunken (Right kidney=4.4X2.1cm, Left kidney=5.6X2.5cm). The disease progressed to ESRD and she was on hemodialysis for a year before her death.

4.13.1.3 Patient 3 (II-4)

The proband (Patient II-4) was the youngest of all. He was diagnosed with renal impairment at 9 years of his life. He underwent ultrasound that revealed bilaterally shrunken kidneys (Right kidney=5.1X3.2cm, Left kidney=8.8X3.5cm) and small sized cysts at the poorly differentiated corticomedullary junction. The disease progressed to ESRD at 11 years. The patient underwent kidney transplant, donor being his mother, at the

age of 12 years. The transplanted graft functioned normally for only a year and presently the patient undergoes hemodialysis 3-4 times per week.

Table 4.4: Biochemical findings of patients (II-1, II-2, and II-4), family E.

Sr. No.	**Biochemical parameters**	**Results**			**Reference range**
		Patient II-1	**Patient II-2**	**Patient II-4**	
1	Sodium (serum)	143mmol/L	145mmol/L	145mmol/L	136-145mmol/L
2	Potassium (serum)	4.5mmol/L	4.0 mmol/L	5.0 mmol/L	3.5-5.3 mmol/L
3	Phosphate(serum)	3.7mg/dL	2.5mg/Dl	3.9mg/dL	2.5-5.0 mg/dL
4	Calcium(serum)	9.9mg/dL	10.1mg/dL	9.6 mg/dL	9.0-10.7 mg/dL
5	Creatinine (serum)	***3.0 mg/dL**	1.2 mg/dL	***1.5 mg/dL**	0.6-1.3 mg/dL
6	Urea (serum)	**60 mg/Dl**	45 mg/dL	35 mg/dL	10-50 mg/dL
8	Protein (Albumin) spot urine	***16.0mg/dL**	NA	***12.5 mg/dL**	0.0-12.0mg/dL
9	Alkaline phosphatase (LFT)	***447U/L**	100U/L	150 U/L	0.0-258U/L

LFT=liver function test, *indicates values falling outside the normal range.

4.14 Molecular genetic study

4.14.1 *NPHP1* deletion screening

NPHP1 gene deletion screening was performed as described for the family D; patient II-5. None of the affected or healthy members had *NPHP1* gene deletion.

4.14.2 Whole exome sequencing analysis

Proband's DNA (II-4) underwent WES and gave a total of 63,763,000 reads. The average size of read length was 101bp and average depth of target regions was 125.8. Reads were mapped to reference human genome and subsequent filtering steps provided 79,871 variants. The variants were checked for previously associated with NPHP and NPHP-RC genes (discussed in section 4.4). No potential variant was found in genes reported for the disease phenotype. To identify the variant responsible for disease we used three different strategies;

First approach, we used, was to see the variants in genes with relatively high expression in kidneys. For this, we use human protein atlas database (http://www.proteinatlas.org/) which showed 329 such genes. We applied a filter to select variants in these 329 genes for analysis. Afterwards, from the selected variants we further selected the variants that affect the protein structure i-e, nonsynonymous, frameshift, indels, nonsense and splice site variants. Next, a filter was applied to select the variants with MAF<0.01. This reduced the number of variants to 14, from these, the variants following the autosomal recessive mode of inheritance were selected which further reduced the number to 3; a compound heterozygous variation in *KCNJ1* and a homozygous variation in *XPNPEP2*. The second variant was ignored as it was located on X chromosome and the pedigree did not show X-linked trait. Variant in *KCNJ1* was screened in the whole family for validation and segregation (Figure4.6a).

Secondly, from all the homozygous and heterozygous variants (79,871 variants), we applied filter to select the nonsynonymous, frameshift, indels and splice site variant that could alter the protein structure and function. Afterwards, only those variants were selected which were compatible with autosomal recessive mode of inheritance i-e, homozygous or compound heterozygous. This further reduced the number of variants, we then applied a filter to select the variants of unknown MAF or MAF <0.01 in 1000 GP and ExAC database. The variants obtained were checked in in-house exomes (WES data of 100 healthy individuals) and the variants which were unique only to the proband's exome were selected. After this step, we were left with 4 variants (Figure 4.6b).

Thirdly, we applied a filter for WES to select continuous stretches of homozygous peak regions from 79,871 variants and came up with 3081 variants, from these, we excluded the common variants (MAF>1%), synonymous variants, intronic and heterozygous variants which further reduced the number to 40. Short listed homozygous variants were then checked in in-house exomes and the common variants were excluded. This step reduced the variants to 4, interestingly all of these four were common in second and third approach (Figure 4.6c). Prioritizing the variants based on their relevant biological function (using OMIM and literature) and *in silico* prediction, we selected variants in *ZNF154* and *NEK1, NAF1* and *ANBCG5* for segregation study, the variant in *NEK1* was segregated in accordance with mendelian inheritance.

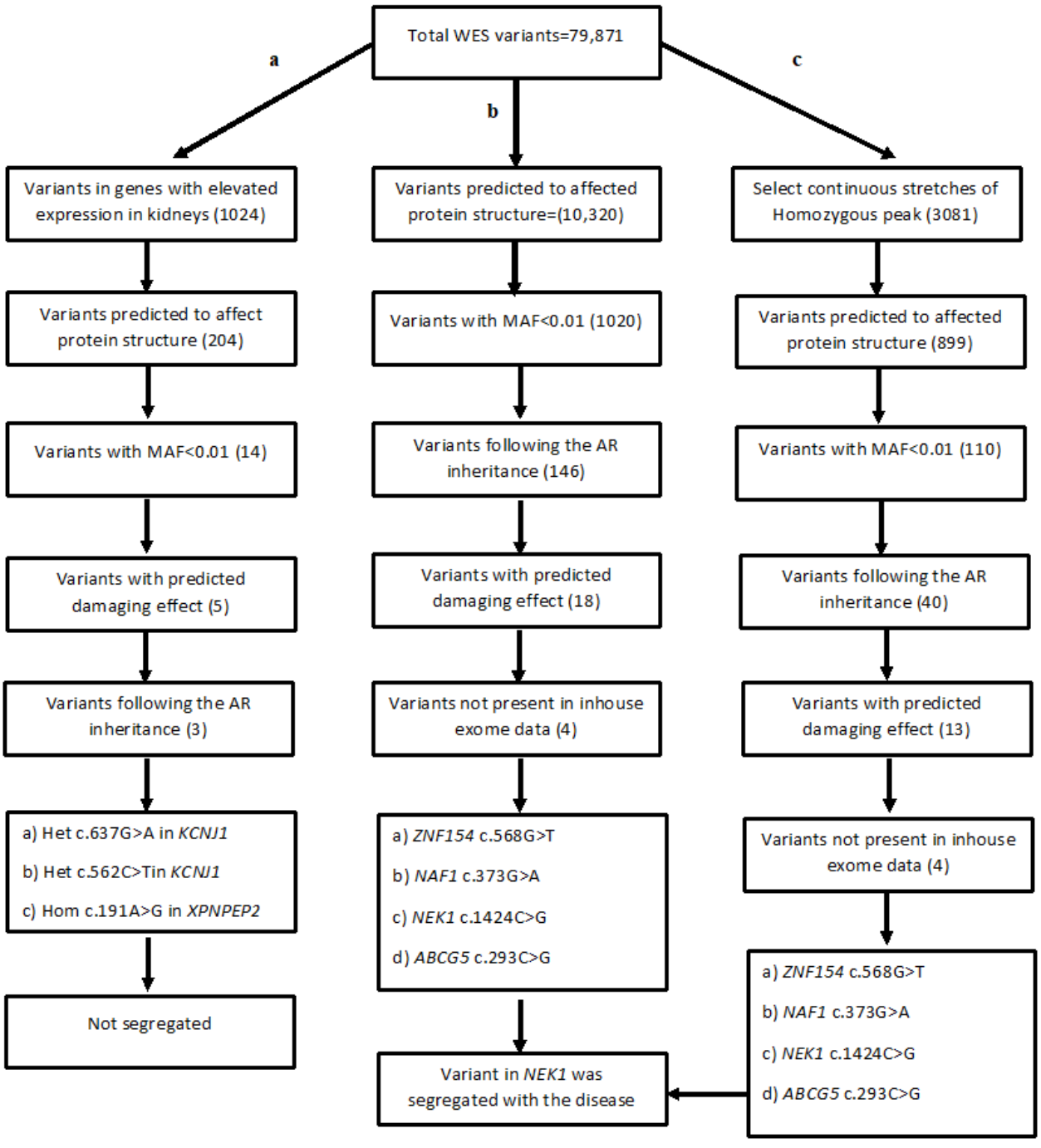

Figure 4.6: Flow chart showing three (a, b and c) different strategies to reach the pathogenic variant from exome data.

4.14.3 Segregation analysis

Segregation study was performed for all the family members for the shortlisted variants (Table 4.5). The unaffected members (I-1, I-2 and II-3) were all heterozygous for c.1424C>G variant in *NEK1* gene and all the affected members (II-1, II-2 and II-4) were homozygous for the c.1424C>G variant (Figure 4.8). None of the other three were found to be segregating with the disease.

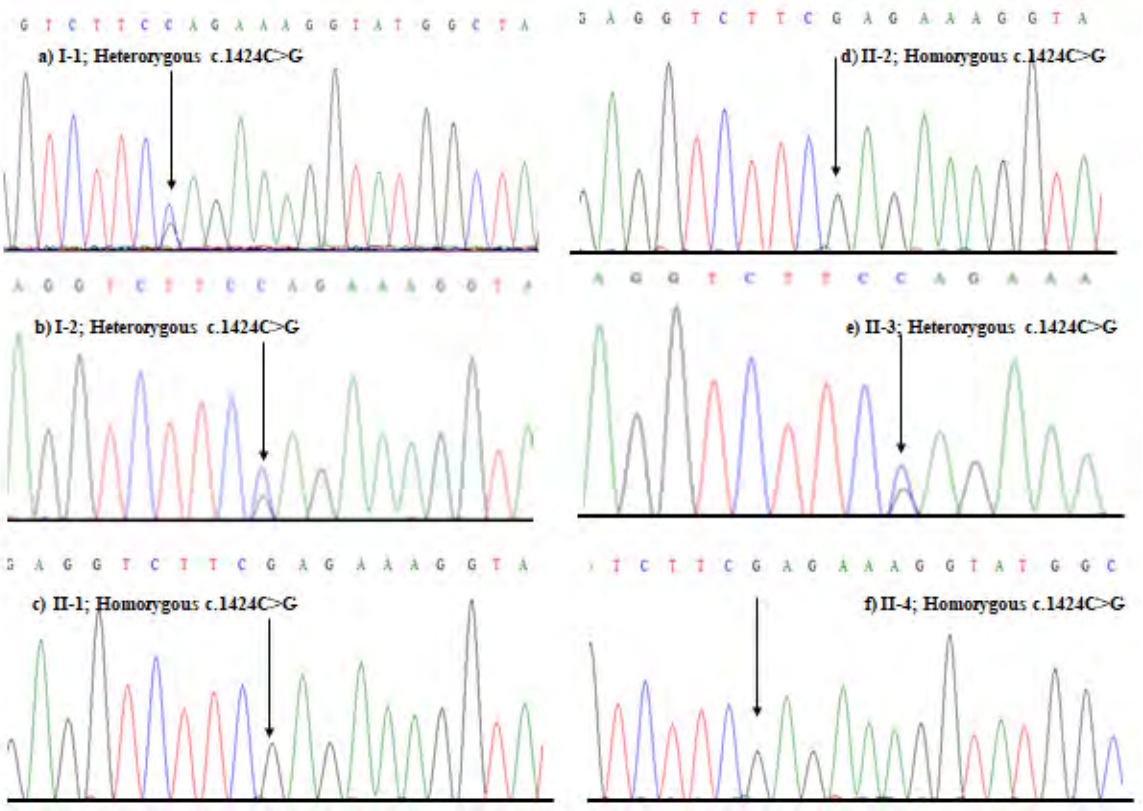

Figure 4.7: Electropherograms obtained using Sanger sequencing of family E. Sequencing results from (a) to (f) are showing *NEK1* c.1424C>G in affected (II-1, II-2, II-4) and unaffected (I-1, I-2, II-3) family members.

Table 4.5: Short listed variants from the WES analysis

Chrom	**Position**	**Gene Name**	**HGVS.c**	**Zygosity**	**Effect**	**AF**	**ExAC**	**PolyPhen2 Scores**	**SIFT Scores**
2	44,059,195	*ABCG5*	c.293C>G	Hom	Missense variant	0.001	0.002	1.0	0.007
4	164,085,536	*NAF1*	c.373G>A	Hom	Missense variant	0.0007	0.0007	1.0	0.004
4	170,477,089	*NEK1*	c.1424C>G	Hom	Missense variant	0.002	0.001	0.89	0.002
19	58,213,749	*ZNF154*	c.568G>T	Hom	Stop-gained variant	0.003	0.001	--	--

Chrom = chromosome. HGVS.c = Human Genome Variation Society. cDNA position, AF = allele frequency from 1000 genome project3, Hom = homozygous, NA = not available, ExAC=Exome Aggregation Consortium.

4.15 Results

WES of the proband (II-4) yielded a large amount of data which, after alignment and variant calling, provided us with 79,871 variants. Complex filtering steps were performed as discussed in above section and we selected 4 variants which we consider for segregation study in the family. Sanger validation proved cosegregation of c.1424C>G in *NEK1* gene with the affected members of the family. Bioinformatics analysis revealed that c.1424C>G; p. Pro475Arg in *NEK1* is predicted to be deleterious according to PolyPhen2, Mutation Taster, and SIFT. It has a minor allele frequency of less than 0.01 in 1000 Genome Project and ExAC database. The novel variant in *NEK1* is located within coiled coil domain of the protein and might affect its ciliary localization (Figure 4.7). The variant was not found in

200 Southern Punjab controls.

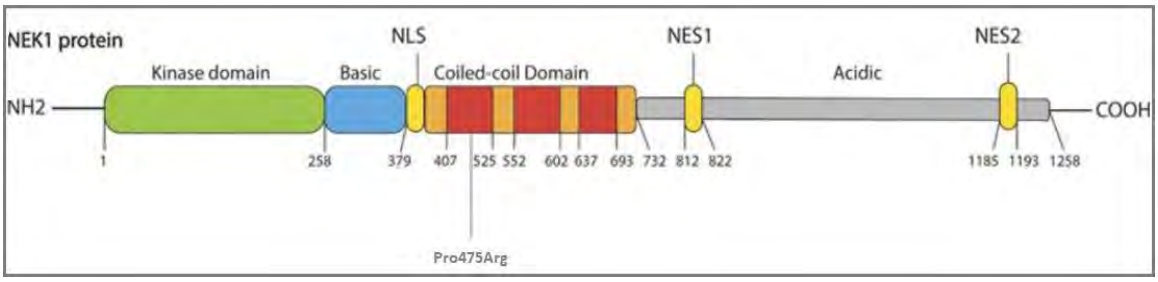

Figure 4.8: NEK1 protein structure (modified from (Monroe et al., 2016))

4.16 Discussion

Since the past few years, NGS has enabled not only the identification of many new genes responsible for NPHP-RC but also helped in demonstrating the links between pathophysiology of NPHP-RC and different pathways e.g. mTOR pathway, DDR pathway, cAMP pathways (Chaki et al., 2012).

ZNF423, SDCCAG8 and *CEP290* encode proteins which play role in DDR signaling and knockdown models of *ZNF423* indicated increased sensitivity to DNA damage (Chaki et al., 2012). NIMA-related kinase 1 encoded by *NEK1* gene is also involved in DDR and functions in regulating renal cells apoptosis after cell damage (Chen, Chen, et al., 2014). Increased kinase activity of NEK1 is required by an injured cell before it recover, so that the cell might sense and repair the DNA and cellular damage more efficiently. Mutated *NEK1* produce insufficient or abnormal NEK1 protein resulting in aberrant death of kidney cells or they may fail to proliferate properly (Chen, Chiang, et al., 2014). In the present study, we identified a missense homozygous mutation (c.1424C>G) in *NEK1* gene in three siblings (II-1, II-2 and II-4) affected with NPHP like ciliopathy.

In the current study we used a stepwise approach to identify causative variant and narrowed down the list of genetic variants that might be responsible for the disease. We did not find any pathogenic mutation in known susceptibility NPHP genes that were shared by affected members of family which lead to the possibility of other variants being responsible for NPHP in the family E. To confirm our results, we used the Sanger sequencing method which narrowed our scope to only one variant; [c.1424C>G, p. Pro475Arg] in *NEK1*. The

variant Pro475Arg in NEK1 is identified as the susceptible genetic variant associated with the disease.

NEK1 protein consists 1286 amino acids protein which is divided into an N-terminus kinase domain, a large central coiled-coil domain (CCD) and C-terminus, CCD helps the protein in ciliary localization (White & Quarmby, 2008). Keeping in mind the role of *NEK1* gene in cilia formation in mouse model of PKD and recent reports demonstrating its localization to basal body and primary cilia like most of NPHP proteins (White & Quarmby, 2008) (Yim, Sung, You, Tian, & Benjamin, 2011), we propose that it might be causing NPHP phenotype in this affected family. The impact of nonsynonymous variant was predicted by multiple algorithms PredictSNP2, MutationTaster, and PolyPhen, all of which supported the pathogenicity of Pro475Arg in *NEK1* encoded protein.

Studies have shown that combination of WES and homozygosity mapping is a powerful tool for identification of novel disease genes in consanguineous families (Braun et al., 2016) (Chaki et al., 2012; Schueler et al., 2015). We performed *NPHP1* gene deletion on the family members and then proceed to WES when no deletion was found. By applying the different strategies to filter data, we identified a novel genetic cause in a family with renal ciliopathy clinically suspected as NPHP in which the unknown genetic causes have been excluded. So far, the mutations in *NEK1* gene have not been described with NPHP-RC, but this rarity is not surprising in such complex heterogenetic diseases as mutations in majority of the recently identified NPHP-RC genes accounts for less than 10 families worldwide (Hoff et al., 2013; Otto et al., 2010; Otto et al., 2008; Schueler et al., 2015). Further molecular and genetic studies will help in determining whether *NEK1* is indeed an NPHP candidate gene.

Our study has some limitations which must be addressed. First, NPHP is a rare disease and the studied family has only three patients and 3 unaffected members, therefore the size of pedigree was relatively small. Secondly, functional investigations to support the pathogenic role of the identified variant cannot be elucidated because of the limited lab facilities.

In conclusion, we report the novel variant in *NEK1* gene through whole exome sequencing and bioinformatics analysis. The study is another good example of genetic characterization

of heterogenetic and complex diseases through WES in an efficient and cost-effective manner.

4.17 Family F (Lab ID: NPH3)

Family F was recruited from Lahore, Pakistan. Diagnosis of NPHP was confirmed based on the initial presenting symptoms and laboratory tests in the local Government hospital, Lahore and family history established the autosomal recessive NPHP. The consanguineous family had five children two of which were affected with NPHP. Their paternal cousins were also affected with the same phenotype. All the four patients from two loop pedigrees had ESRD. Proband was a 15-year-old female. Her elder brother and one of her paternal cousin died of the same disease and the second paternal cousin was kept on dialysis. Pedigree construction (Figure 4.9) was done based on the information provided by the parents of proband (III-3).

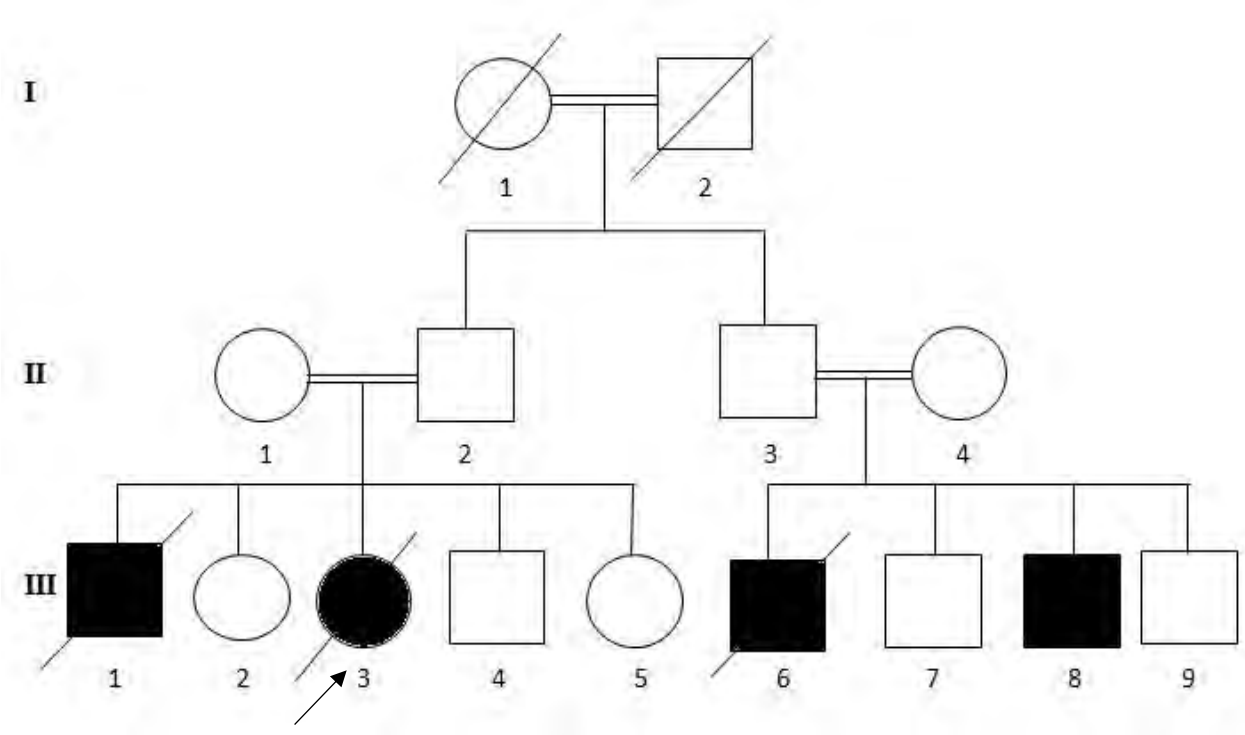

Figure 4.9: Three generation pedigree of family F. Male and female members of the family are represented by squares and circles respectively. Healthy members are represented by unfilled shapes while filled shapes represent affected members; lines across the shapes

represent the deceased members in the family; double lines show the consanguinity. Arrow head points towards proband.

4.17.1 Clinical features of family F

The basic electrolytes of available patients were tested and shown in Table 4.6. Brief history of the patients is given below:

4.17.1.1 Patient 1 (III-1)

Patient III-1 was the first child of consanguineous Pakistani family. He was born after a non-complicated pregnancy with normal birth weight and height. Mild disease manifestations started at the age of 9 years e.g. polyuria, polydipsia, hypokalemia. Upon clinical evaluation NPHP was suspected and renal imaging detects shrunken kidneys with poor corticomedullary border. At 13 years of age, he progressed to ESRD and peritoneal dialysis was initiated which continued for over 3 years, after that the patient died. Unfortunately, his biological sample could not be obtained

4.17.1.2 Patient 2 (III-3)

Patient III-3 was the Proband of family F. She was born without any perinatal or postnatal problems at 39th week of gestation. Initially, at the age of 8 years, she presented with mild symptoms e.g., polyuria and polydipsia due to reduced urine concentrating ability. Growth retardation and anemia became prominent as the renal insufficiency progressed. Renal imaging revealed small sized kidneys with few cysts apparent at corticomedullary border. ESRD developed at the age of 12 years and hemodialysis was initiated. She was alive at the time of sample collection and died at the age 15 years.

4.17.1.3 Patient 3 (III-6)

Patient III-6 was diagnosed with NPHP at the age of 8 years. The disease progressed to ESRD at 12 years and he was kept on peritoneal dialysis, but the renal function deteriorated with time the patient died at the age of 18 years before this study started.

4.17.1.4 Patient 4 (III-8)

Patient III-8 was an 18 years adult person. He was well developed but showed polyuria and anemia at 9 years. His clinical examination revealed high serum creatinine and alkaline phosphatase. He

also had elevated blood urea. Ultrasonography revealed bilaterally shrunken hyperechoic kidneys and abnormal corticomedullary junction. There were no visual, hearing or CNS related abnormalities. He was diagnosed with NPHP based on his family history. Presently, he undergoes maintenance hemodialysis every week.

4.18 Molecular genetic analyses

4.18.1 *NPHP1* gene deletion screening

NPHP1 gene deletion screening was performed as described for the family D; patient II-1. None of the affected or healthy members had *NPHP1* gene deletion.

4.18.2 Whole exome sequencing data analysis

WES of the proband (III-3) sequenced 98,571,884 reads with an average size of 101bp. The reads were mapped to reference sequence and followed by variants calling that provided us with a total of 90,965 variants. Analysis of the genes previously associated with NPHP and NPHP-RC were selected, intronic and synonymous variants were excluded from these and only nonsynonymous, frameshifts, splice site variants were filtered in to obtain 10,228 variants. Next, we applied a filter to select variants with MAF<0.01 in 1000 Genome Project and ExAC database and reduced the number of variants to 1893. Afterwards, variants were further sorted to select only compound heterozygous and homozygous based on the recessive mode of inheritance which gave us 120 variants. We further sorted the damaging variants (at least from two *in silico* prediction tools) from these selected variants. We were left with 23 variants. Inhouse exome data of 100 healthy individuals were sorted out to reject common SNP present in both. 4 variants were unique to this proband which were selected for segregation study (Figure 4.10, Table 4.7).

Table 4.6: Clinical findings of the patients III-3 and III-8, family F.

Sr. No.	Serum biochemistry	Results		Reference range
		Patient III-3	Patient III-8	
1	Sodium	***132**	139	136-145 mmol/L
2	Potassium	***2.9**	3.7	3.5-5.3 mmol/L
3	Phosphate	4.5	4.3	2.7-5.4 mg/Dl
4	Chloride	93	105	98-110mmol/L
5	Bicarbonate	***21**	24	22-28mmol/L
6	Calcium	10	9.9	8.5-10.2 mg/dL
7	Urea	41	50	10-50 mg/dL
8	Creatinine	***1.5**	***1.6**	0.6-1.3 mg/dL
9	Alkaline Phosphatase	80	***350**	0-100U/L

*indicates abnormal levels.

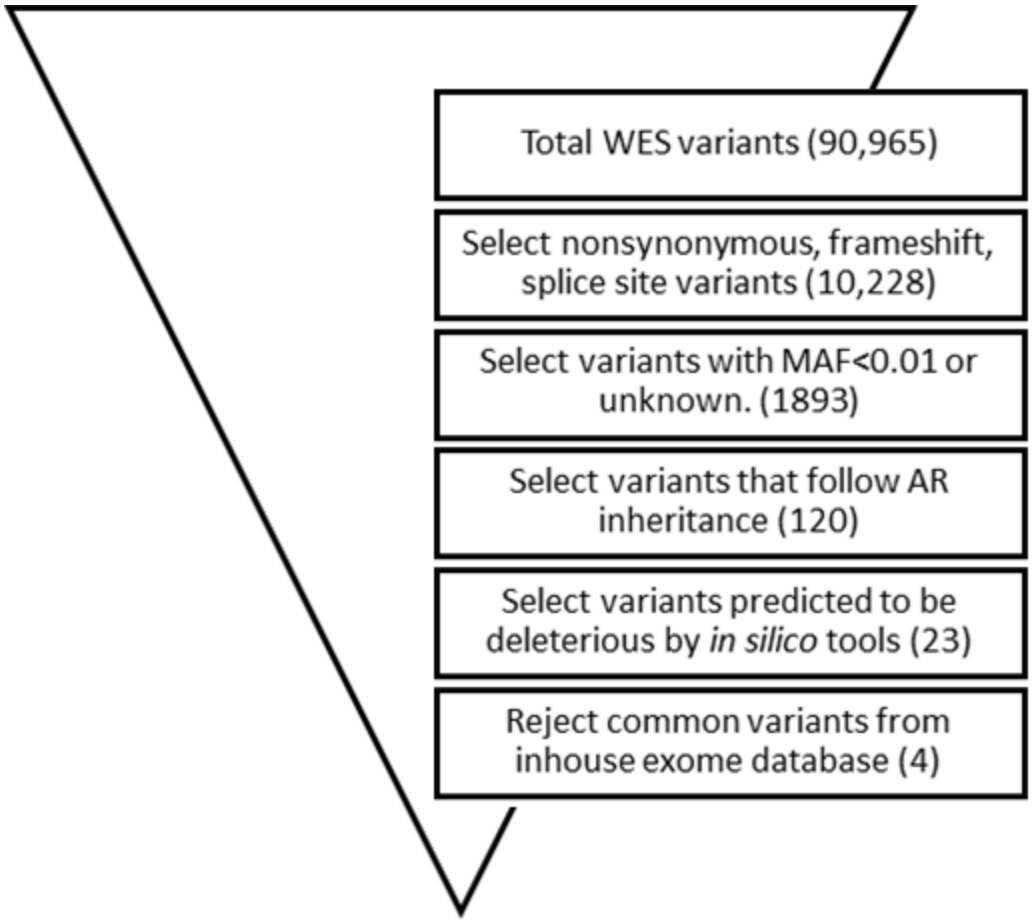

Figure 4.10: Step-wise approach used to identify pathogenic variant(s).

Table 4.7: Shortlisted variants after WES analysis.

Chrom	**Position**	**Gene Name**	**HGVS.c**	**Zyg-osity**	**Effect**	**MAF**	**ExAC**
1	24,411,034	*MYOM3*	c.1894G>A	Hom	Missense variant	0.0005	0.002
6	32,629,806	*HLA-DQB1*	c.599G>A	Hom	Missense variant	0.001	0.0007
6	150,342,155	*RAET1L*	c.517G>A	Hom	Missense variant	0.003	0.001
16	67,331,530	*KCTD19*	c.1023G>T	Hom	Missense variant	0.0001	0.001

Chrom = chromosome. HGVS.c = Human Genome Variation Society. cDNA position, AF = allele frequency from 1000 genome project3, Hom = homozygous, NA = not available, ExAC=Exome Aggregation Consortium.

4.18.3 Segregation analysis

All the available members of family F underwent Sanger sequencing for the shortlisted variants (Table 4.7) and the results showed that the variants did not co-segregated with the affected status (Table 4.8).

Table 4.8 Segregation data of shortlisted variants in family F.

Sr. No	**Variant**	**II-1 Father**	**II-2 Mother**	**II-4 Mother**	**III-3 Patient**	**III-8 Patient**	**III-4 Healthy sibling**	**III-7 Healthy sibling**
1.	*MYOM3*	Heterozygous	Homozygous	Homozygous mutant	Homozygous mutant	Homozygous mutant	--------	-------
2.	*HLA-DQB1*	Heterozygous	Homozygous mutant	Homozygous mutant	Homozygous mutant	Homozygous mutant	Homozygous mutant	--------
3.	*RAET1L*	Homozygous mutant	Heterozygous	Homozygous mutant	Heterozygous	Homozygous Mutant	Homozygous mutant	---------
4.	*KCTD19*	Heterozygous	Heterozygous	Homozygous mutant	Heterozygous	Homozygous mutant	--------	Homozygous mutant

4.19 Discussion

Nephronophthisis is a kidney disorder with genetic and allelic heterogeneity and variable phenotypes (König, 2017). Genetic testing is considered most accurate for the diagnosis of NPHP. Whole exome sequencing is appropriate to identify the underlying genetic cause since it takes less time and is more cost effective and efficient in such diseases where more than few genes are involved (Wang, 2019). In this study, molecular analysis of the patient clinically diagnosed with NPH was carried out to find out the genetic cause of NPHP using Sanger sequencing and WES.

Family described here comprised four (III-1, III-3, III-6 and III-8) patients with similar phenotype suggestive of nephronophthisis. III-1 and III-6 were died before the sample collection while III-3 died during this study. Clinical diagnosis led us to screen *NPHP1* gene for deletion as it accounts for 25% of all NPHP cases. WES was performed on patient III-3 after no *NPHP1* gene deletion was found. To exclude all the genes reported with the

NPHP phenotype (discussed in introduction) and the other ciliopathy genes, WES was carefully searched. Despite careful data analysis we did not identified pathogenic variants in the genes linked to NPHP and NPHP-RC. However, we used the established approach (discussed in 4.18.2 section) to shortlist pathogenic variants from the WES data and came up with four variants that fulfil our criteria. None of these variants was segregated in the family in accordance with autosomal recessive mode of inheritance.

The genetic mutation underlying the disease phenotype was not identified for the possible reasons given; (i) it might have been missed by sequencing techniques due to deep intronic localization which cannot be covered by WES, (ii) the pathogenic variant may be missed due to low coverage of some exonic regions in the exome thus giving false-negative results, (iii) large rearrangements or the copy number variations which may not be captured by this technique (Tiwari et al., 2016).

The molecular diagnosis of the family studied here remain unsolved which is not unexpected as the success rate of genetic diagnosis using whole exome sequencing is nearly 25 %.(Yang et al., 2014). Possibly another novel gene /locus might be the cause of disease in this affected family as the rate of novel genes identification has been increasing for renal ciliopathies owing to the high throughput sequencing technologies. We therefore recommend complementary methods for example whole genome sequencing or autozygosity mapping to aid in identification of molecular cause of the phenotype in this affected family(Tiwari et al., 2016).

CONCLUSION

The present study was done to investigate the pathogenic genetic variants in six unrelated Pakistani families affected with two different inherited nephropathies employing the power of whole exome sequencing and Sanger sequencing in concert with clinical and biochemical study of respective families. Two families affected with inherited distal renal tubular acidosis were resolved with identification of pathogenic recurrent and novel variations in *ATP6V0A4.* One family was clinically misdiagnosed with dRTA, the molecular and subsequent biochemical investigations identified mutation in *AGXT* gene thereby correcting the diagnosis to primary hyperoxaluria type 1. Two families affected with nephronophthisis were resolved with the identification of novel variants in *ANKS6, NPHP4,* and *NEK1* genes. One family affected with nephronophthisis was not resolved at molecular level for which whole genome sequencing is recommended. Current study emphasize that the recurrent mutations in *ATP6V0A4* and *AGXT* gene were really pathogenic and novel variants identified in *ATP6V0A4, ANKS6, NPHP4* and *NEK1* extends the mutation spectrum in these genes respectively. Utility of whole exome sequencing in ascertaining the molecular characterization of inherited nephropathies is also evident from the present study. Furthermore, the study could prove beneficial for better management of the disease and for the prenatal diagnosis of disease in respective families.

REFERENCES

Airik, R., Slaats, G. G., Guo, Z., Weiss, A.-C., Khan, N., Ghosh, A., . . . Elledge, S. J. (2014). Renal-retinal ciliopathy gene Sdccag8 regulates DNA damage response signaling. *Journal of the American Society of Nephrology*, ASN. 2013050565.

Ala-Mello, S., Koskimies, O., Rapola, J., & Kääriäinen, H. (1999). Nephronophthisis in Finland: epidemiology and comparison of genetically classified subgroups. *European Journal of Human Genetics, 7*(2), 205.

Alkanderi, S., Yates, L., Johnson, S., & Sayer, J. (2017). Lessons learned from a multidisciplinary renal genetics clinic. *QJM: An International Journal of Medicine*.

Armstrong, M. E., & Thomas, C. P. (2019). Diagnosis of monogenic chronic kidney diseases. *Current opinion in nephrology and hypertension, 28*(2), 183-194.

Arts, H. H., Doherty, D., van Beersum, S. E., Parisi, M. A., Letteboer, S. J., Gorden, N. T., . . . Kartono, A. (2007). Mutations in the gene encoding the basal body protein RPGRIP1L, a nephrocystin-4 interactor, cause Joubert syndrome. *Nature genetics, 39*(7), 882.

Artuso, R., Fallerini, C., Dosa, L., Scionti, F., Clementi, M., Garosi, G., . . . Mari, F. (2012). Advances in Alport syndrome diagnosis using next-generation sequencing. *European Journal of Human Genetics, 20*(1), 50.

Attanasio, M., Uhlenhaut, N. H., Sousa, V. H., O'Toole, J. F., Otto, E., Anlag, K., . . . Sayer, J. A. (2007). Loss of GLIS2 causes nephronophthisis in humans and mice by increased apoptosis and fibrosis. *Nature genetics, 39*(8), 1018.

Awata, J., Takada, S., Standley, C., Lechtreck, K. F., Bellvé, K. D., Pazour, G. J., . . . Witman, G. B. (2014). Nephrocystin-4 controls ciliary trafficking of membrane and large soluble proteins at the transition zone. *J Cell Sci*, jcs. 155275.

Ayasreh, N., Bullich, G., Miquel, R., Furlano, M., Ruiz, P., Lorente, L., . . . Garin, I. (2018). Autosomal dominant tubulointerstitial kidney disease: clinical presentation of patients with ADTKD-UMOD and ADTKD-MUC1. *American journal of kidney diseases, 72*(3), 411-418.

Bamshad, M. J., Ng, S. B., Bigham, A. W., Tabor, H. K., Emond, M. J., Nickerson, D. A., & Shendure, J. (2011). Exome sequencing as a tool for Mendelian disease gene discovery. *Nature Reviews Genetics, 12*(11), 745.

Batlle, D., & Haque, S. K. (2012). Genetic causes and mechanisms of distal renal tubular acidosis. *Nephrology Dialysis Transplantation, 27*(10), 3691-3704.

Beales, P., Elcioglu, N., Woolf, A., Parker, D., & Flinter, F. (1999). New criteria for improved diagnosis of Bardet-Biedl syndrome: results of a population survey. *Journal of medical genetics, 36*(6), 437-446.

Bergmann, C., Fliegauf, M., Brüchle, N. O., Frank, V., Olbrich, H., Kirschner, J., . . . Kränzlin, B. (2008). Loss of nephrocystin-3 function can cause embryonic lethality, Meckel-Gruber-like syndrome, situs inversus, and renal-hepatic-pancreatic dysplasia. *The American Journal of Human Genetics, 82*(4), 959-970.

Birkenhäger, R., Otto, E., Schürmann, M. J., Vollmer, M., Ruf, E.-M., Maier-Lutz, I., . . . Feldmann, D. (2001). Mutation of BSND causes Bartter syndrome with sensorineural deafness and kidney failure. *Nature genetics, 29*(3), 310.

Bollée, G., Fakhouri, F., Karras, A., Noel, L.-H., Salomon, R., Servais, A., . . . Hummel, A. (2006). Nephronophthisis related to homozygous NPHP1 gene deletion as a cause of chronic renal failure in adults. *Nephrology Dialysis Transplantation, 21*(9), 2660-2663.

Borgal, L., Habbig, S., Hatzold, J., Liebau, M. C., Dafinger, C., Sacarea, I., . . . Schermer, B. (2012). The ciliary protein nephrocystin-4 translocates the canonical Wnt-regulator Jade-1 to the nucleus to negatively regulate beta-catenin signaling. *Journal of Biological Chemistry*, jbc. M112. 385658.

Borthwick, K. J., & Karet, F. E. (2002). Inherited disorders of the H+-ATPase. *Current opinion in nephrology and hypertension, 11*(5), 563-568.

Boyer, O., Nevo, F., Plaisier, E., Funalot, B., Gribouval, O., Benoit, G., . . . Montjean, R. (2011). INF2 mutations in Charcot–Marie–Tooth disease with glomerulopathy. *New England Journal of Medicine, 365*(25), 2377-2388.

Braun, D. A., Schueler, M., Halbritter, J., Gee, H. Y., Porath, J. D., Lawson, J. A., . . . Stein, D. (2016). Whole exome sequencing identifies causative mutations in the majority of consanguineous or familial cases with childhood-onset increased renal echogenicity. *Kidney international, 89*(2), 468-475.

Bredrup, C., Saunier, S., Oud, M. M., Fiskerstrand, T., Hoischen, A., Brackman, D., . . . Bole-Feysot, C. (2011). Ciliopathies with skeletal anomalies and renal insufficiency due to mutations in the IFT-A gene WDR19. *The American Journal of Human Genetics, 89*(5), 634-643.

Capone, V. P., Morello, W., Taroni, F., & Montini, G. (2017). Genetics of congenital anomalies of the kidney and urinary tract: the current state of play. *International journal of molecular sciences, 18*(4), 796.

Chaki, M., Airik, R., Ghosh, A. K., Giles, R. H., Chen, R., Slaats, G. G., . . . Cluckey, A. (2012). Exome capture reveals ZNF423 and CEP164 mutations, linking renal ciliopathies to DNA damage response signaling. *Cell, 150*(3), 533-548.

Chen, Y., Chen, C.-F., Polci, R., Wei, R., Riley, D. J., & Chen, P.-L. (2014). Increased Nek1 expression in renal cell carcinoma cells is associated with decreased sensitivity to DNA-damaging treatment. *Oncotarget, 5*(12), 4283.

Chen, Y., Chiang, H.-C., Litchfield, P., Pena, M., Juang, C., & Riley, D. J. (2014). Expression of Nek1 during kidney development and cyst formation in multiple nephron segments in the Nek1-deficient kat2J mouse model of polycystic kidney disease. *Journal of biomedical science, 21*(1), 63.

Cheng, J., Fu, Y., Chen, W., Hwang, B., Chen, S., & Lin, C. (1987). Type I primary hyperoxaluria associated with type I renal tubular acidosis. *The International journal of pediatric nephrology, 8*(4), 235-238.

Choi, H. J. C., Lin, J.-R., Vannier, J.-B., Slaats, G. G., Kile, A. C., Paulsen, R. D., . . . Boulton, S. J. (2013). NEK8 links the ATR-regulated replication stress response and S phase CDK activity to renal ciliopathies. *Molecular cell, 51*(4), 423-439.

Cochat, P., Hulton, S.-A., Acquaviva, C., Danpure, C. J., Daudon, M., De Marchi, M., . . . Hoppe, B. (2012). Primary hyperoxaluria Type 1: indications for screening and guidance for diagnosis and treatment: Oxford University Press.

Copelovitch, L., & Kaplan, B. S. (2010). An expanded syndrome of dRTA with hearing loss, hyperoxaluria and beta2-microglobulinuria. *NDT plus, 3*(5), 439-442.

Coppieters, F., Lefever, S., Leroy, B. P., & De Baere, E. (2010). CEP290, a gene with many faces: mutation overview and presentation of CEP290base. *Human mutation, 31*(10), 1097-1108.

Coussa, R., Otto, E., Gee, H. Y., Arthurs, P., Ren, H., Lopez, I., . . . Khan, A. (2013). WDR19: an ancient, retrograde, intraflagellar ciliary protein is mutated in autosomal recessive retinitis pigmentosa and in Senior-Loken syndrome. *Clinical genetics, 84*(2), 150-159.

Daga, A., Majmundar, A. J., Braun, D. A., Gee, H. Y., Lawson, J. A., Shril, S., . . . Tan, W. (2018). Whole exome sequencing frequently detects a monogenic cause in early onset nephrolithiasis and nephrocalcinosis. *Kidney international, 93*(1), 204-213.

Deen, P., Verdijk, M., Knoers, N., Wieringa, B., Monnens, L., van Os, C. H., & van Oost, B. A. (1994). Requirement of human renal water channel aquaporin-2 for vasopressin-dependent concentration of urine. *Science, 264*(5155), 92-95.

Delous, M., Baala, L., Salomon, R., Laclef, C., Vierkotten, J., Tory, K., . . . Ozilou, C. (2007). The ciliary gene RPGRIP1L is mutated in cerebello-oculo-renal syndrome (Joubert syndrome type B) and Meckel syndrome. *Nature genetics, 39*(7), 875.

den Hollander, A. I., Koenekoop, R. K., Yzer, S., Lopez, I., Arends, M. L., Voesenek, K. E., . . . Brunner, H. G. (2006). Mutations in the CEP290 (NPHP6) gene are a frequent cause of Leber congenital amaurosis. *The American Journal of Human Genetics, 79*(3), 556-561.

Devuyst, O., Knoers, N. V., Remuzzi, G., & Schaefer, F. (2014). Rare inherited kidney diseases: challenges, opportunities, and perspectives. *The Lancet, 383*(9931), 1844-1859.

Devuyst, O., Meij, I., Jeunemaitre, X., Ronco, P., Antignac, C., Christensen, E. I., . . . Müller, D. (2009). EUNEFRON, the European Network for the Study of Orphan Nephropathies: Oxford University Press.

Divers, J., & Freedman, B. I. (2010). Susceptibility genes in common complex kidney disease. *Current opinion in nephrology and hypertension, 19*(1), 79.

Dixon-Salazar, T., Silhavy, J. L., Marsh, S. E., Louie, C. M., Scott, L. C., Gururaj, A., . . . Sztriha, L. (2004). Mutations in the AHI1 gene, encoding jouberin, cause Joubert syndrome with cortical polymicrogyria. *The American Journal of Human Genetics, 75*(6), 979-987.

Eckardt, K.-U., Alper, S. L., Antignac, C., Bleyer, A. J., Chauveau, D., Dahan, K., . . . Rampoldi, L. (2015). Autosomal dominant tubulointerstitial kidney disease: diagnosis, classification, and management—a KDIGO consensus report. *Kidney international, 88*(4), 676-683.

Eckardt, K.-U., Coresh, J., Devuyst, O., Johnson, R. J., Köttgen, A., Levey, A. S., & Levin, A. (2013). Evolving importance of kidney disease: from subspecialty to global health burden. *The Lancet, 382*(9887), 158-169.

Enerbäck, S., Nilsson, D., Edwards, N., Heglind, M., Alkanderi, S., Ashton, E., . . . van't Hoff, W. (2018). Acidosis and deafness in patients with recessive mutations in FOXI1. *Journal of the American Society of Nephrology, 29*(3), 1041-1048.

Escobar, L., Mejía, N., Gil, H., & Santos, F. (2013). Distal renal tubular acidosis: a hereditary disease with an inadequate urinary H+ excretion. *Nefrología (English Edition), 33*(3), 289-296.

Estévez, R., Boettger, T., Stein, V., Birkenhäger, R., Otto, E., Hildebrandt, F., & Jentsch, T. J. (2001). Barttin is a Cl-channel β-subunit crucial for renal Cl-reabsorption and inner ear K+ secretion. *Nature, 414*(6863), 558.

Failler, M., Gee, H. Y., Krug, P., Joo, K., Halbritter, J., Belkacem, L., . . . Schueler, M. (2014). Mutations of CEP83 cause infantile nephronophthisis and intellectual disability. *The American Journal of Human Genetics, 94*(6), 905-914.

Fry, A. C., & Karet, F. E. (2007). Inherited renal acidoses. *Physiology, 22*(3), 202-211.

Gagnadoux, M., Bacri, J., Broyer, M., & Habib, R. (1989). Infantile chronic tubulo-interstitial nephritis with cortical microcysts: variant of nephronophthisis or new disease entity? *Pediatric nephrology, 3*(1), 50-55.

Gattone II, V. H., Wang, X., Harris, P. C., & Torres, V. E. (2003). Inhibition of renal cystic disease development and progression by a vasopressin V2 receptor antagonist. *Nature medicine, 9*(10), 1323.

Gazzo, A. M., Daneels, D., Cilia, E., Bonduelle, M., Abramowicz, M., Van Dooren, S., . . . Lenaerts, T. (2015). DIDA: A curated and annotated digenic diseases database. *Nucleic acids research, 44*(D1), D900-D907.

Gee, H. Y., Otto, E. A., Hurd, T. W., Ashraf, S., Chaki, M., Cluckey, A., . . . Fang, H. (2014). Whole-exome resequencing distinguishes cystic kidney diseases from phenocopies in renal ciliopathies. *Kidney international, 85*(4), 880-887.

Georges, B., Cosyns, J.-P., Dahan, K., Snyers, B., Carlier, B., Loute, G., & Pirson, Y. (2000). Late-onset renal failure in Senior-Loken syndrome. *American journal of kidney diseases, 36*(6), 1271-1275.

Glaudemans, B., van der Wijst, J., Scola, R. H., Lorenzoni, P. J., Heister, A., van der Kemp, A. W., . . . Bindels, R. J. (2009). A missense mutation in the Kv1. 1 voltage-gated potassium channel–encoding gene KCNA1 is linked to human autosomal dominant hypomagnesemia. *The Journal of clinical investigation*, *119*(4), 936-942.

Go ´mez J, Gil-Pen ˜a H, Santos F,et al. (2016) Primary distal renal tubular acidosis: novel findings in patients studied by next-generation sequencing. Pediatr Res 79: 496–501.

Gong, F., Alzamora, R., Smolak, C., Li, H., Naveed, S., Neumann, D., Pastor-Soler, N. M. (2010). Vacuolar H+-ATPase apical accumulation in kidney intercalated cells is regulated by PKA and AMP-activated protein kinase. *American Journal of Physiology-Renal Physiology*, *298*(5), F1162-F1169.

Gorden, N. T., Arts, H. H., Parisi, M. A., Coene, K. L., Letteboer, S. J., van Beersum, S. E., . . . Knutzen, D. (2008). CC2D2A is mutated in Joubert syndrome and interacts with the ciliopathy-associated basal body protein CEP290. *The American Journal of Human Genetics*, *83*(5), 559-571.

Grampa, V., Delous, M., Zaidan, M., Odye, G., Thomas, S., Elkhartoufi, N., . . . Lebreton, C. (2016). Novel NEK8 mutations cause severe syndromic renal cystic dysplasia through YAP dysregulation. *PLoS genetics*, *12*(3), e1005894.

Graser, S., Stierhof, Y.-D., Lavoie, S. B., Gassner, O. S., Lamla, S., Le Clech, M., & Nigg, E. A. (2007). Cep164, a novel centriole appendage protein required for primary cilium formation. *J Cell Biol*, *179*(2), 321-330.

Gregory, M. J., & Schwartz, G. J. (1998). *Diagnosis and treatment of renal tubular disorders.* Paper presented at the Seminars in nephrology.

Habbig, S., Bartram, M. P., Müller, R. U., Schwarz, R., Andriopoulos, N., Chen, S., . . . Liebau, M. C. (2011). NPHP4, a cilia-associated protein, negatively regulates the Hippo pathway. *The Journal of cell biology*, *193*(4), 633-642.

Halbritter, J., Bizet, A. A., Schmidts, M., Porath, J. D., Braun, D. A., Gee, H. Y., . . . Davis, E. E. (2013). Defects in the IFT-B component IFT172 cause Jeune and Mainzer-Saldino syndromes in humans. *The American Journal of Human Genetics, 93*(5), 915-925.

Halbritter, J., Porath, J. D., Diaz, K. A., Braun, D. A., Kohl, S., Chaki, M., . . . Otto, E. A. (2013). Identification of 99 novel mutations in a worldwide cohort of 1,056 patients with a nephronophthisis-related ciliopathy. *Human genetics, 132*(8), 865-884.

Harris, P. C., & Rossetti, S. (2008). Molecular diagnostics of ADPKD coming of age: Am Soc Nephrol.

Hasan, M., Sutradhar, I., Gupta, R. D., & Sarker, M. (2018). Prevalence of chronic kidney disease in South Asia: a systematic review. *BMC nephrology, 19*(1), 291.

Hildebrandt, F. (2009). Nephronophthisis *Genetic Diseases of the Kidney* (pp. 425-446): Elsevier.

Hildebrandt, F. (2010). Genetic kidney diseases. *The Lancet, 375*(9722), 1287-1295.

Hildebrandt, F., Attanasio, M., & Otto, E. (2009). Nephronophthisis: disease mechanisms of a ciliopathy. *Journal of the American Society of Nephrology, 20*(1), 23-35.

Hildebrandt, F., Otto, E., Rensing, C., Nothwang, H. G., Vollmer, M., Adolphs, J., . . . Brandis, M. (1997). A novel gene encoding an SH3 domain protein is mutated in nephronophthisis type 1. *Nature genetics, 17*(2), 149.

Hildebrandt, F., Strahm, B., Nothwang, H.-G., Gretz, N., Schnieders, B., Singh-Sawhney, I., . . . Group, A. S. (1997). Molecular genetic identification of families with juvenile nephronophthisis type 1: rate of progression to renal failure. *Kidney international, 51*(1), 261-269.

Hildebrandt, F., & Zhou, W. (2007). Nephronophthisis-associated ciliopathies. *Journal of the American Society of Nephrology, 18*(6), 1855-1871.

Hill, N. R., Fatoba, S. T., Oke, J. L., Hirst, J. A., O'Callaghan, C. A., Lasserson, D. S., & Hobbs, F. R. (2016). Global prevalence of chronic kidney disease–a systematic review and meta-analysis. *PLoS One, 11*(7), e0158765.

Hinkes, B., Wiggins, R. C., Gbadegesin, R., Vlangos, C. N., Seelow, D., Nürnberg, G., . . . Hoskins, B. E. (2006). Positional cloning uncovers mutations in PLCE1 responsible for a nephrotic syndrome variant that may be reversible. *Nature genetics, 38*(12), 1397.

Hinkes, B. G., Mucha, B., Vlangos, C. N., Gbadegesin, R., Liu, J., Hasselbacher, K., . . . Hildebrandt, F. (2007). Nephrotic syndrome in the first year of life: two thirds of cases are caused by mutations in 4 genes (NPHS1, NPHS2, WT1, and LAMB2). *Pediatrics, 119*(4), e907-e919.

Hoefele, J., Nayir, A., Chaki, M., Imm, A., Allen, S. J., Otto, E. A., & Hildebrandt, F. (2011). Pseudodominant inheritance of nephronophthisis caused by a homozygous NPHP1 deletion. *Pediatric nephrology, 26*(6), 967-971.

Hoefele, J., Wolf, M. T., O'Toole, J. F., Otto, E. A., Schultheiss, U., Dêschenes, G., . . . Hildebrandt, F. (2007). Evidence of oligogenic inheritance in nephronophthisis. *Journal of the American Society of Nephrology, 18*(10), 2789-2795.

Hoff, S., Halbritter, J., Epting, D., Frank, V., Nguyen, T.-M. T., Van Reeuwijk, J., . . . Helmstädter, M. (2013). ANKS6 is a central component of a nephronophthisis module linking NEK8 to INVS and NPHP3. *Nature genetics, 45*(8), 951.

Hogg, R. J., Furth, S., Lemley, K. V., Portman, R., Schwartz, G. J., Coresh, J., . . . Kausz, A. T. (2003). National Kidney Foundation's Kidney Disease Outcomes Quality Initiative clinical practice guidelines for chronic kidney disease in children and adolescents: evaluation, classification, and stratification. *Pediatrics, 111*(6), 1416-1421.

Huangfu, D., Liu, A., Rakeman, A. S., Murcia, N. S., Niswander, L., & Anderson, K. V. (2003). Hedgehog signalling in the mouse requires intraflagellar transport proteins. *Nature*, *426*(6962), 83.

Hurd, T. W., & Hildebrandt, F. (2011). Mechanisms of nephronophthisis and related ciliopathies. *Nephron Experimental Nephrology*, *118*(1), e9-e14.

Hurd, T. W., Otto, E. A., Mishima, E., Gee, H. Y., Inoue, H., Inazu, M., . . . Konishi, M. (2013). Mutation of the Mg2+ transporter SLC41A1 results in a nephronophthisis-like phenotype. *Journal of the American Society of Nephrology*, ASN. 2012101034.

Hussain, S., Akhtar, N., Qamar, R., Khan, N., & Naeem, M. (2018). Molecular Study of Nephronophthisis in 7 Unrelated Pakistani Families. *Iranian journal of kidney diseases*, *12*(4), 240-242.

Hwang DY, Cohen JB (1996) U1 snRNA promotes the selection of nearby 5 splice sites by U6 snRNA in mammalian cells. Genes Dev 10:338–350.

Jouret, F., Bernard, A., Hermans, C., Dom, G., Terryn, S., Leal, T., . . . de Jonge, H. R. (2007). Cystic fibrosis is associated with a defect in apical receptor–mediated endocytosis in mouse and human kidney. *Journal of the American Society of Nephrology*, *18*(3), 707-718.

Karet, F. E. (2002). Inherited distal renal tubular acidosis. *Journal of the American Society of Nephrology*, *13*(8), 2178-2184.

Knoers, N. V. (2009). Inherited forms of renal hypomagnesemia: an update. *Pediatric nephrology*, *24*(4), 697-705.

Koboldt, D. C., Steinberg, K. M., Larson, D. E., Wilson, R. K., & Mardis, E. R. (2013). The next-generation sequencing revolution and its impact on genomics. *Cell*, *155*(1), 27-38.

König, J., Kranz, B., König, S., Schlingmann, K. P., Titieni, A., Tönshoff, B., . . . Hansen, M. (2017). Phenotypic spectrum of children with nephronophthisis and related

ciliopathies. *Clinical Journal of the American Society of Nephrology, 12*(12), 1974-1983.

Konrad, M., Schlingmann, K. P., & Gudermann, T. (2004). Insights into the molecular nature of magnesium homeostasis. *American Journal of Physiology-Renal Physiology, 286*(4), F599-F605.

Kose E, Kose SS, Alparslan C, et al. (2014) Val2Ala mutation in the ATP6V0A4 gene causes early-onset sensorineural hearing loss in children with recessive distal renal tubular acidosis: a case report. Ren Fail 36:808–810.

Krishnan, R., Eley, L., & Sayer, J. A. (2008). Urinary concentration defects and mechanisms underlying nephronophthisis. *Kidney and Blood Pressure Research, 31*(3), 152-162.

Kruegel, J., Rubel, D., & Gross, O. (2013). Alport syndrome—insights from basic and clinical research. *Nature Reviews Nephrology, 9*(3), 170.

Laing, C. M., Toye, A. M., Capasso, G., & Unwin, R. J. (2005). Renal tubular acidosis: developments in our understanding of the molecular basis. *The international journal of biochemistry & cell biology, 37*(6), 1151-1161.

Lata, S., Marasa, M., Li, Y., Fasel, D. A., Groopman, E., Jobanputra, V., . . . Verbitsky, M. (2018). Whole-exome sequencing in adults with chronic kidney disease: a pilot study. *Annals of internal medicine, 168*(2), 100-109.

Lesser CF, Guthrie C (1993) Mutations in U6 snRNA that alter splice site specificity: implications for the active site. Science 262:1982–1988.

Li X, Chai Y, Tao Z, et al. (2012) Novel mutations in ATP6V0A4 are associated with atypical progressive sensorineural hearing loss in a Chinese patient with distal renal tubular acidosis. Int J Pediatr Otorhinolaryngol 76:152– 154.

Lloyd, S. E., Pearce, S. H., Fisher, S. E., Steinmeyer, K., Schwappach, B., Scheinman, S. J., . . . Goodyer, P. (1996). A common molecular basis for three inherited kidney stone diseases. *Nature, 379*(6564), 445.

Luo, F., & Tao, Y. H. (2018). Nephronophthisis: A review of genotype–phenotype correlation. *Nephrology*.

Machuca, E., Benoit, G., & Antignac, C. (2009). Genetics of nephrotic syndrome: connecting molecular genetics to podocyte physiology. *Human molecular genetics, 18*(R2), R185-R194.

Macia, M. S., Halbritter, J., Delous, M., Bredrup, C., Gutter, A., Filhol, E., . . . Braun, D. A. (2017). Mutations in MAPKBP1 cause juvenile or late-onset cilia-independent nephronophthisis. *The American Journal of Human Genetics, 100*(2), 323-333.

McCarthy, H. J., Bierzynska, A., Wherlock, M., Ognjanovic, M., Kerecuk, L., Hegde, S., . . . Jones, C. (2013). Simultaneous sequencing of 24 genes associated with steroid-resistant nephrotic syndrome. *Clinical Journal of the American Society of Nephrology, 8*(4), 637-648.

McMahon, A. P., Ingham, P. W., & Tabin, C. J. (2003). 1 Developmental roles and clinical significance of Hedgehog signaling.

Milliner, D. S. (2005). The primary hyperoxalurias: an algorithm for diagnosis. *American journal of nephrology, 25*(2), 154-160.

Mohebbi, N., & Wagner, C. A. (2018). Pathophysiology, diagnosis and treatment of inherited distal renal tubular acidosis. *Journal of nephrology, 31*(4), 511-522.

Molinari, E., Srivastava, S., Sayer, J. A., & Ramsbottom, S. A. (2017). From disease modelling to personalised therapy in patients with CEP290 mutations. *F1000Research, 6*.

Mollet, G., Silbermann, F., Delous, M., Salomon, R., Antignac, C., & Saunier, S. (2005). Characterization of the nephrocystin/nephrocystin-4 complex and subcellular

localization of nephrocystin-4 to primary cilia and centrosomes. *Human molecular genetics, 14*(5), 645-656.

Monroe, G. R., Kappen, I. F., Stokman, M. F., Terhal, P. A., van den Boogaard, M.-J. H., Savelberg, S. M., . . . Hengeveld, R. C. (2016). Compound heterozygous NEK1 variants in two siblings with oral-facial-digital syndrome type II (Mohr syndrome). *European Journal of Human Genetics, 24*(12), 1752.

Müller, R.-U., Haas, C. S., & Sayer, J. A. (2018). Practical approaches to the management of autosomal dominant polycystic kidney disease patients in the era of tolvaptan. *Clinical Kidney Journal, 11*(1), 62-69. doi: 10.1093/ckj/sfx071

Nakai, K., & Sakamoto, H. (1994). Construction of a novel database containing aberrant splicing mutations of mammalian genes. *Gene, 141*(2), 171-177.

O'toole, J. F., Liu, Y., Davis, E. E., Westlake, C. J., Attanasio, M., Otto, E. A., . . . Nuutinen, M. (2010). Individuals with mutations in XPNPEP3, which encodes a mitochondrial protein, develop a nephronophthisis-like nephropathy. *The Journal of clinical investigation, 120*(3), 791-802.

Olbrich, H., Fliegauf, M., Hoefele, J., Kispert, A., Otto, E., Volz, A., . . . Reinhardt, R. (2003). Mutations in a novel gene, NPHP3, cause adolescent nephronophthisis, tapeto-retinal degeneration and hepatic fibrosis. *Nature genetics, 34*(4), 455.

Otto, E. A., Hurd, T. W., Airik, R., Chaki, M., Zhou, W., Stoetzel, C., . . . Murga-Zamalloa, C. A. (2010). Candidate exome capture identifies mutation of SDCCAG8 as the cause of a retinal-renal ciliopathy. *Nature genetics, 42*(10), 840.

Otto, E. A., Loeys, B., Khanna, H., Hellemans, J., Sudbrak, R., Fan, S., . . . Attanasio, M. (2005). Nephrocystin-5, a ciliary IQ domain protein, is mutated in Senior-Loken syndrome and interacts with RPGR and calmodulin. *Nature genetics, 37*(3), 282.

Otto, E. A., Ramaswami, G., Janssen, S., Chaki, M., Allen, S. J., Zhou, W., . . . Wolf, M. T. (2011). Mutation analysis of 18 nephronophthisis associated ciliopathy disease

genes using a DNA pooling and next generation sequencing strategy. *Journal of medical genetics, 48*(2), 105-116.

Otto, E. A., Schermer, B., Obara, T., O'Toole, J. F., Hiller, K. S., Mueller, A. M., . . . Landau, D. (2003). Mutations in INVS encoding inversin cause nephronophthisis type 2, linking renal cystic disease to the function of primary cilia and left-right axis determination. *Nature genetics, 34*(4), 413.

Otto, E. A., Tory, K., Attanasio, M., Zhou, W., Chaki, M., Paruchuri, Y., . . . Becker, C. (2009). Hypomorphic mutations in meckelin (MKS3/TMEM67) cause nephronophthisis with liver fibrosis (NPHP11). *Journal of medical genetics, 46*(10), 663-670.

Otto, E. A., Trapp, M. L., Schultheiss, U. T., Helou, J., Quarmby, L. M., & Hildebrandt, F. (2008). NEK8 mutations affect ciliary and centrosomal localization and may cause nephronophthisis. *Journal of the American Society of Nephrology, 19*(3), 587-592.

Oud, M. M., Van Bon, B. W., Bongers, E. M., Hoischen, A., Marcelis, C. L., De Leeuw, N., . . . Brunner, H. G. (2014). Early presentation of cystic kidneys in a family with a homozygous INVS mutation. *American journal of medical genetics Part A, 164*(7), 1627-1634.

Pal, A., & Reidy, K. J. (2017). Genetic syndromes affecting kidney development *Kidney development and disease* (pp. 257-279): Springer.

Park E, Cho MH, Hyun HS, et al. (2018) Genotype-phenotype analysis in pediatric patients with distal renal tubular acidosis. Kidney Blood Press Res 43:513–521.

Pela, I., Provenzano, A., & Giglio, S. (2011). Transient hyperoxaluria in a patient with inherited distal renal tubular acidosis. *Pediatric nephrology, 26*(2), 323-324.

Pereira, P., Miranda, D., Oliveira, E., & Simões e Silva, A. (2009). Molecular pathophysiology of renal tubular acidosis. *Current genomics, 10*(1), 51-59.

Perinpam, M., Enders, F. T., Mara, K. C., Vaughan, L. E., Mehta, R. A., Voskoboev, N., . . . Lieske, J. C. (2017). Plasma oxalate in relation to eGFR in patients with primary hyperoxaluria, enteric hyperoxaluria and urinary stone disease. *Clinical biochemistry, 50*(18), 1014-1019.

Phillips, C. L., Miller, K. J., Filson, A. J., Nürnberger, J., Clendenon, J. L., Cook, G. W., . . . Bacallao, R. L. (2004). Renal cysts of inv/inv mice resemble early infantile nephronophthisis. *Journal of the American Society of Nephrology, 15*(7), 1744-1755.

Picca, S., Colombini, E., & Cochat, P. (2017). Primary Hyperoxaluria *Pediatric Dialysis Case Studies* (pp. 315-323): Springer.

Raj, V., Gordillo, R., Warnecke, D., & Chand, D. (2016). Overview of Nephronophthisis: A Genetically Heterogeneous Ciliopathy. *Pediatr Neonatal Nurs Open Access, 2*(3), 2470-0983.2115.

Ring, T., Frische, S., & Nielsen, S. (2005). Clinical review: renal tubular acidosis–a physicochemical approach. *Critical Care, 9*(6), 573.

Rosenthal, W., Seibold, A., Antaramian, A., Lonergan, M., Arthus, M.-F., Hendy, G. N., . . . Bichet, D. G. (1992). Molecular identification of the gene responsible for congenital nephrogenic diabetes insipidus. *Nature, 359*(6392), 233.

Roy, A., Al-bataineh, M. M., & Pastor-Soler, N. M. (2015). Collecting duct intercalated cell function and regulation. *Clinical Journal of the American Society of Nephrology, 10*(2), 305-324.

Ruf R, Rensing C, Topaloglu R, et al. (2003) Confirmation of the ATP6B1 gene as responsible for distal renal tubular acidosis. Pediatr Nephrol 18:105–109.

Rumsby, G. (1998). Identification of new mutations in primary hyperoxaluria type 1 (PH1). *Journal of nephrology, 11*, 15-17.

Salomon, R., Saunier, S., & Niaudet, P. (2009). Nephronophthisis. *Pediatric nephrology, 24*(12), 2333.

Sang, L., Miller, J. J., Corbit, K. C., Giles, R. H., Brauer, M. J., Otto, E. A., . . . Kwong, M. (2011). Mapping the NPHP-JBTS-MKS protein network reveals ciliopathy disease genes and pathways. *Cell, 145*(4), 513-528.

Santos, F., Gil-Peña, H., & Alvarez-Alvarez, S. (2017). Renal tubular acidosis. *Current opinion in pediatrics, 29*(2), 206-210.

Santos, F., Ordóñez, F. A., Claramunt-Taberner, D., & Gil-Peña, H. (2015). Clinical and laboratory approaches in the diagnosis of renal tubular acidosis. *Pediatric nephrology, 30*(12), 2099-2107.

Sayer, J. A. (2008). The genetics of nephrolithiasis. *Nephron Experimental Nephrology, 110*(2), e37-e43.

Sayer, J. A., Otto, E. A., O'Toole, J. F., Nurnberg, G., Kennedy, M. A., Becker, C., . . . Fausett, B. V. (2006). The centrosomal protein nephrocystin-6 is mutated in Joubert syndrome and activates transcription factor ATF4. *Nature genetics, 38*(6), 674.

Schaefer, E., Stoetzel, C., Scheidecker, S., Geoffroy, V., Prasad, M. K., Redin, C., . . . Muller, J. (2016). Identification of a novel mutation confirms the implication of IFT172 (BBS20) in Bardet–Biedl syndrome. *Journal of human genetics, 61*(5), 447.

Schäfer, T., Pütz, M., Lienkamp, S., Ganner, A., Bergbreiter, A., Ramachandran, H., . . . Czarnecki, P. G. (2008). Genetic and physical interaction between the NPHP5 and NPHP6 gene products. *Human molecular genetics, 17*(23), 3655-3662.

Schäffer, A. A. (2013). Digenic inheritance in medical genetics. *Journal of medical genetics*, jmedgenet-2013-101713.

Schueler, M., Braun, D. A., Chandrasekar, G., Gee, H. Y., Klasson, T. D., Halbritter, J., . . . Zhou, W. (2015). DCDC2 mutations cause a renal-hepatic ciliopathy by disrupting Wnt signaling. *The American Journal of Human Genetics, 96*(1), 81-92.

Schuermann, M. J., Otto, E., Becker, A., Saar, K., Rüschendorf, F., Polak, B. C., . . . Haller, M. (2002). Mapping of gene loci for nephronophthisis type 4 and Senior-Løken syndrome, to chromosome 1p36. *The American Journal of Human Genetics, 70*(5), 1240-1246.

Shearer, A. E., DeLuca, A. P., Hildebrand, M. S., Taylor, K. R., Gurrola, J., Scherer, S., . . . Smith, R. J. (2010). Comprehensive genetic testing for hereditary hearing loss using massively parallel sequencing. *Proceedings of the National Academy of Sciences, 107*(49), 21104-21109.

Shi, X., Garcia III, G., Van De Weghe, J. C., McGorty, R., Pazour, G. J., Doherty, D., . . . Reiter, J. F. (2017). Super-resolution microscopy reveals that disruption of ciliary transition-zone architecture causes Joubert syndrome. *Nature cell biology, 19*(10), 1178.

Shiba, D., Manning, D. K., Koga, H., Beier, D. R., & Yokoyama, T. (2010). Inv acts as a molecular anchor for Nphp3 and Nek8 in the proximal segment of primary cilia. *Cytoskeleton, 67*(2), 112-119.

Shiba, D., & Yokoyama, T. (2012). The ciliary transitional zone and nephrocystins. *Differentiation, 83*(2), S91-S96.

Shimkets, R. A., Warnock, D. G., Bositis, C. M., Nelson-Williams, C., Hansson, J. H., Schambelan, M., . . . Findling, J. W. (1994). Liddle's syndrome: heritable human hypertension caused by mutations in the β subunit of the epithelial sodium channel. *Cell, 79*(3), 407-414.

Simms, R. J., Eley, L., & Sayer, J. A. (2009). Nephronophthisis. *European Journal of Human Genetics, 17*(4), 406.

Simms, R. J., Hynes, A. M., Eley, L., & Sayer, J. A. (2011). Nephronophthisis: a genetically diverse ciliopathy. *International journal of nephrology, 2011*.

Simon, D. B., Bindra, R. S., Mansfield, T. A., Nelson-Williams, C., Mendonca, E., Stone, R., . . . Bakkaloglu, A. (1997). Mutations in the chloride channel gene, CLCNKB, cause Bartter's syndrome type III. *Nature genetics, 17*(2), 171.

Simon, D. B., Karet, F. E., Hamdan, J. M., Di Pietro, A., Sanjad, S. A., & Lifton, R. P. (1996). Bartter's syndrome, hypokalaemic alkalosis with hypercalciuria, is caused by mutations in the Na–K–2CI cotransporter NKCC2. *Nature genetics, 13*(2), 183.

Simon, D. B., Karet, F. E., Rodriguez-Soriano, J., Hamdan, J. H., DiPietro, A., Trachtman, H., . . . Lifton, R. P. (1996). Genetic heterogeneity of Barter's syndrome revealed by mutations in the K+ channel, ROMK. *Nature genetics, 14*(2), 152.

Simon, D. B., & Lifton, R. P. (1996). The molecular basis of inherited hypokalemic alkalosis: Bartter's and Gitelman's syndromes. *American Journal of Physiology-Renal Physiology, 271*(5), F961-F966.

Simon, D. B., Nelson-Williams, C., Bia, M. J., Ellison, D., Karet, F. E., Molina, A. M., . . . Koolen, M. (1996). Gitelman's variant of Barter's syndrome, inherited hypokalaemic alkalosis, is caused by mutations in the thiazide-sensitive Na–Cl cotransporter. *Nature genetics, 12*(1), 24.

Simons, M., Gloy, J., Ganner, A., Bullerkotte, A., Bashkurov, M., Krönig, C., . . . Jenny, A. (2005). Inversin, the gene product mutated in nephronophthisis type II, functions as a molecular switch between Wnt signaling pathways. *Nature genetics, 37*(5), 537.

Smulders, Y. M., Frissen, P. J., Slaats, E. H., & Silberbusch, J. (1996). Renal tubular acidosis: pathophysiology and diagnosis. *Archives of internal medicine, 156*(15), 1629-1636.

Soliman, N. A., Hildebrandt, F., Otto, E. A., Nabhan, M. M., Allen, S. J., Badr, A. M., . . . El-Kiky, H. (2012). Clinical characterization and NPHP1 mutations in

nephronophthisis and associated ciliopathies: a single center experience. *Saudi journal of kidney diseases and transplantation: an official publication of the Saudi Center for Organ Transplantation, Saudi Arabia*, *23*(5), 1090.

Soriano, J. R. (2002). Renal tubular acidosis: the clinical entity. *Journal of the American Society of Nephrology*, *13*(8), 2160-2170.

Srivastava, S., Molinari, E., Raman, S., & Sayer, J. A. (2018). Many Genes—One Disease? Genetics of Nephronophthisis (NPHP) and NPHP-Associated Disorders. *Frontiers in pediatrics*, *5*, 287.

Srivastava, S., & Sayer, J. A. (2014). Nephronophthisis. *Journal of pediatric genetics*, *3*(2), 103-114.

Stehberger, P. A., Schulz, N., Finberg, K. E., Karet, F. E., Giebisch, G., Lifton, R. P., . . . Wagner, C. A. (2003). Localization and regulation of the ATP6V0A4 (a4) vacuolar H+-ATPase subunit defective in an inherited form of distal renal tubular acidosis. *Journal of the American Society of Nephrology*, *14*(12), 3027-3038.

Taskiran, E. Z., Korkmaz, E., Gucer, S., Kosukcu, C., Kaymaz, F., Koyunlar, C., . . . Vadnagara, K. (2014). Mutations in ANKS6 cause a nephronophthisis-like phenotype with ESRD. *Journal of the American Society of Nephrology*, ASN. 2013060646.

Thomas, C., Mansilla, M., Sompallae, R., Mason, S., Nishimura, C., Kimble, M., . . . Stewart, Z. (2017). Screening of living kidney donors for genetic diseases using a comprehensive genetic testing strategy. *American Journal of Transplantation*, *17*(2), 401-410.

Tiwari, A., Lemke, J., Altmueller, J., Thiele, H., Glaus, E., Fleischhauer, J., . . . Berger, W. (2016). Identification of novel and recurrent disease-causing mutations in retinal dystrophies using whole exome sequencing (WES): benefits and limitations. *PLoS One*, *11*(7), e0158692.

Torres, V. E., & Harris, P. C. (2009). Autosomal dominant polycystic kidney disease: the last 3 years. *Kidney international*, *76*(2), 149-168.

Tory, K., Lacoste, T., Burglen, L., Morinière, V., Boddaert, N., Macher, M.-A., . . . Niaudet, P. (2007). High NPHP1 and NPHP6 mutation rate in patients with Joubert syndrome and nephronophthisis: potential epistatic effect of NPHP6 and AHI1 mutations in patients with NPHP1 mutations. *Journal of the American Society of Nephrology*, *18*(5), 1566-1575.

Utsch, B., Sayer, J. A., Attanasio, M., Pereira, R. R., Eccles, M., Hennies, H.-C., . . . Hildebrandt, F. (2006). Identification of the first AHI1 gene mutations in nephronophthisis-associated Joubert syndrome. *Pediatric nephrology*, *21*(1), 32-35.

Vargas-Poussou R, Mouillier P, Le Pettier N, et al. (2006) Genetic investigation of autosomal recessive distal renal tubular acidosis: evidence for early sensorineural hearing loss associated with variants in the ATP6V0A4 gene. J Am Soc Nephrol 17:1437–1443.

Vilboux, T., Doherty, D. A., Glass, I. A., Parisi, M. A., Phelps, I. G., Cullinane, A. R., . . . Soldatos, A. (2017). Molecular genetic findings and clinical correlations in 100 patients with Joubert syndrome and related disorders prospectively evaluated at a single center. *Genetics in Medicine*, *19*(8), 875.

Vivante, A., & Hildebrandt, F. (2016). Exploring the genetic basis of early-onset chronic kidney disease. *Nature Reviews Nephrology*, *12*(3), 133.

Wang, Y., Chen, F., Wang, J., Zhao, Y., & Liu, F. (2019). Two novel homozygous mutations in NPHP1 lead to late onset end-stage renal disease: a case report of an adult nephronophthisis in a Chinese intermarriage family. *BMC nephrology*, *20*(1), 173.

Wagner, C. A., Finberg, K. E., Breton, S., Marshansky, V., Brown, D., & Geibel, J. P. (2004). Renal vacuolar H+-ATPase. *Physiological reviews, 84*(4), 1263-1314.

Waldherr, R., Lennert, T., Weber, H.-P., Födisch, H., Michalk, D., Müller-Wiefel, D., & Schärer, K. (1982). The Nephronophthisis Complex; a Clinicopathologic Study *Renal Insufficiency in Children* (pp. 7-22): Springer.

Watnick, T., & Germino, G. (2003). From cilia to cyst. *Nature genetics, 34*(4), 355.

West, B., Luke, A., Durazo-Arvizu, R. A., Cao, G., Shoham, D., & Kramer, H. (2008). Metabolic syndrome and self-reported history of kidney stones: the National Health and Nutrition Examination Survey (NHANES III) 1988-1994. *American journal of kidney diseases, 51*(5), 741-747.

White, M. C., & Quarmby, L. M. (2008). The NIMA-family kinase, Nek1 affects the stability of centrosomes and ciliogenesis. *BMC cell biology, 9*(1), 29.

Williams, E. L., Acquaviva, C., Amoroso, A., Chevalier, F., Coulter-Mackie, M., Monico, C. G., . . . Salido, E. (2009). Primary hyperoxaluria type 1: update and additional mutation analysis of the AGXT gene. *Human mutation, 30*(6), 910-917.

Wolf, M., Saunier, S., O'Toole, J., Wanner, N., Groshong, T., Attanasio, M., . . . Waldherr, R. (2007). Mutational analysis of the RPGRIP1L gene in patients with Joubert syndrome and nephronophthisis. *Kidney international, 72*(12), 1520-1526.

Wolf, M. T., & Hildebrandt, F. (2011). Nephronophthisis. *Pediatric nephrology, 26*(2), 181-194.

Xu, J., Barone, S., Li, H., Holiday, S., Zahedi, K., & Soleimani, M. (2011). Slc26a11, a chloride transporter, localizes with the vacuolar H+-ATPase of A-intercalated cells of the kidney. *Kidney international, 80*(9), 926-937.

Yakulov, T. A., Yasunaga, T., Ramachandran, H., Engel, C., Müller, B., Hoff, S., . . . Walz, G. (2015). Anks3 interacts with nephronophthisis proteins and is required for normal renal development. *Kidney international, 87*(6), 1191-1200.

Yamamura T, Nozu K, Miyoshi Y, et al. (2017) An in vitro splicing assay reveals the pathogenicity of a novel intronic variant in ATP6V0A4 for autosomal recessive distal renal tubular acidosis. BMC Nephrol 18:353.

Yang, Y., LU, X., Chen, W., Li, L., Zhu, X., Huang, C., & Liu, S. (2019). Two novel AGXT mutations cause the infantile form of primary hyperoxaluria type I in a Chinese family: Research on missed mutation. *Frontiers in pharmacology, 10*, 85.

Yang, Y., Muzny, D. M., Xia, F., Niu, Z., Person, R., Ding, Y.,Buhay, C. (2014). Molecular findings among patients referred for clinical whole-exome sequencing. *JAMA, 312*(18), 1870-1879.

Yenchitsomanus, P.-t., Kittanakom, S., Rungroj, N., Cordat, E., & Reithmeier, R. A. (2005). Molecular mechanisms of autosomal dominant and recessive distal renal tubular acidosis caused by SLC4A1 (AE1) mutations. *Journal of molecular and genetic medicine: an international journal of biomedical research, 1*(2), 49.

Yim, H., Sung, C. K., You, J., Tian, Y., & Benjamin, T. (2011). Nek1 and TAZ interact to maintain normal levels of polycystin 2. *Journal of the American Society of Nephrology*, ASN. 2010090992.

Zhang, C., Ren, H., Shen, P., Xu, Y., Zhang, W., Wang, W., . . . Chen, N. (2015). Clinical evaluation of Chinese patients with primary distal renal tubular acidosis. *Internal Medicine, 54*(7), 725-730.

Zhuang Y, Weiner AM (1986) A compensatory base change in U1 snRNA suppresses a 5¢ splice site mutation. Cell 46:827– 835

Zollinger, H., Mihatsch, M., Edefonti, A., Gaboardi, F., Imbasciati, E., & Lennert, T. (1980). Nephronophthisis (medullary cystic disease of the kidney). A study using electron microscopy, immunofluorescence, and a review of the morphological findings. *Helvetica paediatrica acta, 35*(6), 509-530.

Electronic Database Information

- UCSC genome Browser: https://genome.ucsc.edu/
- Ensembl genome Browser: http://www.ensembl.org/index.html
- NCBI database: https://www.ncbi.nlm.nih.gov/
- Exome Aggregation Consortium (EXAC): http://exac.broadinstitute.org/
- Human Gene Mutation Database: http://www.hgmd.cf.ac.uk/
- Online Mendelian Inheritance in Man (OMIM)

APPENDIX A: TURNITIN REPORT

APPENDIX B: PRIMERS LIST

Table 1. Primers used for amplification of *NEK1*

Exon	Primer	Sequence	Product size (bp)	AT (°C)
17	F	GCAGTGGAGGGACTATAGC	287	58.5
	R	ATCCTGGACGAACTCCAGG		

Table 2. Primers used for amplification of *AGXT*

Exon	Primer	Sequence	Product size (bp)	AT (°C)
10	F	TCTCACCCACGCACTGAGC	318	59
	R	CTGGATACCCCTTGGAGA		

Table 3. Primers used for amplification of *NPHP4*

Exon	Primer	Sequence	Product size (bp)	AT (°C)
22	F	TCATCGTGGACAGTCGGA	221	58
	R	CCAAATGCAACTTCCCTGT		

Table 4. Primers used for amplification of *ANKS6*

Exon	Primer	Sequence	Product size (bp)	Tm
9	F	CATGGAGTCTTTCCTGCAGAG	368	61
	R	TGGATTCGTCGGTTTGAGGT		

Table 5. Primers used for screening *NPHP1* deletion

Exon	Primer	Sequence	Product size (bp)	AT (°C)
(NPH1del)	F	GCTCCTTCCTGAGAAGACAG	142	56.5
	R	CCACCTCTCATCCAGACACT		

Table 6. Primers used for amplification of *ZNF154*

Exon	Primer	Sequence	Product size (bp)	AT (°C)
5	F	GTTCAGCAGCAGAGAACCC	297	60
	R	GCACTCATATGGCCTTTCC		

Table 7. Primers used for amplification of *NAF1*

Exon	Primer	Sequence	Product size (bp)	AT (°C)
2	F	CTACTTTCCCAATACCATATCAG	574	54.7
	R	CCAGATCACTACTCTCTTTTACA		

Table 8. Primers used for amplification of *PCNT*

Exon	Primer	Sequence	Product size (bp)	AT (°C)
28	F	GAAGCGACGATTGCCGAGAG	319	66
	R	CACCATCCATGCGAGGCTGTG		

Table 9. Primers used for amplification of *KCNJ1*

Exon	**Primer**	**Sequence**	**Product size (bp)**	**AT (˚C)**
2	F	TCACGTGACCATTGGATATGG	354	60
	R	CCAGCGTCAACTACAAAGTTG		

AT=Annealing temperature, F=Forward, R=Reverse

Table 10. Primers used for amplification of *ATP6V0A4*

Exon	Primer	Sequence	Product size (bp)	AT(˚c)
4	F	GCTATTGCTGGGGAACGTTAAG	437	60
	R	GCAAACATCCACAAATAGCTCG		
5	F	AGCCCAGGCAACAGAGTGAG	502	62.2
	R	GAATGACCTGCCTGGTCATG		
6	F	ACAGTGAGCTGAGATCGCGC	401	65
	R	GCTGCCACAGCACCTGGATC		
7	F	GATCCAGGTGCTGTGGCAGC	373	64
	R	AGAGGGAGACGACCATGCAG		
8	F	CTTAAGAGAGCATGCACGTG	458	60.5
	R	TCACCAATGGCCTAGCCATG		
10	F	CATGTCGGTAGAGCTGTGTC	564	58
	R	GCCGCCTAGGATAGTACTAG		
12	F	GCAGAAATGACTCAGTGCAG	561	59
	R	ACCAGAAAGGCATAGCCAGC		
13	F	AGAGTTCAAGGCCAGGTGAC	481	57.5
	R	GAAGGAAGCAATCCTACCAC		
14	F	TCGTGAGTCTCAGAGAGATC	426	52.3
	R	CTGATTCCCACAGCTACTAC		
15	F	ATGATTGTGCCACTGCACTC	592	60
	R	ATGCTGAAAGGAACGGCAC		
16	F	CTGCTGTGGTCATGTGGCTC	395	56.5
	R	AAGTGCACCTCTGAGTAGAC		
17	F	CTCAGATTGTAGCCTCAGTG	465	53
	R	TGGGTAGAAGGTGTAGACAG		
18	F	GTATGCATTGAGCTGGACTG	467	55
	R	CTTGGAGAGACTCTGCTCAG		
19	F	CCGTTGTTTGCCAGTAGTGC	483	62
	R	TCAAGATCACGCCACTGCAC		
20	F	GCTATTGCTGGGGAACGTTAAG	437	61
	R	GCAAACATCCACAAATAGCTCG		
21	F	GCACAATGTCCGCTCACTAC	510	59
	R	AGCAGTGACAGGGCTACTGC		
22	F	GCTGGGGAACGTTAAGACAC	426	58
	R	CATCCACAAATAGCTCGGAG		
23	F	GGAGTTGGAGACCATCCTAG	676	56
	R	TGTGAGCCTATCTCAGATGC		
24	F	CTCAGGATTCTCATGGCAGC	445	58
	R	CCTCTGACGTGGTTAAGTCG		

APPENDIX C: PUBLICATION